Taylor & Francis
Taylor & Francis Group

Journal of Toxicology and Environmental Health, Part B
Critical Reviews

ISSN: 1093-7404 (Print) 1521-6950 (Online) Journal homepage: http://www.tandfonline.com/loi/uteb20

Inhalation Exposure to Carbon Nanotubes (CNT) and Carbon Nanofibers (CNF): Methodology and Dosimetry

Günter Oberdörster, Vincent Castranova, Bahman Asgharian & Phil Sayre

To cite this article: Günter Oberdörster, Vincent Castranova, Bahman Asgharian & Phil Sayre (2015) Inhalation Exposure to Carbon Nanotubes (CNT) and Carbon Nanofibers (CNF): Methodology and Dosimetry, Journal of Toxicology and Environmental Health, Part B, 18:3-4, 121-212, DOI: 10.1080/10937404.2015.1051611

To link to this article: http://dx.doi.org/10.1080/10937404.2015.1051611

Journal of Toxicology and Environmental Health, Part B, 18:121–212, 2015
Published with license by Taylor & Francis
ISSN: 1093-7404 print / 1521-6950 online
DOI: 10.1080/10937404.2015.1051611

INHALATION EXPOSURE TO CARBON NANOTUBES (CNT) AND CARBON NANOFIBERS (CNF): METHODOLOGY AND DOSIMETRY

Günter Oberdörster[1], Vincent Castranova[2], Bahman Asgharian[3], Phil Sayre[4]

[1]Department of Environmental Medicine, University of Rochester, Rochester, New York, USA
[2]Formerly with the National Institute for Occupational Safety and Health, West Virginia University School of Pharmacy, Morgantown, West Virginia, USA
[3]Applied Research Associates, Raleigh, North Carolina, USA
[4]Formerly with the U.S. Environmental Protection Agency, Washington, DC, USA

Dedicated to Professor Paul Morrow, 1922–2013
In respectful and fond memory of a devoted scientist, inspirational colleague, caring mentor, selfless friend, and in gratitude for his lasting groundbreaking contributions to inhalation toxicology

Carbon nanotubes (CNT) and nanofibers (CNF) are used increasingly in a broad array of commercial products. Given current understandings, the most significant life-cycle exposures to CNT/CNF occur from inhalation when they become airborne at different stages of their life cycle, including workplace, use, and disposal. Increasing awareness of the importance of physicochemical properties as determinants of toxicity of CNT/CNF and existing difficulties in interpreting results of mostly acute rodent inhalation studies to date necessitate a reexamination of standardized inhalation testing guidelines. The current literature on pulmonary exposure to CNT/CNF and associated effects is summarized; recommendations and conclusions are provided that address test guideline modifications for rodent inhalation studies that will improve dosimetric extrapolation modeling for hazard and risk characterization based on the analysis of exposure-dose-response relationships. Several physicochemical parameters for CNT/CNF, including shape, state of agglomeration/aggregation, surface properties, impurities, and density, influence toxicity. This requires an evaluation of the correlation between structure and pulmonary responses. Inhalation, using whole-body exposures of rodents, is recommended for acute to chronic pulmonary exposure studies. Dry powder generator methods for producing CNT/CNF aerosols are preferred, and specific instrumentation to measure mass, particle size and number distribution, and morphology in the exposure chambers

Address correspondence to Günter Oberdörster, DVM, PhD, Department of Environmental Medicine, University of Rochester, 601 Elmwood Avenue, Med. Ctr. Box 850, Rochester, NY 14642, USA. E-mail: gunter_oberdorster@urmc.rochester.edu

are identified. Methods are discussed for establishing experimental exposure concentrations that correlate with realistic human exposures, such that unrealistically high experimental concentrations need to be identified that induce effects under mechanisms that are not relevant for workplace exposures. Recommendations for anchoring data to results seen for positive and negative benchmark materials are included, as well as periods for postexposure observation. A minimum data set of specific bronchoalveolar lavage parameters is recommended. Retained lung burden data need to be gathered such that exposure-dose-response correlations may be analyzed and potency comparisons between materials and mammalian species are obtained considering dose metric parameters for interpretation of results. Finally, a list of research needs is presented to fill data gaps for further improving design, analysis, and interpretation and extrapolation of results of rodent inhalation studies to refine meaningful risk assessments for humans.

Carbon nanotubes (CNT) and carbon nanofibers (CNF) are commonly used in commerce, and applications are expected to increase in the near future (Zhao and Castranova 2011; De Volder et al. 2013). Since approximately 2004, the U.S. Environmental Protection Agency (EPA) has reviewed over 60 notices for commercialization of these materials under Section 5 of the Toxic Substances Control Act. Releases during the manufacture of these fibrous carbon nanomaterials, and during the incorporation of CNT/CNF into finished products, coupled with results from experimental animal studies showing asbestos-like effects, raised considerable human health concerns (Nowack et al. 2013). These exposures are commonly in the form of CNT/CNF-containing aerosols, resulting in a need to monitor exposure and assess inhalation effects upon workers (National Institute for Occupational Safety and Health [NIOSH] 2013). Available data indicate that releases through use and disposal of products containing CNT/CNF are far lower (Kingston et al. 2014). In order to assess the inhalation toxicity of these fibrous carbon nanomaterials, it is critical to consider whether and how testing of these materials differs from methods recommended in existing standard test guidelines for assessing effects of aerosols of soluble chemicals and larger solid particulates.

This review summarizes the effects of CNT/CNF reported after dosing of the respiratory tract and examines respiratory tract testing conducted in rodents to date for these materials. It specifically addresses the challenges posed by inhalation testing with CNT/CNF, including methods of particle generation, options for animal exposure systems, consideration of critical physicochemical properties for characterization of the materials, and importance to characterize exposures, determine doses and evaluate responses when examining exposure-dose-response relationships. Modifications to existing standard test guidelines were recommended to accommodate these challenges.

DOSING METHODS FOR THE RESPIRATORY TRACT

Human exposure to CNT and CNF may occur throughout their life cycle, from their manufacture at the workplace to their final disposal, depending on whether processes along the life cycle yield airborne inhalable or respirable particulate elements of CNT and CNF. Although dermal exposure and ingestion via contaminated food and water may also occur, the major exposure route is inhalation with the respiratory tract as portal of entry, which is the focus of this review. When assessing potential effects of airborne CNT and CNF in animal studies, equivalent human exposure conditions ideally need to be mimicked by considering exposure methods and mode and dosimetric aspects. Although dosing of the respiratory tract might also be achieved using bolus type delivery methods, such as intratracheal instillation (IT) or oropharyngeal aspiration of material suspended in a physiological medium

such as 0.9% saline, inhalation is considered the gold standard.

Table 1 highlights some differences between the different methods of dosing the rodent respiratory tract with nanomaterials. A main difference is the delivery of material either as a bolus exposure (instillation, aspiration) or by inhalation, with the former representing a nonphysiological mode of delivery of the liquid suspended material within a fraction of a second (very high dose rate), whereas the latter physiological inhalation deposits aerosolized materials over an extended period of time (days, weeks, or months, termed low dose rate). The high dose rate issue for instillation or aspiration may be mitigated by administering bolus-type deliveries at lower doses over the course of weeks. However, multiple exposures require multiple anesthetizations, which subsequently increase stress to animals and require careful animal monitoring.

A high dose rate and high doses may overwhelm normal defense mechanisms and thus result in significant initial pulmonary inflammation, and may also affect disposition of the administered material to secondary organs. In addition, the necessary pretreatment of nanomaterials with dispersants to prevent their agglomeration in the vehicle medium used for instillation/aspiration delivery alters the particle surface, which is likely to impact their biokinetics and induction of effects. Inhalation of pristine unmodified nanomaterials avoids these sources of potential introduction of artifacts from surface modifications. The impact of high doses also needs to be considered when the amounts exceed by orders of magnitude dose levels that are expected to be deposited in the respiratory tract of humans under realistic inhalation exposure scenarios. The selection of high bolus doses is often justified by arguments that the delivered dose is the same—per unit alveolar surface area—as is deposited per unit alveolar surface area in humans exposed to occupational exposure levels over a 40-yr working life. This ignores completely the effect of dose rate, that is, delivery of the same dose over a long period (days, months, years) versus within a fraction of a second (Oberdörster 2012; Baisch et al. 2014). Responses induced by such high doses are likely due to mechanisms, such as particle overload or effects of homeostasis, that are not operative at relevant low doses (Slikker et al. 2004). For example, overload doses of poorly soluble particles (PSP) of low toxicity overwhelm the alveolar macrophage clearance function, which was shown to induce lung tumors in rats (International Life Sciences Institute [ILSI] 2000).

Another disadvantage of bolus type delivery is the uneven distribution of the administered material throughout the respiratory tract relative to inhalation. A more central deposition of the delivered dose and its uneven distribution in the lower respiratory tract occur (Brain et al. 1976; Pritchard et al. 1985; Dorries and Valberg 1992; Driscoll et al. 2000). On the other hand, the great advantage of bolus-type delivery is the ease of delivering material to the lung, requiring no special equipment. Results also allow for the ranking of pulmonary toxicity of materials, and may be useful for qualitative risk assessment, although results are inadequate for purposes of quantitative risk assessment. Bolus delivery does not simulate normal human inhalation exposure conditions, and therefore an important component for risk assessment, that is, exposure to defined airborne concentrations over time, is missing. In general, instillation or aspiration may be considered as "proof of principle studies" or "hypothesis-forming studies" for identifying mechanisms and obtaining information on biodistribution, which needs to be verified subsequently by inhalation.

Other bolus type delivery methods that are not listed in Table 1 include laryngeal aspiration and intratracheal microspray of liquid suspended nanomaterials (NM) and intratracheal insufflation of NM powders (Morello et al. 2009; Penn Century [www.penncentury.com]). The latter two involve delivery of a preset dose in a syringe-type dispenser either as liquid spray or as dry powder, with the tip of the cannula-type sprayer inserted into the rodent trachea approximately 3–5 mm above the main-stem

TABLE 1. Methods of Dosing Rodent Lower Respiratory Tract with Particles

Method	Anesthesia	Depos. all Reg. Resp. Tr.	Evenness of Deposition	Physiol. Mode	Dose Rate	Use for Toxicity Ranking	Use for Quant. Risk Assessm.	NP Pre-treatment to avoid Agglomer	Repeat/ Long-term Exposures	Animal Stress at daily Exposure	Special Expertise/ Equipment Required	Costs
Bolus Type												
Intranasal instillation A	yes	yes	good to poor	no	high	yes	no	yes	limited	high	no	low
Intratrach instillations A	yes	No	good to poor	no	high	yes	no	yes	limited	high	no	low
Orophar. aspiration B	yes	no	good to poor	no	high	yes	no	yes	limited	high	no	low
Inhalation C												
whole body	no	yes	excell.	yes	low	yes	yes	no D	yes	low	yes	high
nose only	no	yes	excell.	yes	low	yes	yes	no D	yes	med	yes	high

A - synchronize with inspiration; B - caveat: significant inflammation in rats; C - requires larger amounts of material: D- most aerosolization methods result in significant, yet realistic, agglomeration of NPs.

carina, to be delivered in synchrony with the inspiration of the animal. Advantages and disadvantages of these are essentially the same as those for other bolus type delivery systems, except that insufflation does not require dispersant pretreatment of the dry NM.

Delivery of airborne engineered nanomaterials (ENM) to the lung by inhalation is achieved in different ways, with the most common being whole-body and nose-only exposures. The former requires individual placement of rodents in compartmentalized areas in order to avoid huddling of the animals and permits some free movement, whereas their movement is severely restricted by placing them in narrow tubes during nose-only exposure with the noses protruding into the plenum with continuously supplied aerosol. This induces significant stress in the animals (Phalen 2009), as evidenced by a retarded body weight gain during longer term nose-only exposures (Coggins et al. 1993, 2011; Pauluhn and Mohr 1999; Rothenberg et al. 2000). In contrast, contamination of the fur by aerosolized materials is restricted to the head and perhaps shoulder area, whereas during whole-body exposure aerosol deposition occurs on the whole-body surface area, resulting in some additional gastrointestinal (GI) tract exposure due to preening (see more discussion under "Types of Inhalation").

In addition to these two most common inhalation methods, intratracheal inhalation has been used, which prevents any external exposure of fur and allows simulation of different breathing scenarios, including breath holding. This requires less material to be aerosolized, but requires anesthesia throughout the exposure (Oberdörster, Cox, and Gelein 1997; Kreyling et al. 2009).

RESPONSES TO CNT/CNF EXPOSURES

Since the mid 1990s, material scientists have developed and perfected methods to arrange carbon atoms in a crystalline graphene lattice with a tubular morphology, thus creating CNT. CNT may be produced as a single tubular structure to form a single-walled carbon nanotube (SWCNT), as a tube within a tube forming a double-walled carbon nanotube (DWCNT), or as multiple tubes within a tube forming a multiwalled carbon nanotube (MWCNT). SWCNT have a diameter of 1–2 nm, while MWCNT are synthesized with diameters ranging from 10 to 80 nm depending upon the number of encapsulated tubes forming the CNT structure. CNT range in length from 0.5 to over 30 μm. Therefore, CNT exhibit high aspect ratios and may be classified as man-made fibrous materials, according to the World Health Organization (WHO) respirable fiber definition, that is, a particle longer than 5 μm, <3 μm in diameter, and with an aspect ratio of >3:1 (WHO 1981).

CNT (1) are resistant to acid or heat treatment, (2) exhibit high tensile strength, (3) possess unique electrical properties, and (4) may be easily functionalized. Therefore, applications as structural materials, electronics, heating elements, in production of conductive fabric, for bone grafting and dental implants, and in drug delivery systems are being developed. Recent in vitro findings regarding catalytic degradation of carboxylated, but not pristine, SWCNT have also been verified for in vivo conditions (Allen et al. 2008; 2009; Liu, Hurt, and Kane 2010a; Kotchey et al. 2013) With the anticipated increase in the synthesis and commercialization of CNT, human and environmental exposure during the life cycle of CNT, that is, production, distribution, use, and disposal, is anticipated. Therefore, it is critical to determine the bioactivity of CNT and characterize the dose and time dependence of possible adverse health effects of exposure to inform risk assessment and development of prevention strategies.

A complication in evaluating the potential adverse health effects resulting from pulmonary exposure to CNT is the wide range of physicochemical properties among different CNT. For example, CNT might be synthesized by three distinctively different processes, resulting in differences in chirality and degrees of catalyst contaminants, and exposures may be to raw CNT or CNT purified to remove catalytic metals. CNT may be produced with

a wide variety of fiber widths and lengths, and airborne CNT exhibit a wide range of structural sizes and shapes from micrometer agglomerates to nanometer nanoropes. Lastly, CNT may be functionalized to alter their physicochemical properties, such as hydrophobicity versus hydrophilicity. In addition, doping of MWCNT with nitrogen was found to reduce their toxicity significantly (Carrero-Sanchez et al. 2006; Elias et al. 2007).

At present, data are inadequate to determine to what degree biological responses to a given CNT and CNF can be generalized as one nanoparticle class. Indeed, reported effects following exposure of rodents to CNT by bolus-type delivery or inhalation revealed that although responses are qualitatively similar, the magnitude and time course of responses may vary significantly, suggesting that quantitative differences in bioactivity are likely (Shvedova et al. 2005; 2008; Ryman-Rasmussen, 2009b). Three recent 13-wk inhalation studies in rats with two different types of MWCNT and one 13-wk rat inhalation study with CNF showed similar results, yet different LOAEL and/or NOAEL were derived (Ma-Hock et al. 2009a; Pauluhn 2010; DeLorme et al. 2012; Kasai et al. 2014). The results also suggested that MWCNT and CNF might be generically placed into the same hazard category. However, additional subchronic inhalation studies with different types of MWCNT and CNF are urgently needed to substantiate this suggestion. Indeed, the International Agency for Research on Cancer (IARC) (Grosse et al. 2014) recognized this uncertainty when classifying only Mitsui-7 MWCNT as possibly carcinogenic to humans (Group 2 B) and other MWCNT and SWCNT as not classifiable with respect to carcinogenicity (Group 3).

Indeed, a most recent key study involving 2 year whole body inhalation exposures of rats to three concentrations of Mitsui-7 MWCNT confirmed a significant dose-dependent induction of neoplastic lesions in the lung (adenoma and carcinoma) at the medium concentration (0.2 mg/m^3; 26%) and high concentration (2 mg/m^3; 32%) in male rats and at only the high concentration (2 mg/m^3; 22%) in female rats. The low concentration (0.02 mg/m^3; 4%) was not different from controls (4–6 %). (Fukushima, personal communication, 2015). A paper with full details of this milestone study is in preparation. The apparently greater sensitivity of males vs females is opposite to earlier findings of chronic inhalation studies with poorly soluble particles of low cytotoxicity. (Lee et al, 1985) With this confirmation of the carcinogenicity of inhaled Mitsui-7 MWCNT the IARC classification is likely to change to: Probably carcinogenic to humans (Group 2 A).

PULMONARY RESPONSE TO SWCNT

Due to the low density of CNT, it is anticipated that respirable particles may be generated during manufacturing, as a result of transfer, weighing, mixing, and blending of CNT. Therefore, inhalation is considered a primary route for human exposure. The pulmonary effects attributed to exposure of rodents to SWCNT were first reported in 2004. Warheit et al. (2004) exposed rats by IT instillation to high doses of a raw form of SWCNT (0.25–1.25 mg/rat), with the CNT sample containing 30–40% amorphous carbon, 5% nickel, and 5% cobalt. Although suspended in phosphate-buffered saline (PBS) containing 1% Tween 80, the SWCNT were highly agglomerated. Pulmonary exposure to SWCNT resulted in a rapid but transient inflammatory and injury response, as evidenced by increased levels of bronchoalveolar lavage fluid (BALF) neutrophils, lactate dehydrogenase (LDH) activity, and protein. Granulomas, predominantly in the terminal bronchioles, were reported 1 wk postexposure and persisted through 3 mo postexposure. A 15% rise in mortality rate within 1 d postexposure was noted and attributed to physical blockage of conducting airways by large SWCNT agglomerates. Lam et al. (2004) also reported rapid and persistent granulomas in mice after IT instillation of mice to very high doses of SWCNT (0.1–0.5 mg of SWCNT/mouse). These investigators compared raw (containing 25% metal catalyst) to purified (approximately 2% iron [Fe])

SWCNT and found the granulomatous reaction was not dependent on metal contamination of SWCNT. The high mass doses induced a maximal response, which may have masked an additional effect of the higher Fe content.

Mangum et al. (2006) exposed rats by pharyngeal aspiration to purified SWCNT (0.5 mg/rat; 2.6% Co and 1.7% Mo) suspended in 1% Pluronic. Data showed no apparent inflammatory responses. However, cell proliferation and platelet-derived growth factor (PDGF) protein levels were significantly increased 1 d postexposure and significant interstitial fibrosis was noted at 21 d postexposure. Shvedova et al. (2005) exposed mice by pharyngeal aspiration to purified SWCNT (10–40 μg/mouse). The suspended SWCNT preparation, sonicated but with no dispersant, contained micrometer-sized agglomerates as well as some smaller nanorope structures. A rapid and transient inflammation and pulmonary damage were noted. In addition, granulomatous lesions and interstitial fibrosis within 7 d postexposure, which lasted through the 59-d course of the study, were observed. Granulomas were associated with the deposition of agglomerates in the terminal bronchioles and proximal alveoli, while interstitial fibrosis was associated with deposition of more dispersed SWCNT structures in the distal alveoli. This distinction between deposition site (proximal vs. distal alveoli) and response (granulomas vs. interstitial fibrosis) was confirmed using gold-labeled SWCNT, which allowed nanoropes structures to be visualized in lung tissue (Mercer et al. 2008). As in the Lam et al. (2004) study, the transient inflammatory/injury response and persistent granulomatous and fibrotic lesions were not markedly affected by the presence or absence of catalytic metals using raw versus pure SWCNT (Shvedova et al. 2005; 2008).

Mercer et al. (2008) compared the pulmonary response of mice after pharyngeal aspiration of a poorly dispersed versus well-dispersed (acetone-dispersed, washed, and suspended in PBS with sonication) preparation of SWCNT. It was found that transient inflammation and persistent interstitial fibrosis were fourfold greater on an equal delivered mass burden basis for well-dispersed SWCNT compared to poorly dispersed SWCNT. Shvedova et al. (2008) reported the pulmonary response of mice to inhalation of SWCNT (5 mg/m^3, 5 h/d, 4 d). Qualitatively, short-term inhalation produced pulmonary responses similar to bolus exposure by pharyngeal aspiration, that is, transient inflammation and damage but persistent granulomas and interstitial fibrosis. Aerosolization of dry SWCNT resulted in smaller structures (count median diameter [CMD] approximately 220 nm) than suspension of SWCNT for aspiration (a mixture of μm size agglomerates and smaller nanorope structures). Quantitatively, SWCNT were estimated to be fourfold more potent on an equal mass burden basis (5–10 μg/lung) in producing inflammation and fibrosis after inhalation (deposited lung burden was estimated from aerosol concentration, minute ventilation, duration of exposure, and estimated deposition fraction) than was aspiration of less dispersed SWCNT (Shvedova et al. 2008). Of interest, the degree of the response to aspiration of well-dispersed SWCNT was similar to that for short-term inhalation, using a similar type of SWCNT (Mercer et al. 2008; Shvedova et al. 2008), suggesting that aspiration exposure may be appropriate for testing well-dispersed CNT for purposes of hazard identification.

Murray et al. (2012) compared the potency of SWCNT to crocidolite asbestos after aspiration in mice. At 1 and 7 d postexposure, SWCNT (40 μg/mouse) were significantly more potent in inducing transforming growth factor (TGF)-beta, a fibrogenic factor, than asbestos (120 μg/mouse). In addition, SWCNT were substantially more potent in inducing alveolar interstitial fibrosis as evidenced by lung collagen and alveolar wall connective tissue thickness than asbestos at 28 d postexposure. Shvedova et al. (2014) confirmed the greater fibrotic potency of SWCNT compared to asbestos at 1 year after aspiration in mice. The high bolus doses expressed by mass need to be considered which in addition raises the question about comparing responses by different metrics: Would surface characteristics such as area, charge, and chemistry be more appropriate?

Recently, Shvedova et al. (2013) presented data suggesting that SWCNT may act as a cancer promoter. In this study, mice were exposed to SWCNT (80 μg/mouse) or phosphate-buffered saline vehicle by pharyngeal aspiration. Two days after aspiration, mice were inoculated (iv) with Lewis lung carcinoma cells. In vehicle control mice, inoculation with cancer cells resulted in lung tumors 21 d after iv injection. However, lung tumor growth was significantly greater in mice preexposed to SWCNT as measured by the following: (1) 5-fold increase in lung weight, (2) 2.5-fold elevation in the number of visible tumors, and (3) 3-fold rise in the area of metastatic nodules. Data indicated that this tumor promotion was associated with SWCNT-induced upregulation of granulocyte myeloid-derived suppressor cells, which would depress antitumor immunity. This may be viewed as an important hypothesis-forming study. However, the extremely high bolus dose and dose rate need to be compared to dose-response relationships following realistic inhalation exposures.

In summary, pulmonary exposure of mice to SWCNT induced granulomatous lesions associated with deposition of micrometer-sized agglomerates as well as rapid and progressive interstitial fibrosis associated with migration of smaller SWCNT structures into the alveolar septa. Although most studies were conducted in mice, exposure of rats to SWCNT also induced granulomas and fibrosis. It should be noted that most of these SWCNT studies involved bolus exposure, resulting in high lung burdens at a very high dose rate. The single inhalation study with SWCNT involved a relatively high aerosol concentration (5 mg/m^3) and 5-d exposure duration (Shvedova et al. 2008). Therefore, dose rate was still relatively high. Thus, there is the need for 13-wk inhalation studies in rodents. Lung burdens from reported bolus exposure studies may be used as guidance for determination of aerosol exposure concentration (ideally resulting in low, medium, and high doses). Current knowledge gaps include (1) determination of worker exposure to SWCNT (aerosol concentration and size distribution of airborne structures), (2) characterization of the effect of catalytic metals on pulmonary responses to SWCNT, (3) determination of whether inhaled SWCNT can translocate to the pleura or other organs and produce intrapleural or systemic effects, (4) determination of whether inhaled SWCNT induce lung cancer, (5) evaluation of the degree to which SWCNT agglomerates are dispersed into smaller structures upon contact with pulmonary surfactant or cellular enzymes, (6) determination of the biopersistence of SWCNT, and (7) elucidation of mechanisms involved in these adverse responses.

PULMONARY RESPONSE TO MWCNT

Muller et al. (2005) exposed rats by IT instillation to MWCNT (0.5–5 mg/rat) suspended in 1% Tween 80. Dose-dependent inflammation, granulomas, and fibrosis were noted, with the unground MWCNT (6 μm length) being more potent than ground MWCNT (0.7 μm length). At 60 d postexposure, 81% of unground MWCNT were retained in the lung, as determined by 0.5% Co impurities, compared to 36% for short MWCNT. Li et al. (2007a) compared the pulmonary response of mice exposed to purified MWCNT by IT instillation (50 μg/mouse bolus dose) versus inhalation (32.6 mg/m^3, 6 h/d, for 5–15 d [estimated deposited dose of 70–210 μg]). MWCNT aerosolized from dry material were less agglomerated than when suspended in 1% Tween 80. Intratracheal instillation produced inflammation and severe destruction of alveolar structures, while inhalation predominately resulted in moderate pathology consisting of alveolar wall thickening and cell proliferation but general alveolar structure was retained. This study demonstrated significant differences in the type and degree of pulmonary responses to MWCNT in mice between bolus-type IT instillation and inhalation, with higher doses deposited in lung by inhalation resulting in only moderate effects compared to severe lesions induced by instillation of lower doses. Yu et al. (2013) compared the influence of IT instillation of 100

μg pristine MWCNT to acid-treated MWCNT for 6 mo and noted that pristine MWCNT induced pulmonary autophagy accumulation and more potent tumorigenic responses than the acid-treated MWCNT, suggesting the importance of physicochemical characteristics in toxicity outcome. Similarly, Kim et al. (2010a) found that pristine MWCNT produced more severe acute inflammatory cell recruitment in BALF and multifocal inflammatory granulomas compared to acid-treated MWCNT in mice IT instilled with 100 μg for 1 wk up to 4 mo. In another study, exposure of rats by IT instillation of high doses of purified MWCNT (0.25–1.75 mg/rat) suspended in 1% Tween 80 produced a rapid but transient inflammatory response and persistent alveolar wall thickening (Liu et al. 2008).

Kobayashi et al. (2010) exposed rats by IT instillation to a well-dispersed suspension of MWCNT (10–250 μg/rat). Transient inflammation and damage and a granulomatous response was observed. No fibrosis was found, but a collagen stain for histopathology was not used. In contrast, Porter et al. (2010) reported a rapid and persistent fibrotic response in mice after aspiration of a well-dispersed suspension of purified MWCNT (10–80 μg/mouse dispersed in a diluted artificial lung lining fluid), using Sirius red staining for collagen. In addition, transient inflammation and damage with persistent granulomas at sites of agglomerate deposition were noted. Mercer et al. (2011) conducted morphometric analysis of the interstitial fibrotic response from the Porter et al. (2010) study. Analysis indicates a time- and dose-dependent fibrotic response. At 80 μg of MWCNT/mouse, interstitial fibrosis at 28 d postexposure was significantly above control measured as the thickness of alveolar wall collagen. At 56 d postexposure, interstitial fibrosis at 40 μg of MWCNT/mouse was significantly greater than control at 40 μg of MWCNT/mouse, with nonsignificant trends observed at lower doses.

Similarly, Aiso et al. (2010) reported transient inflammation and damage, and persistent granulomas and alveolar wall fibrosis in rats after IT instillation of different MWCNT (40–160 μg/rat). In a recent report, mice were exposed by inhalation (5 mg/m^3, 5 h/d, 12 d) to Mitsui-7 MWCNT (lung burden of 28 μg/lung) and alveolar interstitial fibrosis was monitored for 336 d postexposure (Mercer et al. 2013a). The thickness of alveolar septal collagen increased 14 d postexposure and continued to progress to 70% above control by 336 d postexposure.

Han et al. (2010; 2015) exposed mice by aspiration to carboxylic or hydroxyl functionalized MWCNT (20–40 μg/mouse). These functionalized MWCNT were well dispersed in PBS. Similar to other reports, transient inflammation (1 and 7 d post), elevated cytokine production (1 day post), and lung injury (1 day post) were found at 20 and 40 μg/mouse. Surface functionalization of MWCNT was reported to affect bioactivity, with carboxylated or acid-treated MWCNT being less inflammatory and fibrotic while amine-functionalized MWCNT were more potent than unmodified MWCNT (Kim et al. 2010a; Yu et al. 2013; Bonner et al. 2013; Li et al. 2013; Sager et al. 2014). Reported biodegradation of carboxylated SWCNT and MWCNT may be attributed to peroxidases (Zhao, Allen, and Star 2011; Kotchey et al. 2013).

Pauluhn (2010) exposed male and female rats by nose-only inhalation (0.1–6 mg/m^3, 6h/d, 5 d/wk, 13 wk) to Baytube MWCNT. Aerosolized structures were large, compact agglomerates—defined as assemblages by the author—with a mass median aerodynamic diameter (MMAD) of approximately 3 μm. Subchronic inhalation resulted in persistent inflammation, lung damage, granulomas, alveolar wall thickening, and increased interstitial collagen staining at exposures of 0.4 mg/m^3 or higher. Notably, Pauluhn (2010) did not generate significant amounts of fibrous or loosely agglomerated structures with Baytube MWCNT and described them as assemblages. The non-ibrous morphology of these assemblages was used as explanation to characterize responses as being due to volumetric overload of alveolar macrophages phagocytizing these structures (Pauluhn 2010). The lowest exposure concentration of 0.1 mg/m^3 was

determined to be the NOAEL. Of special importance, the study by Pauluhn (2010) is the only one to determine in a sufficiently long postexposure period the retention halftime (T1/2) of the retained MWCNT (shown later in Table 3). This demonstrated a prolongation of T1/2 with high lung burdens, similar to other persistent particles ranging from more benign (TiO_2; carbon black [CB; [Morrow 1988; Elder et al. 2005]) to highly reactive known human carcinogens (asbestos; crystalline SiO_2 [Bolton et al. 1983; Hemenway et al. 1990]). Inclusion of a sufficiently long postexposure period needs to be a mandatory component of a well-designed repeated inhalation study to determine retention kinetics and regression/progression of effects.

Ma-Hock et al. (2009a) reported pulmonary responses of male and female rats to nose-only inhalation of MWCNT (0.1–2.5 mg/m^3, 6 h/d, 5 d/wk, 13 wk; resultant burden 47–1170 μg/rat [crudely estimated, no clearance assumed]). The aerosolized MWCNT were well dispersed (count median diameter approximately 60 nm). Pulmonary responses included increased lung weight, neutrophilic inflammation, and granulomatous inflammation. No apparent fibrosis was reported. However, Ma-Hock et al. (2009a) did not use a specific collagen stain for histopathologic analysis; consequently, fibrosis may have been underscored. To address this, Treumann et al. (2013) reported results of additional histopathological analyses describing a slight increase of collagen fibers in the medium- and high-dose animals within the microgranuloma, yet no collagen fibers in alveolar walls and pleura. One rat of the lowest exposure group (0.1 mg/m^3) developed minimal granuloma. Data also showed evidence of MWCNT degradation in alveolar macrophages. Overall, data demonstrated that the hallmark of asbestos exposure, pleural inflammation and/or fibrosis, was absent. The lowest exposure concentration of 0.1 mg/m^3 was the LOAEL in this study.

A multidose 2-wk whole-body inhalation study in rats (6 h/d, 5 d/wk) with Mitsui-7 MWCNT determined a NOAEL of 0.2 mg/m^3, whereas significant pulmonary dose-dependent inflammatory effects were seen in groups exposed to 1 and 5 mg/m^3 group (Umeda et al. 2013). Inflammatory indicators were decreased at 4 wk postexposure, but partially still elevated. MWCNT translocated to the peritracheal lymph nodes, which increased in the postexposure observation period. Goblet-cell hyperplasia induced in the 1- and 5-mg/m^3-exposed rats did largely regress during the postexposure period. The retained lung burden (43 μg in 5 mg/m^3 group) at the end of the 2-wk inhalation exposure did not change significantly in the subsequent 4-wk postexposure period, and evidence indicated lengthy in vivo biopersistence of these MWCNT.

In a subsequent whole-body inhalation study, Kasai et al. (2015)[1] exposed female and male F-344 rats to Mitsui-7 MWCNT at 3 concentrations ranging from 0.2 to 5 mg/m^3 (MMAD = 1.4–1.6 μm) for 13 wk (6 h/d, 5 d/wk) using whole-body inhalation chambers. Retained burden in the left lung, determined by a hybrid marker technology (Ohnishi et al. 2013), ranged between 2.3 and 120 μg/rat. Dose-dependent pulmonary inflammation, granulomas, and interstitial fibrosis were observed. Kasai et al. (2015) also observed MWCNT in the mesothelial lining of rodent diaphragms in the highest exposure group (5 mg/m^3). In addition, Kido et al. (2014) subsequently noted that subchronic inhalation exposure to MWCNT resulted in systematic inflammation as indicated by increases in mRNA expression in splenic macrophages. The lowest exposure concentration of 0.2 mg/m^3 was the LOAEL in this study, indicating that a 2-wk inhalation study where a NOAEL of 0.2 mg/m^3 was found for the same MWCNT in their previous investigation (Umeda et al. 2013) was insufficient to derive a longer term NOAEL. It is to be expected that the NOAEL from a chronic 2-yr study might be even lower.

[1]Data were furnished by the Japan Bioassay Research Center to Dr. G. Oberdörster. This study was contracted and supported by the Ministry of Health, Labor, and Welfare of Japan.

Ryman-Rasmussen et al. (2009b) exposed mice to MWCNT by nose-only inhalation (30 or 1 mg/m^3 for 6 h; MMAD 0.18 and 0.16 μm). Lung burdens were not quantified but estimated based on assumed deposition efficiencies. Two to 6 wk postexposure, MWCNT in alveolar macrophages were detected in the subpleural tissue and mesothelial cells lining the lung, as well as subpleural fibrosis in the high-dose group only. Porter et al. (2010) also found MWCNT in the subpleural tissue and subpleural lymphatics, with some fibers penetrating into the intrapleural space 1–2 mo after aspiration of a well-dispersed suspension of MWCNT (20–80 μg/mouse) suspended in diluted artificial lung lining fluid. Mercer et al. (2010) conducted morphometric analyses of the Porter et al. (2010) data and noted significant migration of MWCNT into the intrapleural space as early as 1 d postexposure and at doses of 20 μg/lung. Data demonstrated (using morphometric measurements) that 12,000 MWCNT penetrated into the intrapleural space at 56 d after aspiration of 80 μg of MWCNT in a mouse model, with such penetrations being dose and time dependent at 20 μg/mouse or higher. Liang et al. (2010) found that MWCNT translocate to the lung and induce fibrosis 28 d after intraperitoneal (ip) injection of a large dose of 250 μg MWCNT/mouse or greater. These MWCNT had been functionalized with phosphorylcholine to make them hydrophilic. The Sakamoto et al. (2009) observations also support translocation of intrascrotally administered MWCNT to the thorax, where diaphragmatic granulomatous lesions were found. Recently, Mercer et al. (2013b) reported translocation of inhaled MWCNT (lung burden 28 μg/mouse) from the lung to the chest wall and diaphragm and observed MWCNT in intrapleural lavage fluid. In addition, low but progressive translocation of MWCNT was noted from the lung to the lymphatics, liver, kidneys, heart, and brain over a 336-d postexposure observation period.

Pauluhn and Rosenbruch (2015) compared pulmonary effects and retention kinetics of MWCNT (Baytubes) aerosols generated either as dry powder aerosols or well dispersed from a liquid suspension. Rats were nose-only exposed once for 6 h to large agglomerated aggregates with MMAD of 2.6 μm from powder generation or to smaller well-dispersed structures from liquid nebulization with MMAD of 0.79 μm, at high concentrations of 25–30 mg/m^3. Marked differences were seen in terms of threefold higher initial lung burdens (lung burdens were quantified by NIOSH method 5040 and Doudrick et al. 2013) and about twofold faster clearance of wet-dispersed MWCNT in the 3-mo postexposure period. Macroscopically, lungs from wet-dispersed MWCNT displayed a gray discoloration, which was also seen in the enlarged lymph nodes, whereas dry MWCNT-exposed lungs appeared normal. Histopathological examination revealed a greater alveolar macrophage response and minimal septal thickening in lungs from wet-exposed rats only. Pauluhn and Rosenbruch (2015) emphasized the importance of using relevant exposure scenarios of pristine nanomaterials rather than artificial conditions when testing nanomaterials, to avoid flawed conclusions based on high-dose acute studies. This investigation also highlights the necessity of determining lung burdens rather than only knowing exposure concentrations.

A recent investigation indicated that MWCNT act as a strong promoter of lung tumors (Sargent et al. 2014). In this study, B6C3F1 mice were injected ip with either corn oil (vehicle) or 10 μg/g bw of methylcholanthrene (an initiator). One week later, mice were then exposed by whole-body inhalation (5 h/d, 15 d) to either filtered air or MWCNT (Mitsui-7, 5 mg/m^3, resulting lung burden of 31 μg/lung) generated by an acoustical generator as described by McKinney, Chen, and Frazer (2009). At 17 mo postexposure, mice were euthanized and lung tissue was examined by a board-certified veterinary pathologist for lung tumor formation. MWCNT did not significantly increase the incidence of tumor formation (percent of mice with a tumor) in mice receiving corn oil. However, MWCNT produced a marked rise in tumor incidence in mice treated with the initiator

chemical (initiator alone having a 50% incidence, while the initiator plus MWCNT group displayed a 90% incidence). In addition, MWCNT increased multiplicity (number of tumors/lung) compared to the inducer alone from 1.4 to 3.3 tumors/lung, with tumors being significantly larger in the initiator plus MWCNT group compared to initiator alone. Pathological analysis indicated that tumors were both bronchoalveolar adenomas and bronchoalveolar adenocarcinomas, with significantly more malignant tumors in the initiator plus MWCNT mice. This study is the first to demonstrate lung cancer promotion after inhalation of MWCNT. Although the experimental design of this study was weakened by the absence of negative and/or positive particle control groups, a most recent chronic rat inhalation study (see above) confirmed the induction of both adenomas and carcinomas in the lung. It is of interest that pharyngeal aspiration of 10 μg MWCNT in mice followed by 56 d postexposure revealed significantly enhanced expression of a gene set related to human lung cancer, suggesting this technique may be utilized for early detection of lung cancer (Guo et al. 2012).

In general, available studies indicate that pulmonary exposure of mice or rats to MWCNT induce granulomas and interstitial fibrosis. Evidence also indicates that MWCNT deposited in the lung migrate to the pleura and diaphragm. Results are qualitatively similar for both bolus exposure studies and inhalation studies. Results also appear to be similar after inhalation exposure of both rats and mice when the same MWCNT (Mitsui-7) and aerosol dispersion (MMAD of approximately 1.5 um) were employed, as in the Mercer et al. (2013a); 2013b) and Kasai et al. (2015) studies. Knowledge gaps include (1) determination of typical worker exposure to MWCNT (aerosol concentration and size distribution of aerosolized structures), (2) evaluation of the effects and biopersistence of catalytic metals, fiber dimensions, and surface functionalization on the pulmonary toxicity of MWCNT, (3) determination of the degree to which deposited MWCNT agglomerates disperse into smaller structures upon contact with pulmonary surfactant of cellular enzymes, (4) verification of whether MWCNT can induce or promote lung cancer and mesothelioma, and (5) elucidation of mechanisms involved with adverse pulmonary responses.

PULMONARY RESPONSES TO CNF

Only three studies evaluating responses following exposures to CNF have been reported, two mouse aspiration studies and a 13-wk rat inhalation study. The first mouse study (Murray et al. 2012) administered 120 μg of CNF (98.6% elemental carbon; 1.4% iron; 80 to 160 nm thick; 5–30 μm long) to mice by oro-pharyngeal aspiration, and effects were evaluated at 1, 7, and 28 d postexposure. The second mouse study used the same CNF and dosing, but followed the induced fibrosis for 1 yr postaspiration (Shvedova et al. 2014). The rat inhalation study involved 13-wk (5 d/wk; 6 h/d) inhalation of both male and female rats to 3 concentrations (0.54, 2.5, or 25 mg/m^3) and filtered air controls with evaluation of effects at 1 d and 13 wk postexposure (DeLorme et al. 2012). The CNF were different (99.5% elemental carbon, 0.003% iron; 40–350 nm thick; 1–14 μm long) from those of Murray et al. (2012) or the Shvedova et al. (2014) studies. Pulmonary responses in the high bolus-dosed mice included inflammation (lung lavage increased polymorphonuclear leukocytes [PMN], protein, and LDH activity at d 1, which were still significantly elevated at 28 d postexposure); established oxidative stress responses; and elevated biochemical (collagen) and histochemical (Sirius red) indicators of fibrosis for as long as 1 yr after aspiration (Murray et al. 2012; Shvedova et al. 2014). Effects after inhalation exposure of rats included dose-dependent elevation in lung weight, still increased in the highest dose group at 13 wk postexposure; persistent inflammation (BALF, significant rise in BAL PMN and LDH at highest dose) at 1 d and 17 wk postexposure; interstitial thickening; and proliferation of Type II cells in the subpleural, parenchymal, and bronchiolar region in the high-exposure group, which was persistent for the subpleural

region at 13 wk postexposure. Indicators of cardiovascular effects (C-reactive protein [CRP]; coagulation parameters; histopathology) were not markedly different from controls. A NOAEL of 0.54 mg/m^3 was determined, and a LOAEL of 2.5 mg/m^3 based on minimal inflammation in terminal bronchioles and alveolar ducts (DeLorme et al. 2012).

In summary, pharyngeal aspiration of CNF in mice (high bolus dose) resulted in interstitial fibrosis. Using bolus dosing, the fibrotic potency of CNF was substantially lower than that of SWCNT (Murray et al. 2012; Shvedova et al. 2013). Inhalation exposure of rats to CNF over 13 wk resulted in a far lower degree of fibrosis. DeLorme et al. (2012) indicated that a lower, more worker-relevant dose rate in this inhalation study might explain this difference. However, lung burden was not determined in the inhalation study. The reported MMAD of 3 μm suggests a lower alveolar deposition compared to a more respirable rat aerosol of ≤2 μm MMAD, explaining the low alveolar interstitial fibrosis. Therefore, there remains a need for a subchronic inhalation study to a CNF aerosol, in which retained lung burden in the lower respiratory tract needs to be measured. Knowledge gaps given for SWCNT and MWCNT are also applicable to CNF.

RESPONSES TO INTRAPERITONEAL INJECTION OF MWCNT

Takagi et al. (2008) reported that injection of MWCNT (3 mg, 10^9 fibers/mouse) into the abdomen of p53± mice resulted in mesothelioma similar to the asbestos positive control. The findings in this study have been questioned due to the extremely high dose of MWCNT used (Ichihara et al. 2008). The aforementioned caveats associated with nonphysiological bolus-type dosing need to be considered. However, a follow-up study also found induction of abdominal mesothelioma (25% incidence) after ip injection of 3 μg (10^6 fibers/mouse) of MWCNT (Takagi et al. 2012). Peritoneal and pleural metastatic mesothelioma were also reported after intrascrotal administration of MWCNT (1 mg/kg body weight) into rats, with the extent of response exceeding that of asbestos when compared on the basis of delivered mass as dose metric (Sakamoto et al. 2009). Nagai et al. (2011) administered to rats very high doses (1 and 10 mg/rat) of different MWCNT (agglomerated, nonagglomerated, tangled, thin [50 nm], and thick [150 nm], including Mitsui MWCNT), which resulted in high mortality of the 10-mg-dosed rats and peritoneal mesothelioma at 1 yr in the surviving rats for certain groups. The nonagglomerated thinner MWCNT, including Mitsui, produced greatest peritoneal inflammation and carcinogenicity, which correlated with their crystallinity, sharpness, and rigidity; these properties facilitated piercing of cell membranes as observed in additional in vitro studies. Thick MWCNT produced less inflammation and carcinogenicity, and tangled MWCNT, even when thin, did not induce mesothelioma. Similarly, Muller et al. (2009) noted no mesothelioma over a 2-yr period after abdominal injection of very short MWCNT (<1 μm; 20 mg/rat). These negative findings would have been predicted by results of Poland and coworkers (2008), who found that abdominal injection of 50 μg of long MWCNT/mouse resulted in granulomatous lesions on the diaphragm within 2 wk of exposure, while short MWCNT were ineffective, as were tangled MWCNT. Murphy et al. (2011) reported that intrapleural injection of long MWCNT (5 μg/mouse), but not short MWCNT, resulted in persistent (24 wk) inflammation and fibrosis of the parietal pleural surface similar to that seen with long amosite.

Results of a large 2-yr ip injection study involving 500 male Wistar rats given a low and high dose of 4 different types of MWCNT (50 rats per dose) showed that all MWCNT dosed rats developed mesothelioma (Rittinghausen et al. 2014). Administration of high ip doses by fiber number was the same for all MWCNT at 1 × 10^9 and 5 × 10^9 fibers/rat, equivalent to mass bolus doses ranging from 50 μg to 3 mg. When amosite asbestos was

used as a positive control given as one 10-fold lower ip dose of 0.1×10^9 fibers/rat, 66% mesothelioma incidence resulted, whereas only 1 rat in medium-injected controls developed mesothelioma (2%). Data indicated that MWCNT were capable of inducing mesothelioma and point to the high durability of all CNT. In addition, a higher toxic and carcinogenic potency of straight and more needle-like shaped MWCNT was noted and a lower potential for curled, bent, or tangled MWCNT, which is similar to the findings of Nagai et al. (2011) reported earlier.

While direct intracavitary injection of MWCNT of straight fiber structures resulted in the reported length-dependent inflammatory and fibrosis responses, the occurrence of airborne MWCNT as complex tangles raises questions with regard to their translocation to the pleura upon inhalation and subsequent pleural effects. Appropriate inhalation studies need to be designed. Such an inhalation studies were conducted recently by Mercer et al. (2013a; 2013b; Kasai et al. 2015). Mercer et al. (2013b) reported that MWCNT individual fibers were observed by enhanced dark-field microscopy in pleural lavagate, chest wall, and diaphragm 1 d after inhalation of MWCNT (5 mg/m^3, 5 h/d, 12 d; lung burden of 28 μg/mouse determined by an absorbance assay). The number of MWCNT in the diaphragm significantly increased from 1 d to 336 d postexposure. Kasai et al. (2015) also observed by electron microscopy translocation of MWCNT to the diaphragm after a 13-wk inhalation of Mitsui-7 MWCNT in rats. Fibers were also detected in the pleural lavagate of rats after administration of two types of MWCNT (Mitsui-7 and Nikkiso MWCNT) by intratracheal spraying of large doses (250 μg 5 times over 9 d for a total of 1.25 mg/rat) (Xu et al. 2012). Such high-bolus-dose pulmonary exposure to MWCNT resulted in an increase of inflammatory cells in the pleural cavity, inflammatory and fibrotic lesions of the visceral pleura, and mesothelial hyperplasia in the visceral pleura as determined 6 h after the last dosing. No lesions were observed in the parietal pleura. Xu et al. (2014) recently also exposed rats by intratracheal spraying to long-thick (8 μm × 150 nm) and short-thin (3 μm x 15 nm) MWCNT. Exposure was to 125 μg/rat, 13 times over 24 wk for a total very high dose of 1.625 mg/rat. The short-thin MWCNT sample consisted of agglomerated tangles with few free fibers. Long, but not short, MWCNT translocated to the pleural cavity and deposited in the visceral and parietal pleura. Long MWCNT induced fibrosis in the parietal and visceral pleura, and parietal mesothelial proliferative lesions were found after this 24-wk treatment, confirming—as previously suggested—the importance of fiber length for translocation from deposits in the lung to and effects at remote target sites.

In summary, intracavitary high bolus injection of MWCNT in mice and rats induces mesothelioma. MWCNT were found in the pleural lavage, chest wall, and diaphragm after inhalation exposure of mice or rats to MWCNT. Successive high-dose nonphysiological bolus exposures (over 9 d–24 wk; lung burdens of 1.25–1.63 mg/rat) resulted in pleural inflammation and mesothelial hyperplasia. However, induction of lung tumors or mesothelioma has not yet been demonstrated after realistic inhalation exposure in a noncompromised rodent model. Thus, although the presently available studies confirm a carcinogenic hazard of MWCNT, data cannot be used for quantitative risk characterization of repeated inhalation exposures. The outcome of an ongoing 2-yr rat inhalation study with Mitsui-7 MWCNT (S. Fukushima et al. personal communication, 2014) may provide essential information on the carcinogenic potential of inhaled MWCNT. Other knowledge gaps include (1) determination of dose and time dependence of pleural effects, (2) examination of the impact of fiber dimensions (length and width) and agglomeration/aggregation state on pleural effects, (3) analysis of the effects of functionalization on MWCNT potency, and (4) measuring translocation rates to other potential target sites including liver, spleen, CNS, and bone marrow.

SYSTEMIC CARDIOVASCULAR AND NEUROLOGICAL RESPONSES TO PULMONARY EXPOSURE TO CNT

Li et al. (2007b) observed that multiple aspirations of SWCNT (20 μg/mouse, every 2 wk, for 2 mo) in Apo E -/- mice produced an increased number of aortic plaques. Inhalation of MWCNT (26 mg/m^3 for 5 h; calculated lung burden of 22 μg) resulted in a depression of the responsiveness of coronary arterioles to dilators 24 h postexposure (Stapleton et al. 2011). Further, pharyngeal aspiration of MWCNT (80 μg/mouse) produced an induction of mRNA for certain inflammatory mediators and markers of blood–brain barrier damage in the olfactory bulb, frontal cortex, midbrain and hippocampus 24 h postexposure (Sriram et al. 2009). However, Han et al. (2015) demonstrated that pharyngeal aspiration of MWCNT (40 μg) induced pulmonary inflammatory responses 7 d postexposure with no progression of atherosclerosis in apolipoprotein-E-deficient mice.

A recent MWCNT inhalation study in rats reported 24 h after a 5-h inhalation to 5 mg/m^3 pulmonary inflammation and translocation to systemic organs (Stapleton et al. 2012). Data also showed an impairment of endothelium-dependent dilation in cardiac coronary arterioles, which was not resolved yet by 7 d postexposure, revealing the potential of inhaled MWCNT not only to induce pulmonary inflammatory effects but also to produce serious extrapulmonary effects after a short-term exposure to a high concentration of 5 mg/m^3, resulting in an estimated lung burden of 13 μg/rat. In contrast, Warheit, Reed, and DeLorme (2013) reported no histopathological changes in heart muscle or cardiovascular tissue and no marked changes in C-reactive protein or coagulation parameters between CNF-exposed and air-exposed control rats after a 90-d inhalation of CNF (25 mg/m^3). It is possible that differences of physicochemical properties of these fibrous nanomaterials (hollow vs. solid fibers; retained doses, fiber dimension, surface area, or fiber count/mass) may explain these results. In addition, it is uncertain how long cardiovascular responses persist or adapt after initial exposure (90 d after initial exposure [Warheit, Reed, and DeLorme 2013] vs. 1–7 d postexposure [Stapleton et al. 2012]). Further, identifying cardiovascular effects may require additional specific methods to determine with high sensitivity effects on the cardiovascular system.

Several possible mechanisms have been postulated to explain systemic responses to pulmonary exposure to CNT.

Translocation of CNT to Systemic Sites

Translocation of ip MWCNT from the abdominal cavity to the lung was reported by Liang et al. (2010). However, thus far there is no apparent evidence that systemic effects noted earlier in this report were associated with CNT in the affected tissue. Indeed, aspirated gold-labeled SWCNT were not found in any systemic organ 2 wk postexposure using transmission electron microscopy (TEM) (Mercer et al. 2009). However, the study by Stapleton et al. (2012) found low levels of systemic translocation of inhaled MWCNT into liver, kidneys, and heart. DeLorme et al. (2012) also observed rare events of translocated CNF in brain, heart, liver, kidneys, spleen, intestinal tract and mediastinal lymph nodes, but no histopathological changes were seen. Mercer et al. (2013b) documented translocation of MWCNT to the lymphatics, liver, kidneys, heart, and brain after inhalation of MWCNT (lung burden of 28 μg/mouse). However, this systemic translocation at 336 d postexposure was less than 0.25% of the initial lung burden.

Systemic Inflammation

Erdely et al. (2009) reported that aspiration of SWCNT or MWCNT (40 μg/mouse) induced a significant increase in blood neutrophils and mRNA expression and protein levels for certain inflammatory markers in blood at 4 h postexposure, but not at later times. Such pulmonary CNT exposure also significantly elevated gene expression for mediators, such as Hif–3α and S100a in the heart and aorta at 4 h postexposure. Evidence also indicates that pulmonary exposure to particles alters systemic

microvascular function by inducing activated PMN to adhere to microvessel walls and release reactive species that scavenge NO produced by endothelial cells (Nurkiewicz et al. 2006; 2009). This decreased responsiveness of systemic muscle and coronary arterioles to dilators was observed 24 h after inhalation of nano-TiO_2 at a lung burden of 10 μg (Nurkiewicz et al. 2008; LeBlanc et al. 2009) and after inhalation of MWCNT (Stapleton et al. 2012).

Kido et al. (2014) interpreted their finding of increased mRNA expression of inflammatory cytokines in splenic macrophages after 3 mo of inhalation exposure of rats to MWCNT as indicators of systemic inflammation. Translocated MWCNT were noted in spleen of exposed rats, and both splenic macrophages and T-lymphocytes displayed increased expression of cytokines/chemokines including interleukin (IL)-2, suggesting a potential impact on antitumor activities and general immunosurveillance.

Neurogenic Signals

Intratracheal instillation of SWCNT (250 μg) to rats was found to elevate baroreflex function by twofold (Legramante et al. 2009; Coppeta et al. 2007). Although data specifically for CNT are not yet available, pulmonary exposure to inhaled ultrafine TiO_2 was reported to stimulate sensory neurons in the lung (Kan et al. 2012). Scuri et al. (2010) demonstrated that in vivo inhalation of TiO_2 nanoparticles produced upregulation of lung neutrophins in weanling and newborn rats but not in adults. Further inhibition of sympathetic input to systemic arterioles reversed the decreased responsiveness of microvasculature to dilators after pulmonary exposure to ultrafine TiO_2 (Knuckles et al. 2012).

In summary, although a few studies reported cardiovascular responses after pulmonary exposure to CNT, the results are far from complete. Dose and time-course relationships for a variety of cardiovascular endpoints need to be determined. Mechanisms by which pulmonary particles induce cardiovascular responses require elucidation. Although MWCNT have been observed in cardiovascular tissue after pulmonary exposure, it is unclear whether this tissue burden is sufficient to explain cardiovascular reactions observed. Knowledge gaps concerning relationships between CNT/CNF dimensions, surface area and surface activity, and possible cardiovascular responses need to be addressed. The finding of translocation of inhaled MWCNT to the spleen and activation of splenic macrophages and lymphocytes requires further mechanistic studies regarding systemic inflammatory and immunomodulatory effects.

Relationship Between Physicochemical Properties and Toxicity

Physicochemical properties may affect the potential toxicity of nanomaterials. There are several extensive lists of properties that could apply to nanomaterials, such as the 18 properties noted by the OECD (2010). These properties were examined as part of the OECD nanomaterial testing program, which examined a set of standardized nanomaterials for relevant physicochemical, fate, toxicity, and ecotoxicity endpoints. Other more focused lists are intended to correlate health effects with physicochemical characteristics (Bernstein et al. 2005). There have been efforts to take such focused lists for health effects and narrow them even further to apply to nanomaterials in general (Nanomaterial Registry 2014; Warheit 2008; Nel et al. 2009).The list of properties relevant to all nanomaterials may be narrowed when considering health effects of a particular grouping of nanomaterials. For CNT and CNF, a possible reduced list of traits is contained in Table 2.

TABLE 2. Physicochemical Characteristics which influence Toxicity of CNTs and CNFs

1. Method of Generation
2. Shape (length, width, morphology)
3. Agglomeration/aggregation
4. Surface Properties (area, charge, defects, coating, reactivity)
5. Impurities
6. Density

Method of Generation

The manufacturing technique used to produce CNT or CNF may affect all resultant physicochemical properties, and hence needs to be considered in order to understand the relative potency of the nanoparticle. Carbon nanotube production is accomplished by either chemical, physical, or other processes (Rafique and Iqbal 2011). Chemical vapor deposition (CVD) is a method for large-scale production of CNT, involving use of a hydrocarbon gas such as ethylene, methane, or acetylene; a process gas, either ammonia, nitrogen, or hydrogen; and a substrate such as silicon, glass, or alumina with an associated catalyst particle such as Fe, Co, or Ni. The nanotube diameter is dependent on the catalyst particle size. While most CVD processes produce random groups of CNT, other variants of the process might yield vertically aligned CNT and/or DWCNT. A second chemical process, the high-pressure carbon monoxide reaction method (HiPco), is also suitable for large-scale synthesis of SWCNT. In this method, the catalyst (Fe pentacarbonyl, or a mixture of benzene and ferrocene; Ni may also be used) is introduced in the gas phase, with CO used as the hydrocarbon gas. A third chemical process to produce SWCNT has been developed that uses cobalt and molybdenum catalysts, a silica substrate, and CO gases (CoMoCAT). SWCNT may be either metallic or semiconducting. These traits in turn influence their commercial applications. Physical processes for CNT production include arc discharge and laser ablation. These methods are mostly used for experimental purposes, and produce CNT in highly tangled forms, mixed with carbon contaminants and catalysts and therefore likely require purification, unlike CVD, which does not require extensive posttreatment. Finally, there are miscellaneous processes that are used even less. These include helium arc discharge, electrolysis, and flame synthesis methods. Efforts are currently under way to produce chirality-pure SWCNT in a lab setting. This is of interest since the electronic and optical characteristics of SWCNT are dependent on chirality (Liu, Ma, and Zachariah 2012).

Carbon nanofiber synthesis methods have been summarized by Kim et al. (2013). CNF differ from CNT in that they are generally larger in diameter and noncontinuous. CNF are produced via catalytic CVD using nanosized metal particles such as Fe, dispersed on a ceramic substrate (similar to production of CNT), or by electrospinning of organic polymers such as polyacrylonitrile followed by thermal treatment. CNF have special desirable thermal, electrical, and mechanical properties. A floating catalyst method (Singh et al. 2002) was also established involving metallocenes solutions as catalyst and benzene as feedstock sprayed into a furnace at high temperature to produce CNF in a continuous process at high yield. CNF produced by CVD consist of regularly stacked, truncated conical or planar layers along the filament length, and differ from CNT, which are comprised of concentric graphene tubes that contain an entire hollow core, and are flexible (Murray et al. 2012). In addition, such CNF usually behave as semiconductors, and their layer edges are chemically active. CNF produced by electrospinning and thermal treatment consist of randomly arranged flat or crumpled graphene sheets, with the long axis of the sheets running parallel to the fiber axis (Harris 2005). Electrospinning of two immiscible polymer solutions may produce porous nanosized fibrous carbon materials, and similar to CNT, CNF may be treated to reduce residual catalyst metals.

Shape (Length and Width)

The fiber-like shape of CNT and CNF has some resemblance to asbestos fibers, raising concerns that the well-known fibrogenic, carcinogenic, and mesotheliogenic effects attributed to asbestos inhalation may also be associated with inhalation of CNT/CNF. However, amphibole asbestos are thicker, and consist of straight fibers, many of which exceed 15–20 μm in length. Inhalation of these fibers results in "frustrated" phagocytosis by alveolar macrophages, with associated inflammatory cytokine release and cell death. Serpentine asbestos (chrysotile) consists of more curly

thinner fibrils, and hence may be a better correlate to CNT tangles. Detailed morphological examination using TEM or scanning electron microscopy (SEM) analysis needs to be completed prior to testing.

Ranges of length and width for CNT have been summarized in Donaldson et al. (2006). The lengths of CNT are typically several micrometers, although significantly shorter and longer fibers have been made. SWCNT diameters vary between 0.7 and 3 nm, while MWCNT outer diameters generally are in the 10 to 200 nm range. Although some are straight, most SWCNT and MWCNT are bent or curled to form clumps, assemblages, or ropes that are longer and wider than the individual nanotube singlets. While CNF might be produced by synthesis techniques similar to those of CNT and have a filamentous shape, these differ in several ways from CNT: CNF are composed of regularly stacked truncated conical or planar layers that run along the filament length and provide chemically active end planes in the inner and outer fiber surfaces; unlike CNT, CNF are not comprised of concentric tubes and may or may not contain a hollow core (Kim et al. 2013). CNF are flexible, and have diameters around 100 nm and an aspect ratio above 100 (Kim et al. 2013).

The size of CNT/CNF aerosols is determined by their agglomeration state, which affects their deposition in all regions of the respiratory tract. Depending on the deposited and retained dose, CNT/CNF may induce adverse pulmonary effects and translocate to other organs and tissues. Fibrous particles/fibers are defined as elongated particles with a length-to-diameter ratio (i.e., aspect ratio) equal to or greater than 3 to 1 and longer than 5 μm (EPA 2001; WHO 1981). *Respirable* (EPA 2001) infers that the particle in question might penetrate to the alveolar region upon inhalation. There are considerable differences in fiber respirability between lab rodents and humans as discussed later (Inhalable, Thoracic, and Respirable CNT and CNF Fractions) and in Appendix A. Translocation from deposition sites of inhaled MWCNT from the lungs of mice to pleural sites, to local lymph nodes, and to secondary organs is dependent on agglomeration state and size (Mercer et al. 2013b). In this study, translocation rates and amount translocated to secondary organs were low less than 0.1% over a year, whereas migration to bronchial-associated lymphatics was much higher over 7%. Most of the MWCNT in secondary organs were found in liver, but tiny amounts of short single CNT structures were also detected in brain, heart, and kidneys, in addition to pleural sites. Whether such low translocation of MWCNT might directly produce adverse effects in these distal organs has yet to be determined. Direct ip injection of high doses induced inflammation, granulomas, and mesothelioma (Takagi et al. 2008; Poland et al. 2008; Rittinghausen et al. 2014).

Several studies using intracavitary bolus injection of MWCNT in rodents demonstrated the length dependency of persistent inflammatory responses, which were inversely related to clearance at the parietal pleura (Donaldson et al. 2010; Murphy et al. 2011). These results confirmed earlier pioneering work with ip injection of long and short asbestos demonstrating that the size of lymphatic stomata on the parietal pleural of about 8–10 μm allows efficient clearance of short but not of long (>10–15 μm) fibers (Moalli et al. 1987). Donaldson et al. (2010) and Murphy et al. (2011) also showed that inflammatory response to MWCNT agglomerates or tangles was less and resolved quickly. Similarly, Nagai et al. (2011) and Rittinghausen et al. (2014) reported a low mesotheliogenic response to ip injected tangled MWCNT. It should also be noted that even short 5-μm MWCNT may be proinflammatory when given at high bolus doses, and similarly that lymphatic clearance pathways in the parietal pleura might be blocked by high bolus doses of such short fibers. While the relevance of direct injection of a high bolus dose of CNT into pleural or peritoneal cavity as surrogate for real-world inhalation exposures is questionable, this method may be considered as a proof-of-principle, which needs to be confirmed by realistic inhalation exposures.

Agglomeration/Aggregation

The International Organization for Standardization (ISO 2009) defined agglomeration as a collection of weakly bound (e.g., van der Waals forces) particles where the resulting surface area is similar to the sum of the surface areas of the individual components. Aggregation is defined as strongly bound or fused particles where the resulting external surface area may be significantly smaller than the sum of the individual surface areas (CEN ISO/TS 27687 2008; Jiang, Oberdörster, and Biswas 2009). Agglomeration and/or aggregation of CNT and CNF may have important implications for the biodistribution and toxicity of these materials, since they may be strongly influenced by the physicochemical properties of the agglomerate masses, in addition to the properties of the individual singlets that comprise the agglomerates. For example, the 12-d inhalation study by Mercer et al. (2013b) using highly agglomerated MWCNT aerosols exhibiting a wide range of agglomerated structures revealed a significant increase of singlet MWCNT in lymph nodes and extrapulmonary secondary organs, which indicated preferential translocation of MWCNT as singlets, due to either a slow process of deagglomeration of agglomerates deposited in the lung, or—if the agglomerate structure is kept intact—a slow translocation of MWCNT that were initially deposited as singlets. The former scenario is more likely, given the low number of individual singlet MWCNT that were present in the aerosol.

Deposition of agglomerated MWCNT aerosols in the alveolar region of the lung and subsequent phagocytosis by alveolar macrophages may result in a high burden when expressed as volume. This volumetric load—if exceeding a threshold defined as lung particle overload (Morrow 1988)—results in an impairment of alveolar macrophage clearance function as suggested by Pauluhn (2010). If significant aggregation is present, deaggregation and release of singlet MWCNT in the lung is not likely. The presence of aggregation or agglomeration may affect the surface area of the MWCNT bundle, a dose metric that was suggested as more appropriate to be used when comparing effects—including those associated with lung particle overload—of a wide range of different particle sizes from nano to micro (Oberdörster et al. 1994b; Tran et al. 2000a; Stoeger et al. 2006). If particle surface area is used as the dose metric, the slightly lower surface area of aggregated versus agglomerated structures needs to be considered as defined earlier.

Surface Properties

Surface properties of nanomaterials are important determinants of biological/toxicological activity. For example, surface charge may affect cellular uptake, and because it is the surface of poorly (in vivo) soluble materials that interacts with the organism, surface area (cm^2/g material) as dose metric has been widely applied in nanoparticle toxicology. Yet this metric is often misunderstood by assuming that all nanomaterials fit on a common dose-response relationship if specific surface of each material is used as metric. Rather, the surface area concept implies that expressing an effect—observed in vitro or in vivo—as a function of surface area of poorly soluble materials provides a more meaningful toxicological dose metric for hazard ranking than using mass or number of the tested nanomaterial (Donaldson, Beswick, and Gilmour 1996; Tran et al. 2000b; Oberdörster, Oberdörster, and Oberdörster 2005a). If the only difference is the particle size, with all other properties of a nanomaterial being the same, a common surface area dose-response relationship can be established for this material. Of interest in this regard, the fibrotic potency of SWCNT > MWCNT ≫ CNF correlates with their increasing specific surface areas (Murray et al. 2012; Mercer et al. 2011). An interesting finding supporting the surface area concept is a study by Timbrell et al. (1988) demonstrating that the lung fibrosis score of asbestos in miners

correlated best with the retained asbestos fibers in lung tissue.

Solubility (static in vitro systems) and dissolution (dynamic in vivo system) are important determinants of toxicity of nanomaterials in general (Utembe et al., 2015), but solubility/dissolution are not critical for poorly soluble CNT/CNF. The surface area dose metric concept for particles is different from soluble chemicals, where the dissolved mass is the appropriate dose metric. An expansion of the surface area concept is to express the maximal effect induced by each of a collection of different nanomaterials as effect per unit of their surface area derived from the steepest section of their dose-response relationships. This way the degree of the effect-inducing potential of each nanomaterial can be compared and ranked against each other on the basis of surface reactivity. The surface area normalized maximum responses (per cm^2) of different nanomaterials then may reflect their different hazard potential for purposes of hazard ranking (Rushton et al. 2010; Duffin et al. 2007).

The plausibility of the surface area concept is supported by findings that surface properties determine effects upon contact with cells, receptors, organelles. Thus, Sager et al. (2014) found that altering surface properties of MWCNT resulted in different effects and bioactivity profiles in a mouse model. The surface area dose metric concept is also likely to apply to the fibrous structure of CNT and CNF; however, when present as straight single structures, length and diameter also may need to be considered as determinants of their biological/toxicological effects, based on the three-dimensional (3D) paradigm that is well known from asbestos and glass fiber toxicology (Broaddus et al. 2011), but that is unlikely to be applicable for highly tangled/agglomerated CNT.

Ideally, the bioavailable or effective surface area should be the metric for defining surface reactivity (response per unit surface area). The gas (mostly nitrogen) adsorption method after Brunauer, Emmett, and Teller (BET) (Brunauer, Emmett, and Teller 1938) is generally used to determine specific surface area, which, however, needs to be considered only as a surrogate for a biologically available surface, whose real definition is still elusive. Donaldson et al. (2013) noted the central importance of a biologically effective dose (BED) in toxicology, which drives toxic responses and includes particle surface area as one metric. Peigney et al. (2001) developed a mathematical model to estimate the surface area of bundles of parallel CNT by accounting for the void spaces and also the number of layers in MWCNT. Evidence indicated that the calculated values are in good agreement with measured data by BET. Given that CNT agglomerates do not usually consist of straight, well-aligned parallel tubes, these theoretical calculations are—like BET—not providing information on bioavailable surface area.

Surface modification, for example, carboxylation, might affect biopersistence. Carboxylation of SWCNT and MWCNT makes them more vulnerable to oxidative destruction by peroxidases, which reduces their biopersistence significantly and may point to new possibilities to produce less reactive CNT through surface modifications (Zhao, Allen, and Star 2011; Kotchey et al. 2013). Carboxylation also makes the CNT more hydrophilic and less agglomerated. Carboxylation may decrease the ability of these nanoparticles to enter epithelial cells and cross cell membranes, enter the alveolar interstitium, and produce fibrosis (Wang et al. 2011; Sager et al. 2014). The ROS-inducing potential of CNT expressed per unit surface area may also be determined as a measure to categorize CNT and CNF based on their surface reactivity. Cell-free assays and electron spin resonance (ESR) spectroscopy were shown to be effective methods to assess this property (Rushton et al. 2010; Tsuruoka et al. 2013). In contrast to raw CNT, CNT purified to remove catalytic metals do not generate high levels of ROS in cell-free systems (Kagan et al. 2006).

Other surface properties and modification, like zeta potential, electrostatic charge, coatings, and defects, may also significantly influence their biological/toxicological responses (Fenoglio et al. 2008; Shvedova et al. 2005; Tabet et al. 2011; Li et al. 2013;

Salvador-Morales et al. 2008). Indeed, Li et al. (2013) observed that MWCNT functionalized with polyetherimide, which resulted in a strong positive surface charge, were more fibrogenic than bare MWCNT after aspiration in a mouse model. In addition, surface charge influences the agglomeraton state of CNT/CNF, which impacts their aerodynamic behavior when aersolized.

Impurities

Impurities that might affect pulmonary toxicity of CNT and CNF may be present and fall into three classes (Donaldson et al. 2006): support material, organics, and metals. Support material includes aluminates, silicates, and magnesium oxide. Residual organics include amorphous particles, or microstructured particles such as graphite sheets, which might arrange into carbon nanofibers or spheres. Little toxicity information is available that correlates adverse pulmonary effects with impurity amounts of either support material or residual organics. The most commonly used metals in CNT synthesis include Co, Fe, Ni, and Mo. CNT may be processed to remove most of the metal catalysts, such as those encapsulated in layers of amorphous soot or graphite.

Transition metal complexes and free Fe and Ni are known catalysts of biological free radical reactions. Therefore, where metal content was attributed to effects seen, correlations need to be considered in light of metal bioavailability. The effects of Fe and Ni catalysts on the pulmonary toxicity responses of CNT in three studies were recently reviewed by NIOSH (2013). Generally, higher Fe contents up to 18% were not associated with a higher lung response (Shvedova et al. 2008; Mercer et al. 2008), suggesting low bioavailability. In contrast, bioavailability of a high Ni- content affected the outcome granuloma formation (Lam et al. 2004). Bioavailability of metal impurities is a key determinant, as is potential contamination with endotoxin (lipopolysaccharide, LPS) which needs to be carefully tested (Esch et al. 2010).

Density

The relative density or specific gravity of nanomaterials is often regarded as being of little or no importance for interpretation of biological/toxicological effects. However, material density and bulk density need to be considered because inhalation is the main route of human exposure to CNT and CNF, and aerosol density is an important property to predict and understand their aerodynamic behavior and deposition fractions throughout the respiratory tract (Park et al. 2004). Further, because (1) cellular uptake of deposited materials, in particular by macrophages, results in a volumetric loading that was suggested to impair cell function if exceeding approximately 6% of the normal cell volume (Morrow 1988), and (2) volume and density are highly correlated, data on material density and bulk density need to be included in a listing of physicochemical properties for CNT/CNF characterization.

Material density of nanomaterials is specifically important for aerosols consisting of singlet particles in the aerodynamic size range, that is, above approximately 0.3 μm. In contrast, for singlet nanoparticles below 100 nm in the aerosol the main mechanism for their deposition in the respiratory tract is by diffusion, for which particle density does not play a role. Because airborne nanomaterials rarely occur as singlets, the aerodynamic behavior of their larger agglomerate sizes is determined by the effective density of the agglomerates. Difficulties in determining the effective aerosol density were described for regular particles (Park et al. 2004; Ku et al. 2007; Liu, Ma, and Zachariah 2012; Miller et al. 2013), but solutions have not yet been proposed for bundles/agglomerates of CNT and CNF aerosols. To overcome this problem, gas pycnometry was used to determine bulk density of bundled MWCNT (Pauluhn and Rosenbruch 2015) using the method of ISO 15901–1 (ISO 2005a). Wang et al. (2015) derived an expression for the effective density based on fractal-like structure of CNT and fit the equation to measured mass and mobility diameter to obtain

values for effective density as a function of mobility or outer diameter of CNT agglomerates. There is limited applicability of the findings to the respiratory tract because calculations were based on CNT transport in an electric field alone. Extension of this model to other external forces, such as inertia and gravity, is not justified and requires parallel studies. Bulk density may also be assessed by pouring the agglomerated or aggregated CNT or CNF into a graduated cylinder and measuring volume and weight (DIN EN 725–9 2006–05(E) 2006). Depending on conditions of undisturbed pouring (poured density) versus tapping the cylinder (tapping density), different values may occur. However, it needs yet to be determined whether the results approximate the effective aerosol density when using the poured density, whereas the tapping density may approximate the somewhat higher density present after uptake into cells for deriving the volumetric burden in macrophages. Thus, validated methods to measure aerosol densities of CNT still await general acceptance.

Additional Physicochemical Properties

Other physicochemical parameters of CNT/CNF may influence biological/toxicological responses, yet respective information and convincing data are not available. These include chirality of MWCNT, their tip configuration, crystallinity, and fiber stiffness, strength, and hardness. An important parameter may also be the degree of oxidation, which is rarely reported. New findings may reveal other relevant properties. For example, what is the biological significance of the recent discovery of high-speed pulse-like water movement through CNT, as reported by Sisan and Lichter (2014), using numerical simulations of single-file water flow?

Summary

In general, pulmonary exposure of rats or mice by IT instillation, pharyngeal aspiration, or inhalation of SWCNT or MWCNT and CNF results in transient inflammation and lung damage. Granulomatous lesions and interstitial fibrosis, which are of rapid onset and persistent in nature, have also been a common occurrence. Benchmark dose analysis (NIOSH 2013) noted no striking differences in responsiveness to CNT between rat and mouse models. Indeed, inhalation exposure of mice or rats to the same type of CNT (Mitsui-7 MWCNT) resulted in similar responses, that is, pulmonary inflammation, granulomas, interstitial fibrosis, and translocation of MWCNT to the pleura (Mercer et al. 2013a; 2013b; Kasai et al. 2015). The degree of agglomeration does affect deposition site and response. Large agglomerates tend to deposit more centrally at the terminal bronchioles and proximal alveoli and induce a granulomatous response, while more dispersed structures may deposit more peripherally in distal alveoli and produce interstitial fibrosis. The lung most likely might be exposed to more dispersed CNT and CNF structures by inhalation than by bolus-type exposure to a suspension of CNT/CNF. When this is the case, the response to short-term inhalation may differ from that of the same lung burden given as a bolus dose. Thus far, reported data suggest that quantitative differences in bioactivity between different types of CNT are likely. For example, on an equal mass basis, SWCNT appear to be more potent than MWCNT in producing alveolar interstitial fibrosis (Mercer et al. 2011). Limited data available for CNF suggests that the fibrotic potency of CNF is less than that of CNT (Murray et al. 2012). Mercer et al. (2011) proposed that specific surface area, dimensions, or hydrophobicity correlates with the rate of migration of fibrous nanomaterials to the interstitium. However, further investigation is required to resolve this issue.

The influence of manufacturing methods and surface modifications on physical–chemical properties of CNT/CNF needs to be considered when analyzing the correlation between these properties and toxicity. Understanding these correlations may help predict potential toxicities and also for identifying data gaps and research needs to be addressed in future studies.

CONSIDERATIONS AND CONCEPTS FOR REALISTIC RODENT INHALATION

Ideally, human exposure to CNT and CNF needs to be simulated when performing inhalation studies in rodents, not only to identify a potential hazard that is associated with such exposure but also to generate data that can be used for risk assessment. Thus, serious efforts need to be undertaken to obtain knowledge about exposure concentrations, airborne particle size, and size distribution, particularly at the sites of manufacture but also along the life cycle of CNT and CNF (packaging, distribution, incorporation into products, application, disposal), for potential exposure of workers and consumers. Such data are important for generation of an equivalent exposure atmosphere for rodents, taking into consideration differences between humans and rodents with respect to inhalability and respirability (see Inhalable, Thoracic, and Respirable CNT Fractions subsection). Generation of appropriately realistic exposure conditions is critical for purposes of dosimetric extrapolation and for risk assessment.

Available Exposure Data

The first available datum concerning airborne levels of CNT in a workplace was reported by Maynard et al. (2004). This study evaluated aerosolization of SWCNT in a small lab setting that simulated a workplace environment. Results indicated that SWCNT may be aerosolized with sufficient agitation. Estimates of the airborne concentration of SWCNT from personal air samples suggested that workplace respirable dust concentrations were lower than 53 $\mu g/m^3$. Evaluation of activities in a lab handling MWCNT reported significant aerosolization during weighing, transferring, and sonication (Johnson et al. 2010). Particle counts over the size range of 10–1000 nm were 1,576 particles/ml during weighing and 2776 particles/ml during sonication, with CNT structures generated during sonication being less agglomerated than those produced during weighing. Han et al. (2008) measured total airborne dust levels in a lab producing MWCNT in Korea. Processes such as weighing, blending and spraying produced airborne dust levels as high as 400 $\mu g/m^3$. However, not all these particles were MWCNT, and the MWCNT structures generated varied from agglomerates to more dispersed individual fibers. Admixture of background aerosol also needs to be considered. Lee et al. (2010) recently monitored workplace total dust levels at seven MWCNT facilities using personal samplers, area samplers, and real-time monitoring by SMPS, dust monitor and aethalometer. Particle generation was significant during oven opening, catalyst preparation, gel spraying, and preparation and sonication of MWCNT. The highest total particle concentration was 320 $\mu g/m^3$ with a mean 106 $\mu g/m^3$, with number concentrations from approximately 7000 to 75,000 per cubic centimeter. Diameters depended on manufacturing process, with mode diameters ranging from 20 to 30 nm for catalyst preparation and from 120 to 300 nm for ultrasonic dispersion. It should be noted that only a fraction of these airborne particle were MWCNT, with metal nanoparticles being a significant contributor to the total dust aerosolized in these workplaces.

It should be anticipated that within groups of CNT, for example, MWCNT, displaying significant differences between different types of MWCNT with regard to their physical (tangles, agglomerates) and chemical (contaminants, surface chemistry) characteristics, at least quantitative differences of responses are likely. Examples of response differences are apparent from the 13-wk inhalation studies of Pauluhn (2010) and Kasai et al. (2015). The latter study, using a more dispersed MWCNT aerosol, reported CNT-specific toxicity. In contrast, the first study, using approximately 3-μm agglomerates, attributed pulmonary responses to a nonspecific overload mechanism. Surface functionalization may also affect the biological potency of MWCNT. Indeed, Carrero-Sánchez et al. (2006) showed that nitrogen-doped MWCNT given by different routes of administration to mice produced significantly less toxicity than pure MWCNT. In other studies, the biopersistence of carboxylated SWCNT

and MWCNT was significantly reduced by biodegradation via peroxidases, as determined in vitro and in vivo, which reduced inflammatory potential (Allen et al. 2008; Liu, Hurt, and Kane 2010a; Kotchey et al. 2013).

Han et al. (2008) measured size distributions of airborne MWCNT in a research facility and found a majority of non-fibrous particles and CNT agglomerates of different sizes with few single fibers (Figure 1a). Other measurements in commercial and research facilities confirmed that only a few single fibers were found, with the majority of the airborne structures being agglomerates/clusters of different sizes (Tsai et al. 2009; Methner et al. 2010) as illustrated in Figure 1b.

Less information is available for CNF exposure measurements. Measurements by Birch et al. (2011), Evans et al. (2010), and Dahm et al. (2012; 2013) showed varying airborne concentrations, particle shapes, and aerodynamic sizes, depending on the processing site within a manufacturing facility. Similar to the findings with CNT, bundled and entangled structures were mostly found (Figure 2), as well as nonfibrous structures. Maximum concentrations due to uncontrolled transfer and bagging reach 1.1 mg/m^3 (Evans et al. 2010); the dominant mode by particle number of CNF was between 200 and 250 nm for both aerodynamic and mobility equivalent diameters, indicating an effective density close to unity. Depending on the purification process, significant concentrations of polycyclic aromatic hydrocarbons (PAH) and Fe-rich soot were detected in the CNF aerosol, which needs to be considered as causative/contributory factors for potential toxicity. There is an urgent need to obtain more information on the characteristics of CNT and CNF in workplace air. The suggestion that delivery of CNT and CNF to the respiratory tract of experimental animals, by inhalation or by instillation/aspiration, needs to be done with well-dispersed materials is not supported by presently published occupational exposure data, which uniformly demonstrate highly agglomerated structures in the airborne state (Methner et al. 2010; Tsai et al. 2009; Han et al. 2008). It may be possible that one aerosol generation system is equally

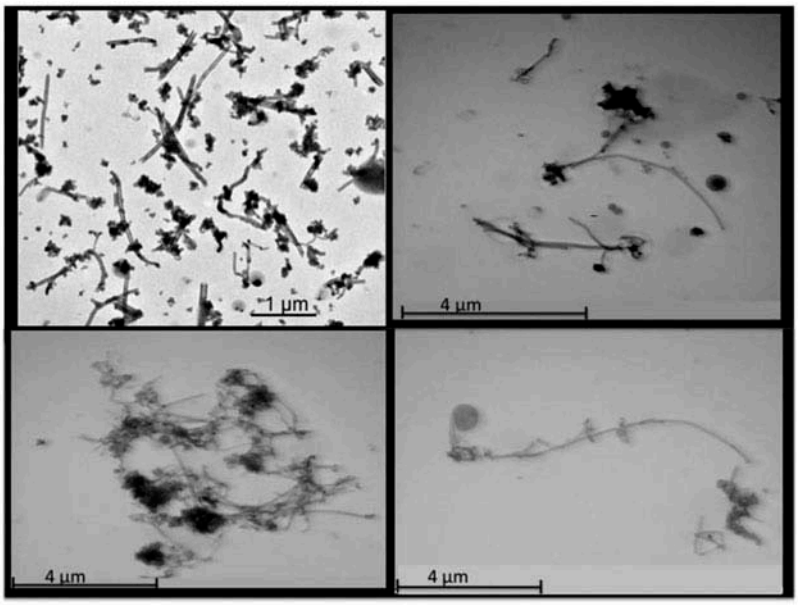

FIGURE 1a. MWCNT aerosols at a research facility.

Aerosols collected at a research facility during manufacture of MWCNT revealing a multiplicity of structures. (Han et al. 2008). Shown are samples collected in the facility after opening the furnace, demonstrating many non-fibrous structures in addition to some single fibers but mostly agglomerates of different sizes. Initially high concentrations could be significantly reduced following installation of proper enclosure and ventilation systems.

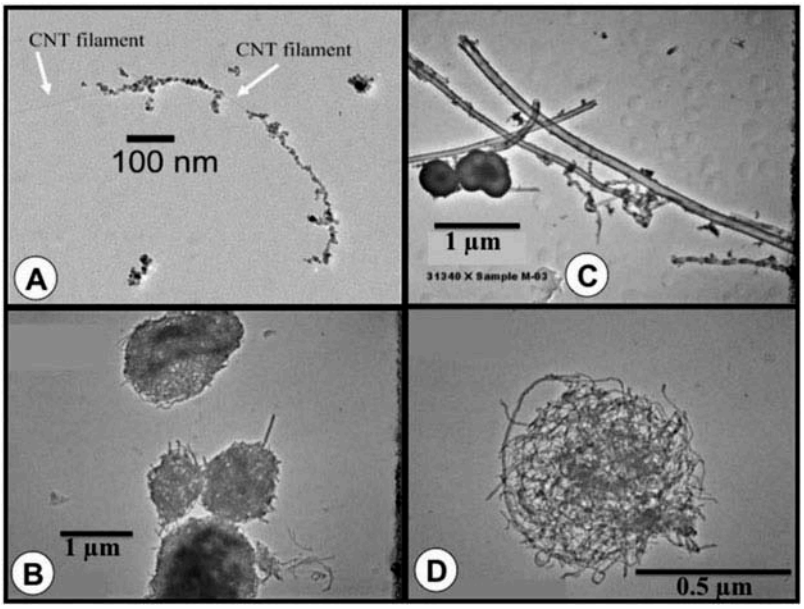

FIGURE 1b. MWCNT aerosols collected at a research facility.

Aerosols collected at a research laboratory generating MWCNT by chemical vapor deposition (A: Tsai et al. 2009***) and several commercial and research facilities manufacturing MWCNT (B, C, D:*** Methner et al. 2010). In the research facility, mostly agglomerates were seen and only some single filaments with numerous attached clusters of nanoparticles were found that consisted of carbon and included Fe from the catalyst (A). The aerosol in a commercial facility was described as "various forms like agglomerates, clusters, bundles, or nests rather than individual fibers or spherical particles" (B, C, D). These were collected under different working tasks (e.g., sawing, dumping). An example of the appearance of the few individual fibers and spherical particles is shown in (C). Total carbon concentrations measured on filters according to NIOSH NMAM Method 5040 (Issue 2, 1998) were equivalent to 1.8 mg/m^3. In general, samples from both facilities indicate that long and individual fibers were hardly seen, in contrast to clusters/tangles of different sizes. The MWCNT aerosol generated experimentally for use in animal inhalation studies seems to be much better dispersed.

well suited for appropriate (workplace representative) aerosolization of all different types of CNT and CNF, but this still needs to be verified.

Workplace Monitoring

ISO/TR12885 (ISO 2008) lists and discusses several air monitoring instruments and techniques for monitoring nano-aerosol exposure at the workplace by airborne mass, number, and size distribution, as discussed later. However, whereas for spherical particles the scanning mobility particle sizer (SMPS) and Differential Mobility Analysing System (DMAS) provide valuable information of their airborne size distribution as mobility diameter of the charged particles, measurements of CNT/CNF of complex structures with these devices are hard to interpret. However, the following methods are well suited for measuring airborne CNT/CNF size distribution.

The micro-orifice uniform deposition impactor (MOUDI) and nano-MOUDI measure aerodynamic diameter, down to 10 nm (at low pressure stages). This measure for CNT/CNF may be used as input into the predictive multiple path particle dosimetry (MPPD) model for rats and humans if data for the density of the airborne structures are available. The advantage of the nano-MOUDI is that airborne particle structures of nanosizes are determined based on their aerodynamic deposition behavior achieved with a low-pressure system. Particle morphology may then be examined (electron) microscopically on the individual stages. Further development into an electrical low pressure impactor (ELPI) was achieved by adding a corona charging unit before the inlet, so that aerodynamically separated particles can be measured by multichannel electrometers in real time based on their charge (Keskinen, Pietarinen, and Lehtimäki 1992).

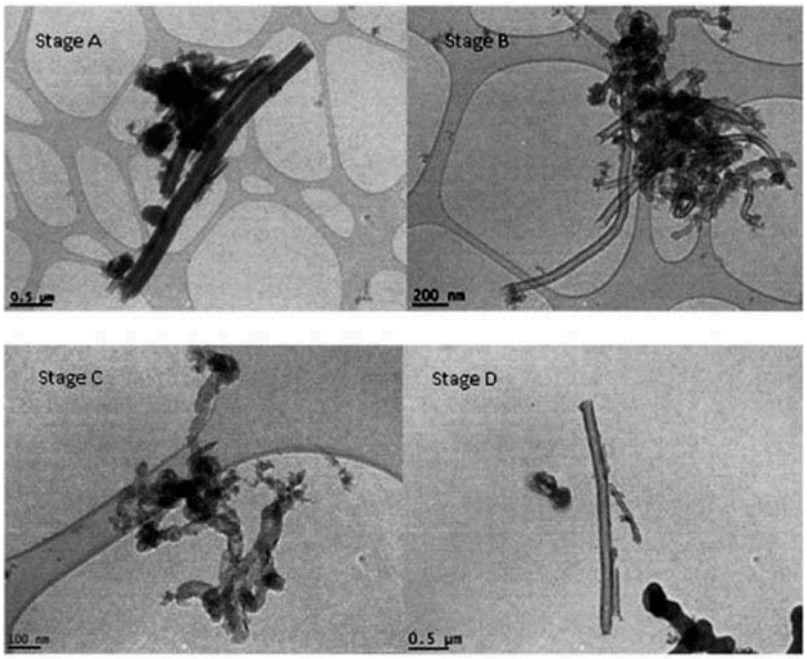

FIGURE 2. CNF aerosols collected on impactor stages during thermal treatment.

Transmission electron microscopy images of airborne CNF size selected by impactors located in a thermal treatment processing area for CNF. Impactor Stage A: 2.5–10 μm; Impactor Stage B: 1.0–2.5 μm; Impactor Stage C: 0.5–1.0 μm; Impactor Stage D: 0.25–0.5. Lacey carbon-coated Ni and SiO-coated Ni grids were used in impactors. *(From:* Birch et al. 2011).

Filter samples for gravimetric measurement ($\mu g/m^3$): Care needs to be taken to adjust filter to same humidity before and after sampling to get net weight.

TEM/SEM: With the use of electrostatic precipitator and filter samples length and diameter distribution, agglomeration state/tangles can be determined.

While the instruments just described provide accurate measurements for aerosol size distribution, caution needs to be observed when measuring CNT and CNF. A condensation nuclei counter (CNC)/condensation particle counter (CPC) may safely be used to count the number of CNT and CNF in the air because there is no size or shape effect involved in the counting process. The differential mobility analyzer (DMA) and SMPS separate submicrometer-sized particles based on their mobility in an electric field. It is conceivable that CNT and CNF of different shapes might attain the same mobility and be separated together thus obscuring size classification. The same limitation holds for the aerodynamic particle sizer (APS), which is based on the time of flight of particles. Aerodynamic drag and torque of CNT depend on the shape and orientation of CNT and CNF in the air. Different size and shape of CNT and CNF may yield similar drag and torque forces under certain flow conditions and hence be grouped together by the instrument. Separation of CNT and CNF in a MOUDI or nano-MOUDI impactor is based on their inertial forces, which is a function of their orientation in the air. Thus, a shape correction needs to be applied when using these instruments. The most reliable technique for size measurements of CNT and CNF is TEM/SEM, which provides both size and shape. However, electron microscope (EM) sizing is time-consuming, provides no real-time measurement, and the measured dimensions (i.e., CMD and geometric standard deviation [GSD]) need to be converted to equivalent diameters if CNT and CNF deposition is going to be calculated. This will be a most difficult task because the density of the aerosol particles has to be known. Given the wide range of structures/shapes of aerosolized CNT (Figures 1

and 2), it becomes apparent that it is not the density of carbon per se that is important as much as the effective density, which may be similar to the packing density. Knowledge regarding the actual density of the CNT aerosol in the workplace air may also be needed for using nano-MOUDI results (MMAD and GSD) as input values for estimating/predicting deposition in rodent and human lung with the MPPD model. While it is presently not possible to integrate a Nano-MOUDI into a personal sampler, number concentration (CNC/CPC) and mass concentration of airborne CNT might be built into such personal sampler. Asbach et al. (2012) and Meier, Clark, and Riediker (2013) tested small samplers that might quality for use as personal samplers.

Inhalable, Thoracic, and Respirable CNT and CNF Fractions

When evaluating the potential toxic and/or carcinogenic effect of CNT/CNF in inhalation studies in lab animals or by in vitro testing via aerosol exposure of primary cells or cell lines, ideally comparable or identical exposure to human scenarios are required to deliver similar doses to target sites or cells of the respiratory tract. In essence, an equivalent human exposure concentration (HEC) needs to be defined based on metrics of exposure. Calculations of a HEC account for interspecies differences in inhalability, respirability, and lung deposition of CNT/CNF. CNT/CNF inhalability, or the inhalable fraction, is defined as the fraction of airborne CNT/CNF that penetrates the extrathoracic airways on inhalation. Similarly, the thoracic fraction is defined as the fraction of airborne CNT/CNF that travels through the head airways and reach the lung. Finally, the respirable fraction is the portion of airborne particles that reaches the alveolar region of the lung. The American Conference of Governmental Industrial Hygienists (ACGIH 2010) established sampling criteria to define these three fractions in terms of induction of hazard in the three regions of the respiratory tract and respective defined airborne particle sizes.

Calculation of CNT/CNF inhalability is the first step in ensuring delivering compatible doses among exposure settings. While CNT/CNF below 10 μm aerodynamic sizes are completely inhalable in humans, only a fraction is inhalable in small animals. In addition, losses of CNT/CNF in the extrathoracic passages of each species are different, which combined with inhalability differences results in different delivered doses (thoracic and respirable fractions) of CNT/CNF to the lower respiratory tract. Therefore, CNT/CNF inhalable, thoracic, and respirable fractions need to be examined and accounted for when extrapolating results of animal inhalation studies to humans based on the delivered dose of CNT/CNF, or when using known human exposure conditions to design realistic rodent inhalation investigations.

There is a wealth of published lab data on penetration of particles into the lungs of humans and animals (Aitken et al. 1999; Asgharian, Kelly, and Tewksbury 2003; Berry and Froude 1989; Breysse and Swift 1990; Hinds, Kennedy, and Tatyan 1998; Hsu and Swift 1999; Kennedy and Hinds 2002). In addition, there are recent developments of semiempirical, predictive models of particle inhalability in humans and lab animals (Ménache, Miller, and Raabe 1995; Brown 2005; Asgharian, Kelly, and Tewksbury 2003). However, there is a major data gap on inhalability and respirability of nonspherical and irregularly shaped particles such as CNT and CNF. Because of their asymmetric geometry, the orientation of CNT/CNF affects penetration and deposition during inhalation in the lungs. Hence, inhalability and respirability models for CNT and CNF need to account for differences in size characteristics and transport properties as compared to spherical particles. A more detailed discussion of inhalable, thoracic, and respirable fractions is provided in Appendix A.

Interspecies Extrapolation

Inhalation studies are conducted in lab animals to observe various biological endpoints. Interpretations of the findings include extrapolation to human exposure scenarios

for purposes of human risk assessment. Conversely, if available, human exposure data can be extrapolated to animal exposures for the design of inhalation studies to examine biological/toxicological responses. Thus, interspecies data extrapolation based on various dose metrics of exposure is needed to either determine a no-observed-adverse-effect level (NOAEL) as input for risk assessment models, or to select realistic exposure levels for animal studies. While dosimetry of extrapolation has often been based on the inhaled dose (inhalable, thoracic, and respirable fractions), it needs to be based upon the deposited dose because the biological outcome is most closely associated with the deposited and not inhaled dose. This is particularly important for purposes of extrapolation when deposited and retained taking into account clearance doses are to be compared between humans and rodents. Figure 3 illustrates a conceptual approach of dosimetric interspecies extrapolation. More information on extrapolation modeling is provided in Appendix B.

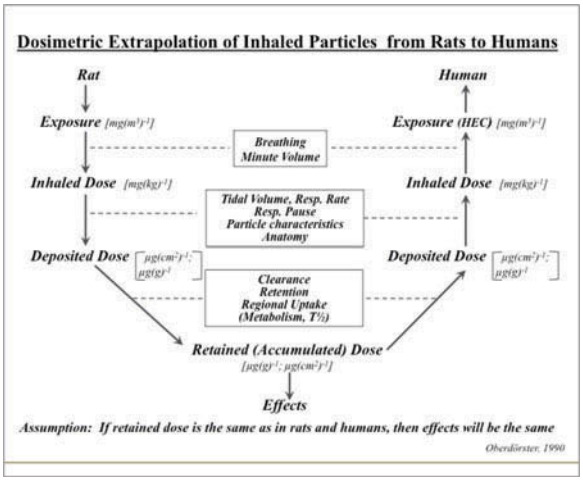

FIGURE 3. Dosimetric Extrapolation of Inhaled Particles from Rats to Humans.

Concept of dosimetric extrapolation of effects of inhaled materials in experimental animals to humans. A Human Equivalent Concentration (HEC) is derived based on study in rats (scenario 2 described in text) by using the MPPD model for rats to estimate the inhaled (delivered) and daily deposited dose in rats resulting from the specific experimental exposure concentrations. Knowing the material rat-specific clearance rates or retention halftime (T1/2) in the lung, the retained dose that has accumulated over the duration in the lung can be calculated, but may also be determined by analytical methods at the end of exposure. Using then human-specific clearance rates—if available—and breathing scenarios as inputs to the MPPD model for humans the HEC can be estimated for either the MMAD and GSD of the experimental aerosol, or for an aerosol size distribution that is known to be present for the human exposure scenario. The HEC is equivalent to the rat exposure in terms of resulting in the same deposited dose—or retained dose—in both species. Through using the MPPD model human and rat inhalability and respirability differences are taken into consideration. Deposited and retained dose can be expressed either per unit of epithelial surface in the respiratory tract—tracheobronchial or alveolar—, or per unit mass of the lung. In addition, the material based dosemetric can be mass (as indicated in the scheme), or surface area or number of CNT/CNF, if respective information is available. [*From:* (Oberdörster 1989)]

Types of Respiratory-Tract Exposures

Rats or mice might be exposed to CNT/CNF by IT instillation, (Warheit et al. 2004), pharyngeal aspiration, (Porter et al. 2010), or inhalation (Shvedova et al. 2008) (Table 1). The major advantages of IT instillation or pharyngeal aspiration are that exposure is technically simple and inexpensive, requiring little specialized instrumentation, and the lung burden is estimated simply from mass of CNT/CNF delivered to the lungs by assuming that between 80 and 90% deposits in the alveolar region (Mercer et al. 2010a). The major disadvantages of IT instillation and pharyngeal aspiration are nonuniform distribution of particles in the lung and the fact that lung burden is delivered as a bolus dose in a fraction of a second rather than gradually over time as with inhalation, that is, the dose rate is many orders of magnitude different. Both IT instillation and pharyngeal aspiration require that CNT/CNF be suspended in a biocompatible fluid. Therefore, agglomeration is an issue, with micrometer-size agglomerates being common when CNT/CNF are suspended in phosphate-buffered saline (PBS; pH 7.4). To improve dispersion of CNT/CNF, 5–10% serum, 1% Pluronic, or 1% Tween 80 has been employed. However, as shown by Dutta et al. (2007) and Haniu et al. (2011), the use of such dispersants significantly affects cellular uptake and masks potential effects of CNT. Porter et al. (2008) argued that CNT/CNF would interact with alveolar lining fluid when deposited in the respiratory region of the lung. Therefore,

they used a dispersion medium that contained 0.6 mg/ml species-specific serum albumin and 0.01 mg/ml disaturated phosphatidyl choline (DSPC) in PBS, that is, albumin and DSPC levels found in the initial aliquot of rodent BALF. This artificial diluted alveolar lining fluid was found to effectively disperse MWCNT, and data suggested that it did not appear to mask particle surface activity. However, Gasser et al. (2010) noted that precoating of MWCNT with lipids from lung surfactant altered the binding of plasma proteins on their surface. Thus, the potential impact of using dispersants when assessing nanomaterial toxicity has to be critically considered, since it affects interaction with cells and tissues. As with inhalation exposure, it is critical to qualitatively evaluate the structure size distribution by electron microscopy of CNT/CNF in suspensions delivered to the lung. The following sections focus on inhalation exposures as the physiologically most appropriate method for delivery of CNT/CNF to the respiratory tract.

Requirements for an Inhalation System

A critical component of acquiring scientific knowledge is the ability for findings from a given lab to be reproduced and extended by other labs. Therefore, simplicity, ease, and consistency of operation in maintaining a stable airborne concentration of CNT/CNF is an important goal in developing aerosol generation systems for CNT/CNF. McKinney, Chen, and Frazer (2009) reported the use of an acoustical generation system for the aerosolization of MWCNT. Automated computer control allowed generation of aerosols of stable concentrations and particle size distribution with little operator manipulation required. In contrast, Baron et al. (2008) reported a generation system for SWCNT that was capable of generating a stable output, using a knife mill generator, but required continuous adjustment by a well-trained technician. This difference in complexity of operation of generation systems reflects the fact that SWCNT agglomerate more avidly than MWCNT. In general, the greater the diameter of the CNT/CNF, the straighter and less curled the fibers, and the easier they are to disperse. Because this principle also applies to workplace exposures, it is important to produce realistic CNT/CNF aerosols with appropriate generation systems.

Inhalation exposures to CNT/CNF using a dry powder aerosolization system is the preferred method that best simulates human exposures under real-world conditions. Generating an aerosol from a liquid suspension might be problematic, as dispersants may have to be added to prevent excessive clumping. Sager et al. (2007) compared the efficiency of dispersing nanoparticles (NP) in PBS with and without BALF or in Dipalmitoylphosphatidylcholine (DPPC) as the major constituent of the alveolar lining fluid, with and without albumin. Based on their finding that DPPC + albumin in PBS was effective, although still less than BALF in PBS, for use during in vivo and in vitro studies, Gasser et al. (2012) confirmed that using a commercially available lung surfactant to coat MWCNT needs to be considered for in vitro studies. Schleh et al. (2013) agreed on the importance of simulating in vivo conditions by coating NP with pulmonary surfactant for in vitro investigations. With regard to surfactant precoating of NP to be delivered to the respiratory tract in suspension, inhalation, or instillation, it has to be considered that adsorption of proteins/lipids is likely to be different from that on pristine particles (Dutta et al. 2007; Haniu et al. 2011; Gasser et al. 2010). Thus, inhalation studies need to aim to mimic real-world conditions by generating aerosols in their original state as would be experienced by humans (Fubini, Ghiazza, and Fenoglio 2010). As discussed earlier, since NP aerosols—including CNT/CNF—are present in the workplace as agglomerates, there is no need to add dispersants when dosing the respiratory tract by inhalation.

As pointed out earlier, it is important to take into consideration inhalability and respirability of rodents versus humans when reproducing real-world human exposure conditions for experimental exposures of rodents. This may be difficult in cases where long CNT and aerodynamically larger agglomerates are present in the workplace aerosol that are respirable by humans depositing in human pulmonary

region, but are less or not respirable by rodents. Enrichment of the aerosol for such longer CNT might be considered to achieve comparable lung burdens in rodents. Conversely, depending on the CNT aerosol generation system, large rodent nonrespirable agglomerates may be present in the experimental aerosol but are not found at the workplace. These may be removed by appropriate preseparators (cyclone; impactor) to avoid exposure to high mass concentrations (large agglomerates represent most of the aerosol mass) that result in unrealistic high nasal deposits and irrelevant exposure-dose-response data. Use of grinding and milling may introduce surface artifacts and contaminants, which need to be controlled carefully. A prerequisite for establishing exposure-dose-response relationships and for dosimetric extrapolation modeling is the availability of reproducible methods to accurately (1) characterize and monitor exposure atmosphere and (2) determine deposited and retained CNT/CNF burdens in the respiratory tract and in extrapulmonary tissues/organs for necessary biokinetic information.

Analysis of Exposure-Dose-Response Relationships

Exposure-dose-response relationships established in rodent inhalation studies as a basis for deriving an HEC may be expressed with different dose metrics, either as exposure-response or as dose-response relationships. The latter is either based on deposited dose or, preferably, on the retained dose in longer term inhalation studies (Figure 3). Comparing these relationships between several materials using different dose metrics may provide information about the relative hazard ranking of these materials. Figure 4 compares exposure-response and dose-response data of subchronic rat inhalation studies with MWCNT (Pauluhn 2010; Ma-Hock et al. 2009a; Kasai et al. 2015), carbon black (CB) (Elder et al. 2005), and CNF (DeLorme et al. 2012). The subchronic CB study was added as a comparison to a well-studied carbon nanomaterial, which is generally viewed as a poorly soluble particle (PSP) of low cytotoxicity that has been used in a number of rodent inhalation studies related to the lung particle overload phenomenon (Morrow 1988). In order to compare the responses to these different materials, the same effect endpoints were selected. Increased lung weight was a common endpoint in all five studies for which exposure-response relationships can be established.

Another sensitive quantitative endpoint, pulmonary inflammation as determined by the increase of polymorphonuclear leukocytes (PMN), was also used to compare exposure-response relationships, although for only four of the subchronic inhalation studies; this endpoint was not included in the MWCNT study by Ma-Hock et al. (2009a). Of greater relevance, however, is a comparison of dose-response relationships, given that deposited and retained doses differ significantly between different investigations, because they depend on the size distributions of the inhaled aerosol. Two of the subchronic rat inhalation studies, Ma-Hock et al. (2009a) and DeLorme et al. (2012), did not determine retained lung burden, so approximate lung burdens have to be estimated based on aerosol sizes as input to the MPPD deposition model (Figure 4b).

Figure 4a shows that exposure-response correlations for the three MWCNT based on increase in lung weight are steeper than those for CB and CNF. Selection of another sensitive endpoint of particle-induced pulmonary inflammation, that is, increase of neutrophils in lung lavage after 3 mo of exposure, demonstrates the steepest dose-response for the two MWCNT, less for CB, and least for CNF. Results of only two MWCNT studies might be included in this plot because no lung lavage data are available from Ma-Hock et al. (2009a).

However, as stated earlier, due to differences in deposition and retention in the lung for different inhaled particulate compounds, the actual retained lung burden rather than inhaled airborne concentration is the preferred metric. Further, expressing the retained lung burden by different metrics of mass, surface area, or volume of the retained particles may provide some mechanistic insight. Figure 4b shows these relationships for the endpoint lung weight for all studies. As explained earlier,

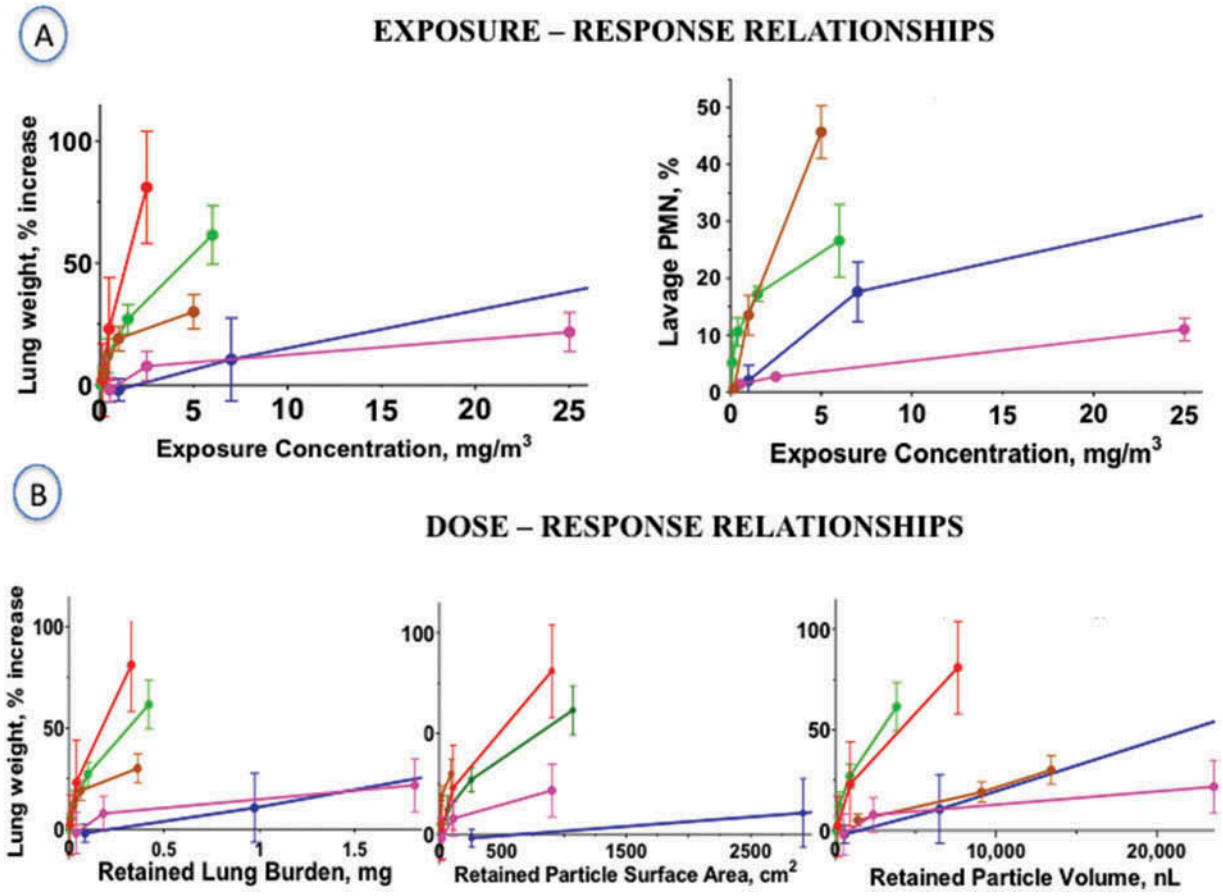

FIGURE 4. Exposure-Response and Dose-Response.

Exposure-Response and Dose-Response relationships of five 3-month inhalation studies in rats with MWCNT, CNF and CB. The carbon black (CB) study is added as a well studied low toxicity particle for comparison.

Percent increase in lung lavage neutrophils (PMN) and retained lung dose were not reported for all of the five subchronic rat inhalation studies. Thus, to approximate retained lung burden of the MWCNT study by Ma-Hock et al. and for the CNF study by DeLorme et al., deposited and retained doses were calculated with the MPPD model, Version 2.90.3, using MMAD and GSD data and the packing density of the materials provided by the authors and a normal rat-specific pulmonary retention halftime (T1/2) of 70 days as model inputs. This T1/2 is appropriate for the rats exposed to the lower concentrations; for the high concentrations and resulting high lung burdens, a prolongation of T1/2 has to be expected (for example, as determined by Pauluhn et al., 2010, Table 3). Therefore, the lung burdens calculated for the high dose groups of these two studies are likely underestimated. The x-axes have been truncated to better separate the individual MWCNT/CNF data, although as a consequence the high exposure/date points could not be displayed.

A: Lung weight and lung lavage neutrophil exposure-responses. B: Lung weight dose-responses based on retained lung burden expressed as mass, surface area and volume of the retained material.

● - MWCNT (Pauluhn, 2010); ● - MWCNT (Ma-Hock et al., 2009a); ● - CNF (DeLorme et al., 2012); ● - CB (Elder et al., 2005); ● - MWCNT (Kasai et al., 2015).

the retained lung burden data for Ma-Hock et al. (2009a) and DeLorme et al. (2012) were estimated. As shown in Figure 4, the metric retained particle surface area revealed that the dose-response curves for the three MWCNT and the CNF nanomaterials are considerably steeper compared to CB. In contrast, when retained doses are expressed as retained mass or retained volume (volume based on bulk, or packing densities), CNF and Mitsui-7 MWCNT were not markedly different from CB.

The example of these studies (Figure 4) indicates the importance of including measurement of lung burden as endpoint in inhalation studies. While exposure-response relationships provide valuable information about the response slope, it is only possible through the knowledge of the actual retained lung burden at different

times during and after exposure to correlate directly a real dose with a measured response and to obtain information about retention and clearance kinetics. At a minimum, four animals per time point need to be scheduled for dosimetric analysis.

Multidose subchronic or chronic inhalation studies are designed to identify a no-observed-adverse-effect level (NOAEL) or a lowest-observed-adverse-effect level (LOAEL). Because of the costs associated with a 2-yr chronic rat inhalation study, subchronic multidose 90-d studies are preferred (Bernstein et al. 2005). Shortening the exposure duration to 4 wk or even 5 d (Pauluhn 2009; Ma-Hock et al. 2009b) still needs to be validated as to the reliability of obtaining sufficient information regarding chronic toxicity in the primary organ of entry as well as secondary remote organs. Mechanisms both of toxicity and of adaptive responses may not have fully developed at shorter exposure durations, such that—until further validation data become available—the present standard of a 90-d assay is thus preferred. In any case, it is mandatory to add a sufficiently long postexposure observation period such that persistence/resolution as well as retention/clearance kinetics in the primary and in secondary organs can be determined (Pauluhn 2009). Ideally, the observation period needs to approximate at least the normal pulmonary retention halftime (T1/2) of low-toxicity poorly soluble particles (PSP), which in the rat is about 60–80 d. This—in conjunction with toxicity endpoints—enables one to identify a potential hazard vis-à-vis other PSP.

Expressing retained lung burden of CNT/CNF with different metrics of mass or surface area or volume (Figure 4b) facilitates a comparison to a PSP such as CB based on the magnitude of an effect per unit of the dose (Rushton et al. 2010). Using the retained particle volume as metric for dose is based on Morrow's hypothesis (1988) that the clearance function of alveolar macrophages becomes significantly impaired when the volume of phagocytized particles of a poorly soluble particle of low cytotoxicity exceeds 6% of the alveolar macrophage volume. With respect to MWCNT, Pauluhn (2009; 2010) suggested that the volume of the CNT/CNF tangles (assemblages) might be used to calculate the volumetric loading of the macrophages. Thus, not the material density of carbon but the much lower effective density of the assemblages needs to be considered. On the other hand, it was suggested that the particle surface area is the appropriate metric because it correlates better than particle volume with an effect on macrophage clearance function and with alveolar inflammatory response in studies involving nanomaterials (Oberdörster, Ferin, and Lehnert 1994a; 1994b; Tran et al. 2000a). Applying the volumetric macrophage overload hypothesis assumes that nanomaterials in general act like PSP particles, whereas the particle surface area concept is based on the understanding that the reactivity (e.g., inflammatory potential) per unit of the material surface area is material dependent and used as an indicator for toxicity ranking (Rushton et al. 2010). As demonstrated in Figure 4b, retained nanomaterial surface area in the five 3-mo inhalation studies supports the surface area concept of particle dose metric.

Of interest in the context of applying dose metrics to evaluate the toxicity of fiber-shaped materials is a study by Timbrell et al. (1988) with asbestos: The exposure metric to characterize asbestos exposure is generally expressed as number of WHO-fibers per cubic centimeter, yet when Timbrell et al. (1988) correlated the severity of fibrosis in asbestos miners with the amount of asbestos fibers retained per unit weight of lung tissue, it turned out that surface area, but not number or mass, was the best dose metric (Figure 5). Surface area-associated reactivity of nano-sized particles was suggested as metric (Dick et al. 2003; Hsieh et al. 2012; Borm et al. 2006; Donaldson, Beswick, and Gilmour 1996). It needs to be realized, though, that surface area—generally measured by gas adsorption (BET)—needs to be viewed as a surrogate for a biologically active or available surface that is yet to be defined. As an example, the reactive oxygen species (ROS)-inducing capacity per unit surface area of a particle may be considered (Rushton et al. 2010).

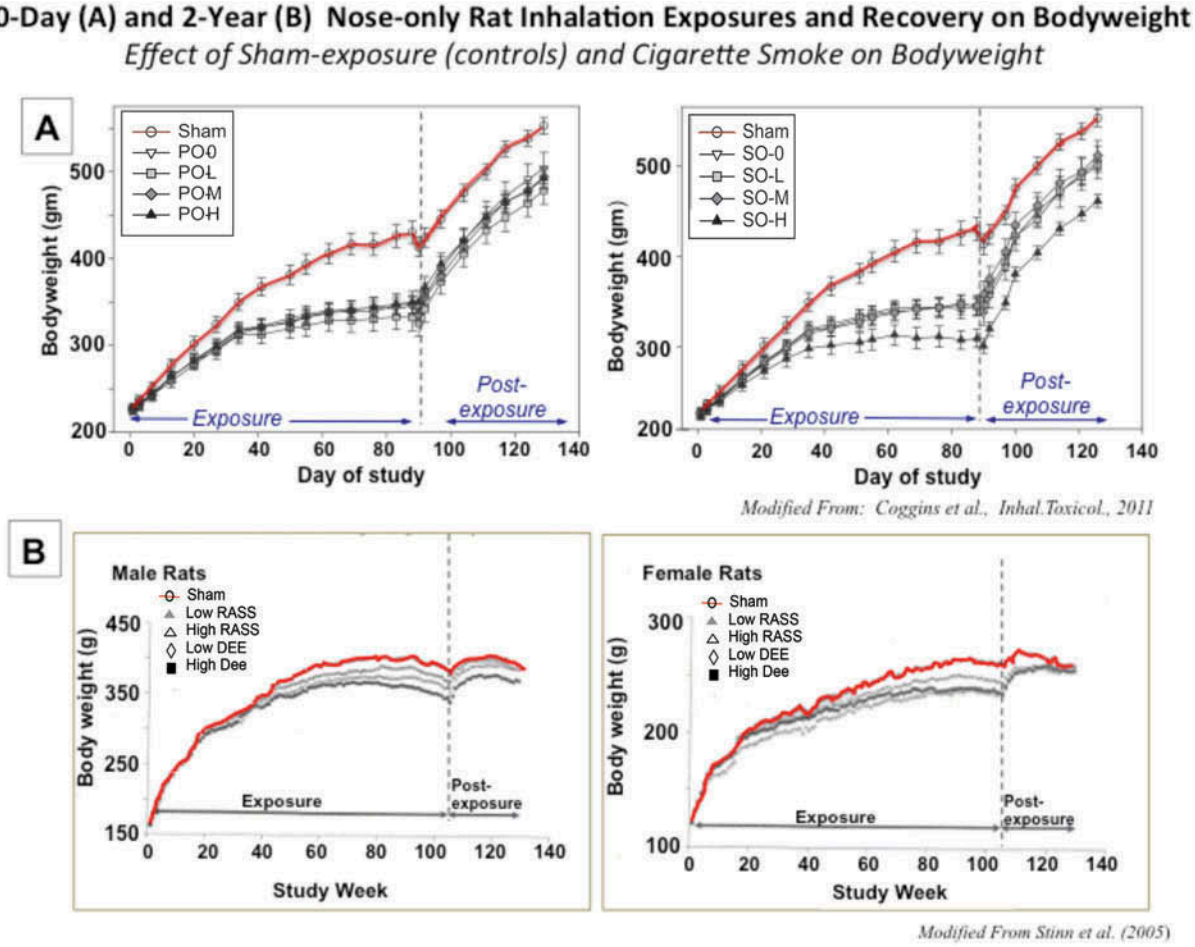

FIGURE 5. MWCNT aerosol size distribution in rodent inhalation study.

A: Subchronic inhalation of different types of cigarettes and air-exposed controls in nose-only tubes.
B: Chronic inhalation of different types of cigarette smoke and diesel engine exhaust and air-exposed controls in nose-only tubes.
Note: Effect of restraint stress on bodyweight in sham (clean air) exposed controls, highlighted in red.

Safety of Lab Personnel

Recommendations for engineering controls to protect lab staff working with nanomaterials have been provided by NIOSH (2012). The types of engineering controls recommended (local exhaust ventilation, chemical hoods, and glove boxes) depend on the state of the nanomaterial (free or bound in a matrix; dry or in a liquid) and the energetics of the lab process or activity. Personal protective equipment (PPE), including gloves, respirators, and protective clothing, is discussed in the NIOSH (2012) publication. It is also of interest to consider NIOSH (2013), which is more specific to CNT and CNF.

STRATEGY/CONCEPTS OF INHALATION TESTING FOR CNT/CNF TOXICITY

Objective

The goal is to assess pulmonary and systemic (secondary target organs) responses to inhaled CNT/CNF in acute and repeat (subchronic; chronic) rodent inhalation studies mimicking relevant exposure conditions of humans. The primary target is the respiratory tract, while secondary targets are extrapulmonary organs that are known or suspected to be affected by nanomaterial translocation from the primary portal-of-entry, including pleura (still part of pulmonary),

cardiovascular, liver, spleen bone marrow, kidneys, central nervous system (CNS), fetus, other (reproductive organs).

In order to identify secondary target sites, biokinetic studies are essential, including retention, clearance, or accumulation of CNT in primary or secondary organs. For this, an appropriately sensitive label is needed to determine the disposition of inhaled material throughout the body, including elimination pathways. Caution needs to be exercised, since any label may alter the physicochemical properties and likely affect biodistribution. In addition, it is important that any label be stable and not dissociate/leach. For carbon-based aerosols, turbidity measurement of retained material in organs/tissue was used and found to yield reproducible results (Elder et al. 2005). However, sensitivity to low concentrations may be problematic, and NIOSH Method 5040 (NIOSH 2013) may be an appropriate alternative. Mercer et al. (2008) attached 10-nm gold NP or fluorescent quantum dots to SWCNT to determine their biodistribution following aspiration in mice. However, such labeling is not feasible for large amounts needed for inhalation exposures. Another method is slow thermal degradation and measurement of CO_2 (Hyung et al. 2007; Peterson and Richards 1999; NIOSH Method 5040 with modifications given in CIB 65 [NIOSH 2013]; Watson, Chow, and Chen 2005). A modified thermal degradation method with increased sensitivity was presented specifically for analyzing CNT/CNF in biological samples. The key is a thorough two-step digestion of tissue to completely eliminate low levels of interfering tissue carbon, yet avoiding harsh treatment to keep CNT/CNF intact (Westerhoff, Doudrick, and Herckes 2012; Doudrick et al. 2013). A promising sensitive method is the use of a hybrid marker (Ohnishi et al. 2013). Suggestions to use specific metallic impurities embedded in the CNT to quantify their retention may be inaccurate due to possible leaching of such metals from CNT in vivo and interference from background levels in tissue. Ideally, ^{14}C-labeled CNT may be used, but pose additional problems related to radio-safety issues, particularly when used as aerosol.

When simulating human exposure conditions for designing appropriate CNT/CNF exposures, available human exposure data need to be adapted with regard to differences in respirability and inhalability between humans and rodents. Three concentrations, logarithmically spaced, are recommended, including expected/predicted human exposure levels. It is essential for performing risk assessment that at least one dose (maximum tolerated dose, MTD) gives a significant response. If human exposure data are not available, a worst-case scenario may be assumed by using a rat (rodent) respirable aerosol at several mg/m^3 as highest concentration. A short-term (approximate 2–4 wk) pilot study is recommended as a range finder in order to estimate a maximal functionally tolerated dose (MFTD) and NOAEL for the longer-term study, and also to verify proper operation of the exposure system and obtain biokinetic data for identification of secondary organs and retained doses in these organs.

Methodology: Inhalation of CNT

Aerosolization of CNT/CNF from a dry powder is preferred, rather than from a liquid suspension, in order to simulate conditions of human exposure to pristine CNT/CNF. Aerosolizing hydrophobic CNT/CNF as an aqueous suspension requires the use of a dispersant, which would alter the surface of CNT/CNF and thereby potentially affect responses and biodistribution (Pauluhn and Rosenbruch 2015). This is particularly important if the goal is to test a specific CNT/CNF under the same conditions to which humans are exposed. A detailed physicochemical characterization of bulk and aerosolized material is desirable. Concerning the bulk CNT/CNF test material, Table 2 provides some guidance.

The CNT/CNF aerosol generated and delivered to the inhalation system requires special attention. A qualitative estimation of structure and size distribution may be determined by electron microscopic evaluation of filter samples taken from the inhalation chamber using

47-mm polycarbonate filters at a sampling rate of 1 L/min. The filters are then analyzed by TEM or SEM to determine the range of CNT/CNF structures and agglomeration in the breathing zone of the exposed animals. Sampling artifacts on the filter have to be considered. CNT/CNF diameter and length may be quantified manually under electron microscopy, although it may be difficult depending on the degree of entanglement and presence of curved structures. Thus, it is currently not feasible to develop a number limit for CNT/CNF due to the absence of counting rules, similar to those for asbestos. Since CNT/CNF aerosols are a mixture of agglomerated structures containing various numbers of individual CNT/CNF, the issue is which structures are bioactive and need to be counted, and which are too agglomerated and are less bioactive and need not be counted. Are singlets more bioactive than large agglomerate? Do small agglomerates dissociate in the lung to single tubes? Is there an agglomerate size limit that is too large to dissociate? Until these questions are answered, development of meaningful counting rules for CNT/CNF is not possible.

Particle size distribution may be quantified using a micro-orifice uniform deposit impactor (MOUDI) and a nano-MOUDI, thus obtaining a mass median aerodynamic diameter (MMAD) and geometric standard deviation (GSD). However, as described earlier, appropriate correction factors need to be applied to account for the shape and orientation effects of CNT/CNF in the airborne state. The particle count mode diameter might be determined by visual inspection of filters from the various stages of the MOUDI and nano-MOUDI under a SEM, and if particles on all stages are counted then the count median diameter derived. However, this is a rather tedious process. Particle bounce from one stage to the next might be minimized by greasing alternate stages of the impactor. The airborne concentration of CNT/CNF generated within the exposure chamber may be assessed by gravimetric analysis of filter samples.

Impaction diameter for CNT/CNF can be established by correlating measured dimensions of CNT/CNF from filter samples to measurements at different stages of the impactor. Similar measurements in a diffusion battery and an elutriator are conducted to obtain equivalent diameters for diffusion and sedimentation. Alternatively, performing CNT/CNF aerosol size distribution with a nano-MOUDI and counting individual structures on each stage by TEM/SEM might be used to plot a count distribution and determine from this plot a count median aerodynamic diameter (CMAD) and GSD. Scanning mobility particle sizers (SMPS) or differential mobility analyzers (DMA) provide count median diameters (CMD) based on the electrical mobility properties of the electrically charged CNT/CNF. However, it is difficult to interpret the results, which are based on the electrical mobility of equivalently charged spherical particles. For purposes of using airborne size distribution to predict deposition in the rodent and human respiratory tract (see MPPD model) the MMAD and GSD obtained with the nano-MOUDI seem to be best suited for inertial losses, which occur in the respiratory tract.

ISO Standard 10808 (ISO 2010a) describes requirements and procedures for monitoring/characterizing aerosolized NP during inhalation exposures. Number-based particle size distribution and mass concentration measurements are described. Four prerequisites for proper measurement of airborne particle number based size distribution should be fulfilled:

> (1) The method used shall be able to monitor particle size distribution in a continuous manner during particle exposures with time resolution appropriate to checking the stability of particle size distribution and concentration. (2) The measurable range of particle sizes and concentrations in the animal's breathing zone shall cover those of the nanoparticle aerosols exposed to the test system during the toxicity test. (3) Particle size and concentration measurements in the animal's breathing zone should be accurate for nanoparticle toxicity testing, and can be validated by means such as calibration against appropriate reference standards (see ISO/IEC 17025: ISO 2005b). (4) The resolution of particle sizing shall be accurate and the range of particle sizes measured shall be sufficiently broad to permit conversion from number-based distribution

> to surface area-based or volume-based distribution. (OECD 2012)

These requirements in ISO 10808 are followed by a note that DMAS is the only currently available method that meets all the above requirements in the size range below 100 nm (see ISO 15900: ISO 2009). However, ISO 10808 also cautions with an important comment that "Estimation of particle size from DMAS measurements can result in significant error for non-spherical particles. Application of DMAS for non-spherical particles is not recommended."

With regard to measurement of airborne mass concentration, ISO 10808 stipulates that the method selected shall be accurate and sensitive, and defined by the limit of quantification. Suggested methods include hte beta attenuation monitor (BAM), tapered oscillating balance (TEOM), piezoelectric microbalance, filter gravimetric, and other methods based on chemical analysis of particles collected on filter media that meet requirements according to ISO/TR 27628 (ISO 2007). A note is added stating that "Mass concentration can be derived from number-based size distribution measurement data by making an assumption regarding particle density, particularly for spherical particles which may match bulk material density (Ku and LaMora, 2009). However, significant errors in calculated mass concentration may result if particle density is inaccurate or unknown. Derived mass concentration from number-based size distribution data should be accepted only when no other accepted methods meet the measuring requirements." In addition, an important caveat also states that "Mass concentration estimation by DMAs (Differential Mobility Analyzer) based on particle size can produce error for non-spherical particles." In case of highly agglomerated structures the effective density will be different from material density, as mentioned earlier.

Thus, an appropriate approach for characterization of CNT/CNF aerosols is the use of a nano-MOUDI for determining aerodynamic size distribution and a filter-based method (gravimetric, chemical) for exposure mass concentration. This would allow derivation of a mass-based exposure limit. Monitoring in real time the consistency of the aerosol concentration throughout the exposure is necessary and can be accomplished by a condensation particle counter (CPC), SMPS, or optical particle counter (e.g., Data-RAM). Although measurements would be best done in the animals' breathing zone, the possibility of confounders from animal dander and/or bedding-generated dust needs to be considered, so the point of measurement may be selected at the entrance of the CNT/CNF aerosol into the inhalation chamber.

Types of Inhalation

Inhalation is considered the gold standard for dosing the respiratory tract. The major advantage of inhalation exposure is that it mimics human pulmonary exposure by distributing the inhaled material throughout the whole respiratory tract in a physiological way over time. It also provides a more even distribution of particles in the lung than bolus exposures to particles in suspension. Lastly, agglomeration is less of a problem with airborne CNT/CNF than when CNT/CNF are delivered as a suspension in biocompatible fluid; therefore, CNT structures and size distribution need to more closely mimic that found in workplace aerosols. Available measurements from workplaces show large diversity ranging from a few single CNT/CNF structures to mostly agglomerates/tangles, depending on the material (Maynard et al. 2009; Han et al. 2008; Tsai et al. 2009; Birch et al. 2011). The major disadvantages of inhalation exposure are that it requires specialized and costly instrumentation and technical expertise that are not universally available in research institutions. Inhalation also requires greater quantities of the test material than bolus exposure.

There are two types of inhalation exposure systems, nose-only and whole-body. Clearly, both modes of inhalation are superior to bolus-type exposures, as discussed earlier (Table 1). OECD Guidelines seem to favor nose-only exposure, but leave the choice of the mode of exposure to the investigators, as stated in

OECD GD 39 (OECD 2009b): "While nose-only is the preferred mode of exposure, special objectives of the study may give preference to the whole-body mode of exposure." The guidelines also state: "When an animal is confined to a restraining tube the observation of its behavior and physical condition is somewhat restricted."

Several studies have addressed pros and cons of either mode of exposure. Phalen (2009) summarized specific advantages for whole-body exposures, such as minimal restraint, controllable environment, and better suitability for chronic studies, and for nose-only exposures, less unintentional exposures of extra-respiratory-tract organs (skin, eyes) and lower amounts of material to be aerosolized. In terms of disadvantages, Phalen (2009) pointed out the unavoidable additional routes of exposures (skin, eyes, oral), the inefficient use of material and higher costs for whole-body exposures versus discomforts due to heat buildup, restraint stress, and the need for extra handling (more labor intensive) associated with nose-only exposures. However, Phalen (2009) also suggested that well-designed nose-only systems permit low stress exposure. For example, acclimatization of rodents prior to nose-only exposure reduces stress; however, as determined by Narciso et al. (2003), full adaptation to restraint requires 14 d of fixed-duration daily restraint. In contrast, the usual length of the period of adaptation to nose-only tube exposure is 5 d. Mauderly (1986) reported altered respiration and minute volume in rats restrained in nose-only tubes without adaptation.

In contrast to significant stress induced by nose-only tube exposure, the nonstressed animals exposed in compartmentalized whole-body chambers tend to sleep and may cover their noses when curling up and thus reduce aerosol inhalation. This should result in lower retained lung burdens. Yeh et al. (1990) compared deposited lung burdens in male and female rats (8 groups total at 5 rats/group) either nose-only or whole-body exposed to the same TiO_2 and brass aerosols for 4 h. The retained lung burdens at 1 h postexposure were consistently higher in all 4 whole-body exposed groups (5 rats each of males and females) compared to the 4 nose-only groups. Although this was significantly different only for the brass-aerosol-exposed rats, results of this study do not substantiate concern that whole-body exposures reduce aerosol intake. The differences in lung burden in the Yeh et al. study (1990) may be due to differences in the breathing patterns observed between nose–only and whole-body exposed rats: Miller et al. (2014), after thorough review of the literature, reported a 38% higher breathing rate in rats restrained in nose only tubes compared to whole-body breathing. This well-demonstrated difference in breathing frequency – most likely due to the higher stress level – between whole-body and nose-only exposures and associated effects on minute ventilation and tidal volume will predictably affect deposition efficiency and deposition sites of inhaled particles in the respiratory tract.

In the context of the efficiency of aerosols depositing in the respiratory tract, an interesting question to consider relates to the relevancy of typically used daytime exposures in nocturnal animals. Indeed, a comparison of lung burdens between daytime- and nighttime-exposed rats for 11.2 h (Hesseltine et al. 1985) revealed an approximately 30% higher retained lung dose in the nighttime-exposed rats, which was attributed to increased respiration accompanying nocturnal activity. Such exposure would be comparable to human daytime exposure. However, exposing rodents during nighttime by either mode of inhalation creates additional problems in terms of limiting food intake (nose-only system) and aerosol contamination of feed (whole body system), and it also adds more work.

In a study evaluating 6-h daily nose-only and whole-body inhalation in pregnant mice to air or water aerosols from gestation day 6 through 15, Tyl et al. (1994) found—compared to whole-body air exposure as control—in both nose-only groups increased maternal toxicity, reduced body weights, and reduced maternal gestational weight gain. In the air nose-only exposed groups 13.3% of the pregnant females died. No significant differences in fetal malformations were found, and evidence indicated that restraint did not markedly affect normal embryo/fetal morphologic development but produced indications

of maternal toxicity. Thomson et al. (2009) interpreted their own findings of enrichment of immune response, apoptosis, and signaling terms in nose-only air-exposed mice as being consistent with effects due to restraint stress.

An undesirable effect due to restraint stress in rats during subchronic nose-only exposures is apparent from published body growth curves shown in studies by Coggins et al. (1993; 2011) and Stinn et al. (2005). These investigations demonstrated convincingly a retardation of body weight gain, even in air-exposed controls, as evidenced by a rise in body weight in the postexposure phase immediately following the termination of subchronic or chronic tube exposures (Figure 6). Rothenberg et al. (2000) found that even short daily nose-only tube exposures of rats to air for 42 d resulted in a 24% lower body weight, although no adverse effects on testes or reproductive performance was found. Pauluhn and Mohr (1999) confirmed this effect of nose-only exposure on body weight reduction in a 4-wk study in rats. Restraint stress-related effects from nose-only exposure in mice were reported by Van Eijl et al. (2006) to include reduced body weight gain and increased adrenal weights in a 3-mo exposure compared to unrestrained littermates. A pronounced hypothermia was prevented in this study by heating the metallic nosepiece to 38°C, which, however, did not reduce stress experienced by animals. Other studies also demonstrated that restraint or immobilization leads to a significant stress response involving activation of the hypothalamic–pituitary–adrenal (HPA) and neuroendocrine axes (Fawcett et al. 1994; Pare and Glavin 1986; Udelsman et al. 1993; Sistonen et al. 1992).

Restraint stress is a main concern for repeat nose-only exposures of rats. Stress-reducing tube designs, which permit easy draining of urine and feces and facilitate dissipation of heat by placing the rat's tail outside the restraint tube, need to be mandatory (Bernstein and Drew 1980). The rat's tail is a crucial site for heat exchange; it lacks fur and is well vascularized with numerous arterio-venous anastomoses facilitating an increase of blood flow during heat stress to dissipate heat via its high surface area to volume ratio (Gordon 1993). Surrounding room air might be sufficient to aid cooling of rats. Rothenberg et al. (2000) suggested room air temperature of 64–70°F to reduce thermal stress during nose-only exposures.

In addition, a multitube arrangement for exposures of many animals in several layers needs to be designed as a flow past nose-only system such that each port has its own aerosol delivery line and separate exhaust for the exhaled air (Baumgartner et al. 1980; Cannon, Blanton, and McDonald 1983). This avoids rebreathing the exhalation of other animals, which is also a concern for vertical flow whole-body chambers consisting of several layers. As suggested by Moss, James, and Asgharian (2006) based on model calculations, the airflow directed to the animal's nose through the delivery line of Cannon-type flow past nose-only tubes should be 2.5- to 4-fold higher than the minute ventilation of the animal to minimize rebreathing exhaled air. Pauluhn and Thiel (2007) confirmed this suggestion by actually measuring that under these conditions there was no increase of CO_2 at the inhalation port of a flow-past nose-only system, verifying that no rebreathing does occur. Given that the additional stress from restraint may be a significant modifying factor of aerosol-induced effects in a nose-only exposure study, the choice of either mode of exposure needs to be carefully weighed against concerns that with whole-body inhalation, exposure of fur/skin and subsequent ingestion of material through preening is greater. However, with respect to oral uptake of CNT, Matsumoto et al. (2012) found that daily gavage of rats to single and MWCNT for 28 d did not produce death or toxicological effects, even at highest daily doses (12.5 mg/kg BW, SWCNT; and 50 mg/kg BW, MWCNT). Thus, lower ingestion of CNT from repeat whole-body exposures is not a concern. In contrast to the many publications describing significant stress from nose-only exposures, OECD (2009b) appears to minimize the significance of restraint tube-induced stress when depicting it as "nose-only mode of exposure-specific mild immobilization stress."

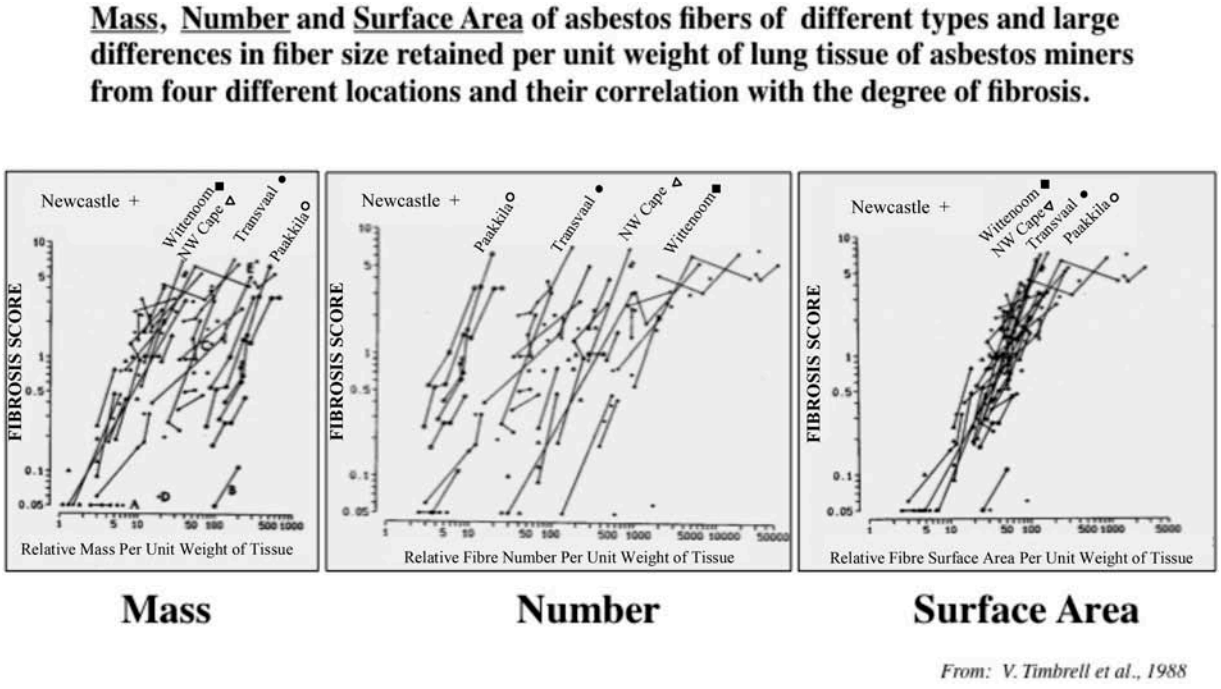

FIGURE 6. MWCNT aerosols collected in rodent inhalation study.

Aerosolized MWCNT collected on filter (A, B) and carbon-coated 200 mesh N: grids (C, D). The MWCNT were aerosolized using an acoustic aerosol generation system (McKinney, Chen, and Frazer 2009) for dry powder generation. Large variations of the airborne structures were observed, ranging from a few single tubes to differently-sized structures of agglomerated CNT to larger tangles resulting in an airborne size distribution as shown in **Figure 5**. The aerodynamic, settling and diffusional behavior cannot be inferred from these pictures; the large tangle in section D may not be inhalable by rodents and is likely not respirable, but can be estimated from their aerodynamic size distribution. Such experimentally generated MWCNT aerosol for rodent exposures needs to be compared to atmospheres found at workplaces. *(See **Figures 1**, **2**).*

Provided that enough material is available for repeat long-term exposures, the low-stress whole-body system is preferable. However, specific circumstances, including low amounts of material to be aerosolized or better respirability of dispersed long and straight asbestos fibers lining up in the narrow flow past delivery line (D. Bernstein personal communication 2015), might justify the use of nose-only systems.

As an alternative to whole-body or nose-only exposure, an IT inhalation system for rats was used to deliver hazardous or radioactive aerosols that prevents any contamination of the skin/fur of the animals (Oberdörster, Cox, and Gelein 1997; Kreyling et al. 2009). Less material is also consumed with this method, and eight or more rats may be exposed simultaneously for several hours, mimicking different breathing scenarios. However, animals are anesthetized and repeat exposures may only be done in weekly intervals, rather than on a daily basis, to minimize stress. Less stressful whole-body exposures need to use compartmentalized systems with individual units for each animal. The aerosol flow needs to be evenly distributed to all units, and daily/weekly rotation of the animals is required if locations are downstream or upstream relative to each other.

Aerosol Generators

Different types of generation systems for CNT/CNF have been used, involving liquid suspension or dry powder generators. As stated earlier, dry powder systems are preferred because they simulate more closely actual human exposures (unless there are situations of real-world exposures to CNT/CNF contained in liquid aerosols). Important for delivery of the generated aerosols to the animal exposure units

is their neutralization via a radioactive source (Phalen 2009).

Generators for droplet (liquid) and dry dust (powder) aerosols were reported (Phalen 2009; Wong 2007). The former include diverse jet and ultrasonic nebulizers, for solutes but also for poorly or insoluble particles suspended in water or physiological fluids (saline, PBS); the latter include various designs ranging from fluidized bed to scrape or brush-type and venturi-type feeder systems as described by Wong (2007) and Phalen (2009). Specific for metallic NP generation, high-voltage electric sparking between two opposing metal electrodes in argon gas, induction of vapor and recondensation or metal evaporation, and subsequent condensation in a high temperature tube furnace has been used (Elder et al. 2006; ISO/FDIS10801: ISO 2010b). The electric spark method was also applied to generate carbon NP for use in inhalation studies in humans and rodents (Frampton et al. 2006; Oberdörster et al. 2004). However, while all of the listed methods can be used to aerosolize spherical NP—albeit with some limitations—CNT/CNF aerosols are best generated by dry powder methods that are not destructive yet deliver well-dispersed CNT/CNF that closely reproduce known or expected human exposures. Currently, there are no generally accepted methods or guidelines specific for inhalation of nano-sized particles. In the past 5 yr, extensive efforts have been applied to develop systems to generate an aerosol of CNT/CNF for animal inhalation studies. Such generation systems include knife mill, acoustical energy, rotating brush, fluidized bed, jet nebulizer, and electrospray aerosolization systems.

Dry Powder Systems

Baron et al. (2008) described a system to generate SWCNT. This system fed acoustically fluidized SWCNT through a knife mill to break up agglomerates. The output of the knife mill was fed through a settling chamber where SWCNT were electrically discharged. At this point, the cutoff aerodynamic diameter was approximately 14 μm. The aerosol was then passed through a cyclone with a 50% cutoff at 4 μm and a second cyclone with a cutoff at 2 μm. The generator system produced a SWCNT aerosol of 5.52 ± 0.25 mg/m^3 over an 8-h period for 4 d. The output efficiency of the generator was 10–12%. Mass median aerodynamic diameter was 4 μm with a count mode aerodynamic diameter of approximately 240 nm (Shvedova et al. 2008). By adjusting the feed rate, this generation system might produce outputs as high as 25 mg/m^3. Although this system produced target concentrations of a dispersed aerosol of SWCNT, it required constant monitoring and periodic adjustment by a well-trained technician to maintain a stable output and size distribution. Since this system employed a knife mill, there is concern that SWCNT may be damaged or shortened during generation. Great caution needs to be exercised because micronization, depending on the method, may significantly increase CNT reactivity, as reported by Ma-Hock et al. (2009a) when ball-milling MWCNT.

McKinney, Chen, and Frazer (2009) described a system that produced an aerosol of MWCNT using an acoustical generation system. Bulk MWCNT (5 g) were placed in a large cylindrical acrylic chamber (18 inches high and 14 inches diameter) enclosed at both ends with flexible latex diaphragms (0.02 inches thick) held tightly in place with rubber O-rings. The cylinder was lined with conductive foil tape, which was grounded to prevent static charge buildup. A 15-inch loudspeaker was placed below the bottom diaphragm of the cylinder. The speaker was driven by a computer-generated analog signal (a frequency sine wave swept back and forth from 10 to 18 Hz over a 20-s period) through an audio amplifier, thus spanning the resonant frequency of the chamber plus diaphragms. The output of the generator was controlled by varying the amplitude of the signal driving the speaker. MWCNT, forming a fluidized cloud in the chamber, were collected from the chamber by passing clean air into a port at the bottom edge of the cylinder and collecting the aerosolized MWCNT from a port at the opposite top edge of the cylinder at an airflow of ≤15 LPM

(L/min). This MWCNT aerosol then entered an exposure chamber where concentration and particle size distribution were monitored. Mass output was 10.01 ± 0.18 mg/m^3. Mass median aerodynamic diameter was 1.5 μm with a geometric standard deviation of 1.7. Count mode aerodynamic diameter was ~400 nm. Output of the generator was tightly controlled by three different computerized feedback loops to control aerosol concentration by altering power of the amplifier, trans-diaphragm pressure by altering airflow into the box enclosing the cylinder chamber, and exposure chamber pressure by altering airflow out of the exposure chamber. It was stable over many hours of operation. Larger agglomerates can be removed by a 2-μm cutoff cyclone (Figure 7).

An improved dispersion method for aerosolizing MWCNT was developed by Taquahashi et al. (2013) with the goal of generating predominantly single dispersed fibers by effectively removing agglomerates without changing length and diameter. Two preparatory steps were involved, starting with suspending MWCNT in *tert*-butyl alcohol (TB) followed by filtration through a vibrating metal sieve of 25 μm, then snap-freezing by liquid nitrogen and vacuum sublimination, which removed all TB. Small cartridges loaded with the prepared MWCNT were air pressure injected at 6-min intervals into the inhalation chamber, which was continuously supplied with an airflow of 15 L/min. The resulting sawtooth-like concentration was very stable over 2 h at average concentrations of 1.3 and 2.8 mg/m^3, depending on the cartridge loads.

Another MWCNT aerosol generation system was developed by Kasai et al. (2014) for whole-body rat inhalation exposure. This system, termed a "cyclone sieve method," involves delivery of MWCNT from a hopper-type dust feeder into a vertical cylindrical container in which an upward spiraling airstream of filtered air keeps the MWCNT in suspension through gravitational and centrifugal forces. At the upper end of the cylinder a vibrating sieve (53 μm) limits passage only to smaller aerosols to the animal exposure chamber, whereas larger agglomerates settle down into a collection flask at the bottom. This system generates a well-dispersed MWCNT aerosol without larger agglomerates, one that maintained a stable concentration over a 6-h exposure period. Moreover, particle size distribution was similar for airborne mass concentrations ranging from 0.2 to 5 mg/m^3, with MMAD between 1.04 and 1.33 μm and GSD between 2.7 and 3.4. This system was used successfully in the recently finished 90-d (Kasai et al. 2015) and an ongoing 2-yr rat inhalation studies with MWCNT (Fukushima personal communication 2014).

Myojo et al. (2009) described a generation system for MWCNT employing a rotating brush and fluidized bed (RBG—1000 generator, PALAS GmbH, Karlsruhe, Germany). MWCNT were fed (2–20 mm/h) to a rotating brush (1200 rpm) and suspended into an airstream (13.3 L/min). The aerosolized MWCNT were fed into a two-component fluidized bed (bed: irregular stainless-steel beads) to remove agglomerates and stabilize concentration. MWCNT aerosol concentration increased linearly with feed rate to the rotating brush (feed rate of 2–20 mm/h, resulting in an output of 5000–20,000 particles/cm^3). The generator produced a well-dispersed aerosol of MWCNT, as evidenced by electron micrographs of filter samples. However, MMAD or CMD were not provided. At a feed rate of 2 mm/h, MWCNT aerosol concentration was 4 mg/m^3. Calculated concentration of MWCNT surface area ranged from approximately 50 to 400 μm^2/cm^3. Generator efficiency was 11–13%.

Ma-Hock et al. (2009a; 2009b) used a piston-fed rotating stainless-steel brush together with a cyclone separator to aerosolize MWCNT: A high output of 30 mg/m^3 with MMAD 0.5–1.3 μm, and GSD 3.1–5.4; CMD 580 nm (Optical Particle Counter) and 60 nm (SMPS). Larger agglomerates were present. A similar piston-fed rotating stainless steel brush was successfully used in an earlier study for generating glass-fiber aerosols (Bernstein et al. 1995).

Fujitani, Furuyama, and Hirano (2009) used a sieve shaker generator to disperse MWCNT mixed with 5-mm stainless-steel balls in an aluminum cyclone separator, followed by a second cyclone. The maximal concentration

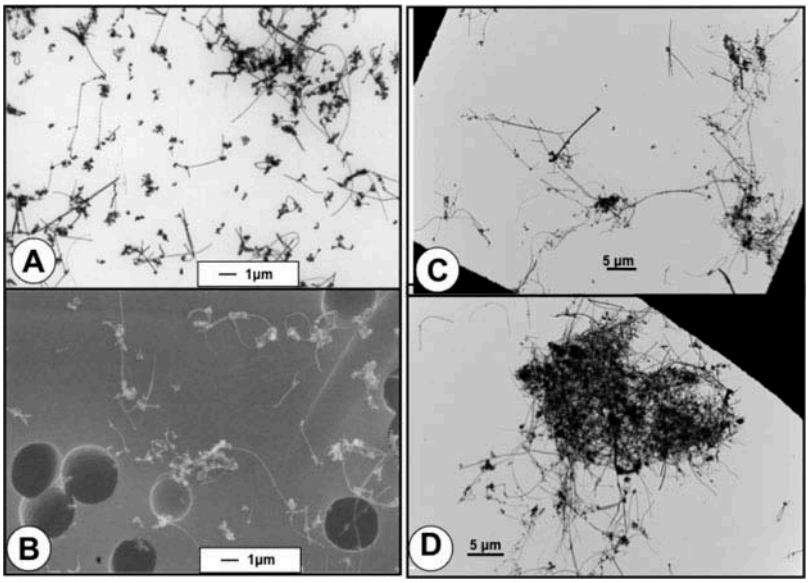

FIGURE 7. MWCNT aerosols collected in rodent inhalation study.

Aerosolized MWCNT collected on filter (A, B) and carbon-coated 200 mesh N: grids (C, D). The MWCNT were aerosolized using an acoustic aerosol generation system (McKinney et al., 2009) for dry powder generation. Large variations of the airborne structures were observed, ranging from a few single tubes to differently-sized structures of agglomerated CNT to larger tangles resulting in an airborne size distribution as shown in Figure 8. The aerodynamic, settling and diffusional behavior cannot be inferred from these pictures; the large tangle in section D may not be inhalable by rodents and is likely not respirable, but the aerodynamic behavior can be estimated from their aerodynamic size distribution. Such experimentally generated MWCNT aerosol for rodent exposures needs to be compared to atmospheres found at workplaces. (See Figures 1, 2).

was 1.2 mg/m^3, with a CMD of 300 nm and an aerodynamic diameter of 1–2 µm; the aerosol was well dispersed and also had larger agglomerates. Concerns are the potential of contamination from steel balls, aluminum, and shortening of CNT.

Mitchell et al. (2007) used a screw feeder system to feed MWCNT into a jet mill, and placed a cyclone separator before inhalation chamber entry. Varying states of agglomeration were seen, more with higher concentration of 5 mg/m^3. The MMAD ranged from 0.7 to 1.8 µm, and GSD from 2 to 2.5; CMD measured by DMA was 350–400 nm; no information was provided concerning exposure stability.

For inhalation of Baytubes, a Wright dust feeder was used. MWCNT were compressed into a Wright dust feeder and a slow-moving blade abrasion generated an aerosol that passed through a cyclone before dilution and entering the exposure system (Pauluhn 2010). Specifically, Baytubes (tight agglomerates of MWCNT) were first micronized, then packed into a dust feeder. Resulting MMAD values as measured by impactor were 2.74–3.42, and GSD 2–2.14 for concentrations of 0.4–5.68 mg/m^3 and agglomerate count by SMPS from 320 to 1763/cm^3.

The CNF aerosols in the subchronic inhalation study by DeLorme et al. (2012) were generated by feeding dry CNF material into a glass tube into which a high-pressure air stream was directed that carried the resulting CNF aerosol into the exposure chamber. Different concentrations were achieved by varying the feed rate into the airstream and/or varying the on/off period of the feeder. Resulting MMAD ranged from 1.9 to 3.3 µm at concentrations from 0.5 to 25 mg/m^3, indicating agglomerated CNF structures.

Li et al. (2007a) described an MWCNT aerosol generation system consisting of a dry powder generator with two sequential depositor tiers to retain larger agglomerates before the aerosol entered the animal exposure

chamber. The resulting MWCNT aerosol was "almost respirable," but the concentration decreased continually over a period of 90 min so that the exposures had to be repeated 4 times within a 6-h exposure session.

Table 3 compares design, exposures, and results of the two 90-day inhalation studies using different MWCNT and one CNF inhalation study. The similarity in dosimetry and responses is apparent, although there are significant differences in some of the histological findings. A NOAEL of 0.1 mg/m^3 was found by Pauluhn (2010), whereas this level was a LOAEL in the Ma-Hock et al. (2009a) study. Of interest is that the increase in lung weight as indicator of overall respiratory toxicity seems to be similar between the Pauluhn (2010) and Ma-Hock et al. (2009a) investigations when based on retained lung burden (Table 3). Exposure-response and dose-response relationships are shown in Figure 4.

Liquid CNT Suspension Systems

Functionalized CNT/CNF that are well dispersed in aqueous or physiological saline can be dispersed using jet nebulizers. Careful characterization with regard to size and size distribution and agglomeration state of the generated aerosol with appropriate instrumentation is mandatory, as it is for the dry powder generation systems. CNT/CNF that are not well dispersed in deionized water or saline require use of dispersants for liquid-phase aerosol generation, which poses the same problem/concern as for bolus-type dosing by instillation or aspiration in terms of altering surface properties, with potential consequences for disposition and effects of deposited CNT/CNF in the respiratory tract. In addition, it needs to be considered that dissolution/leaching of contaminants (catalysts) may occur in the suspension, which may also affect surface properties. In general, dispersion dryers before entry into exposure chamber need to be used with CNT/CNF aerosol generated from liquid suspensions.

Oyabu et al. (2011) described the generation of a well-dispersed aerosol of MWCNT using a nebulization system developed for NP by Shimada et al. (2009). Briefly, an aqueous suspension of MWCNT dispersed in 0.5 mg/ml Triton X-100 was atomized by a pressurized nebulizer equipped with an ejector to break liquid threads into droplets (Nanomaster, JSR Corp., Tokyo, Japan). The nebulizer received clean air (35 L/min) at an inlet pressure of 0.25 MPa and an ejector pressure of 0.20 MPa. Generated droplets were dried in a heater (50°C). The dried MWCNT were then passed into the exposure chamber through a deionizer. The exposure concentration was 0.37 $\pm$ 0.18 mg/m^3. Although neither MMAD nor CMD values were reported, scanning electron micrographs of filter samples from the exposure chamber indicate that this system produced a well-dispersed aerosol of MWCNT with geometric mean diameter of 63 nm and a geometric mean length of 1.1 μm. Use of surfactant may have changed surface properties.

Kim et al. (2010b) modified an electrospray nebulizer to generate a well-dispersed aerosol of MWCNT. The CNT were fed into an electrospray capillary nozzle as a suspension in ethanol at a low feed rate. A high-voltage field between the capillary and a grounded orifice plate produced highly charged particles, with the agglomeration state being controlled by the feeding rate. Two ^{210}Po radiation sources reduced the charges subsequently, and the associated ethanol vapor was reduced efficiently by an activated carbon dryer before MWCNT entered the animal exposure system. Airborne size distribution as determined by SMPS showed a double peak, 150 nm (singlets) and 400 nm (bundles), finely dispersed. The concentration, using one nozzle, was approximately 2 mg/m^3. No dissolution/leaching of metal catalyst or ethanol contamination was to be expected. Several nozzles are required for higher concentrations.

Ryman-Rasmussen et al. (2009a) used a Retsch mixer mill to grind MWCNT. Subsequently, MWCNT were suspended in nonionic surfactant (1% pluronic) in sterile DPBS. Generation of aerosol for nose-only exposure of rats was achieved

TABLE 3. 90-Day Rat Inhalation Studies with MWCNT and CNF, Exposure-Dose-Response Comparison

Material	**Ma-Hock et al. (2009a) MWCNT** (Nanacyl NC7000)	**Pauluhn (2010) MWCNT** (Baytubes)	**Kasai et al. (2015)** (Hodogaya Chemical Co., LTD; MWNT-7)	**DeLorme et al. (2012) CNF** (VGCF-H)
Characterization				
Length/diameter, nm	100–10,000 /5–15 nm	200–1000/10 nm (*micronization*)	2000–5700/40–90nm	1000–14000/40–350 nm
Agglomeration	Yes	Yes (*coiled structures*)	Yes	Yes
Density, g/cm^3	Packing: 0.043	Bulk: 0.11 – 0.33	Bulk; 0.007(production plant)	Bulk: 0.077
Impurities	9.6% Al; <0.2% Co	–0.5% Co	0.2 – 0.4%(*not specified*)	0.003% Fe
BET surf area, m^2/g	250 – 300	255	24–28 m^2/g	13.8
Animals				
Rat strain	Wistar; males/females	Wistar; males/females	F344, males/females	Sprague-Dawley; males/females
Body weight (age)	B.W. not reported (8–9 weeks)	–228 g (m); 180 g (f); (–10 weeks)	B.W. not reported (6 wks)	B.W. not reported(>5 weeks)
Exposure				
Exposure mode	Nose-only	Nose-only	Whole body	Nose-only
Generator	Brush feed generator + cyclone	Wright-Dust Feeder	Cyclon-sieve generator	Accurate Bin Feeder
Duration	90 days: 6 hr/d; 5d/wk	90 days: 6 hr/d; 5d/wk	90 days: 6 hr/d; 5d/wk	90 days: 6 hr/d; 5d/wk
Conctr, mg/m^3	0; 0.1; 0.5; 2.5	0, 0.1; 0.4; 1.5; 6	0; 0.2; 1; 5	0.54; 2.5; 25
MMAD μm (GSD)	2.0(2.8); 1.5(2.1); 0.7(3.6) (*Berner L.P. Cascade Impactor*)	3.05(1.98); 2.74(2.11); 3.42(2.14) (*Marple Cascade Impactor*)	1.5 (2.8); 1.5 (2.8); 1.5 (2.6) (*Micro orifice Uniform Depos. Impact.)*	1.9(3.1); 3.2(2.1); 3.3 (2.0) (*Sierra cyclone/cyclone impactor*)
Size distrib.nm(SMPS)	58 ± 1.8 – 64 ± 1.7	75; 320; 908; 1763	Not done	Not done
Post-expos. recovery	No	6 mos. (males only)	No	3 mos. (males, females; 0.25 mg/m^3)
Dosimetry/Biokinetics				
Lung burden *(90 days, males)*	47; 243; 1170 μg (deposited)[a]	–5, 25; 100; 420 μg (*retained*)[b] (also post-exposure)	9.69;63.60;360.90 μg (retained)[c]	Not determined
Extrapulmonary Translocation	Mediastinal lymphnodes (*inside granulomatous nodules forming acrophages*)	Hilar lymphnodes; other organs not reported	Mediastinal lymphnodes; parietal pleura (diaphragm, capillaries of muscle), spleem	Tracheo-bronchial lymphnodes; rarely in brain, heart, liver, kidneys, spleen, intestinal tract, mediastinal lymphnodes (*no adverse histopath.*)
Retention halftime (T1/2, days)	Not done	151; 350; 318; 375[b]	Not done	Not done
Response				
Body wt. change	No significant difference	No significant difference	No significant difference	15% lower in lowest conc. group; no sign. difference in other groups
Lung weight *(90 days)*	+ 1%; + 23%; + 81% (males)	+0; + 12; +27; +61% (males)	+5;+17;+30% (males)	–2; + 8; +22; (males)
Lymphnode wt.	Increased size (high conc)	Increased wt (1.5 and 6 mg/m^3)	Not reported	not reported
BAL–PMN *(90 days)*	Not reported	–0.5; 3.8; 13; 19%	0.6;13.5;45.7%	1.4; 2.7; 11.0%
BAL-PMN post-exposure *(3 mos)[6 mos]* high dose only	Not done	(22%) [19%]	Not done	(13%) [not done]
Neutrophilic, histiocytic inflam.	Yes	Yes	Yes	Yes

(*Continued*)

TABLE 3. (Continued)

Material	**Ma-Hock et al. (2009a) MWCNT** (Nanacyl NC7000)	**Pauluhn (2010) MWCNT** (Baytubes)	**Kasai et al. (2015)** (Hodogaya Chemical Co., LTD; MWNT-7)	**DeLorme et al. (2012) CNF** (VGCF-H)
Granulomat. inflam.	All concentrations	6 mg/m3	All concentrations	Not reported
Interstitial fibrosis	Fibrotic changes	At 1.5 and 6 mg/m^3 groups	At 1 and 5 mg/m^3 groups	Interstitial thickening, no fibrosis
Alv. lipoproteinosis	Yes, 0.5; 2.5	No	No	No
Hypercellularity	Not reported	Yes (0.4 and higher)	Goblet cells in nasal cavity, all conc.	Yes (2.5 and higher conc.)
Lymphnode histology	Granul. inflam, all conctr.	Increased cellularity, all conctr. (signif. at 0.4 and higher)	Not reported	Not reported
Visceral pleura	Not reported	Thickening, collagen at 1.5 and 6 mg/m^3	Inflamm. Infiltration (5 mg/m^3)	Not reported
Blood neutrophilia	Yes (highest conc.)	Not reported	Yes, females only, all conc.	Not reported
Systemic Toxicity	Not detected	Not detected	Yes *(increased mRNA of inflammatory cytokines in spleen, all conc.)*	Not detected
Evaluation				
NOAEL	No	100 μg/m^3	No	540 μg/^{m3}
LOAEL	100 μg/m3	400 μg/^{m3}	200 μg/m^3	2500 μg/m^3

[a] estimated by authors, no clearance considered; [b] based on retained Co in lung; [c] extrapolated from amount determined in left lung and using a left to right lung weight ratio of 1:2.

with six jet Collison nebulizers, followed by removal of large droplets by a particle trap, and water removal by silica gel dryers. MMAD was 714 nm, GSD approximately 2, and CMD 160 nm. High concentrations of 103 mg/m^3 were measured, consisting of approximately 2 μm agglomerates and individual CNT. Concerns are the grinding process and use of dispersant.

Pauluhn and Rosenbruch (2015) also used a Collison-type nebulizer to aerosolize MWCNT in a 6 h nose-only exposure of rats to 30 mg/m^3 with sodium carboxymethyl-*O*-cellulose as dispersant to compare effects of wet dispersion exposure to those of dry powder generation of the same MWCNT. The smaller wet-generated aerosol (MMAD 0.79 μm) induced greater effects than larger pristine dry powder aerosols (MMAD 2.6 μm). It is worthwhile noting that caution against using unrealistic high-dose acute exposure leading to an incomplete picture of potential pulmonary toxicities is required.

A novel approach was suggested by Ahn, Kim, and Yu (2011): Uncoated MWCNT were continuously sonicated in 80°C hot deionized water, which lowered surface tension and facilitated dispersion and then nebulized via a Collison-type nebulizer with subsequent drying of aerosol in a diffusion dryer. This system produced well-dispersed MWCNT without the use of dispersant. Stable and high concentrations of 50 mg/m^3 were obtained. Aerosol size distributions were not determined, and additional information about its use in actual inhalation studies should be forthcoming.

As pointed out before, for any generation method it is important to characterize the generated CNT/CNF aerosol in sufficient detail in order to ensure adequate dosing of the test animals, in particular regarding the respirability of the CNT/CNF aerosols. Limitations of measured data have to be critically considered. For example, the use of DMA to determine equivalent mobility diameters of CNT/CNF (Ku et al. 2007) is based on separation by a mechanism that does not occur in the respiratory tract (i.e., electrical mobility), and DMA measurements may be in error if the size of tangled CNT/CNF exceeds submicrometers. The mobility diameters of doubly and triply charged CNT/CNF are different from singly charged CNT/CNF, on

which the DMA separation is based. Key should be to replicate as best as possible the CNT/CNF aerosol characteristics that humans are exposed to with the proviso that differences in human versus rodent respirability/dosimetry have to be considered. CNT/CNF may be aerosolized in a variety of shapes, which may be grouped to define several CNT/CNF shape categories. A different characterization may be needed for each shape. Obtaining different equivalent diameters for each shape requires the use of different instruments and might prove to be a challenge, given the availability of resources and time.

Endpoints and General Approach

Based on numerous studies showing the potential of nano-sized particles to translocate beyond the portal of entry, thereby potentially producing systemic effects and effects in secondary organs, and given MWCNT-specific results indicating translocation to and effects at pleural tissues, there is a need to expand presently required endpoints (examination of organs, tissues and effects) relative to existing guidelines (EPA 1998; OECD 2009a) and guidance (OECD, 2009b) for subchronic/chronic inhalation studies. These include incorporation of additional effect endpoints for CNT/CNF inhalation studies, as well as data for lung dosimetry and biokinetics.

Biokinetics necessitates the development of appropriate sensitive methods/labels for quantifying biodistribution as briefly discussed previously. To measure lung burdens, sensitive methods are necessary to reliably measure even low levels of retained CNT/CNF (Doudrick et al. 2013; Ohnishi et al. 2013). Because of the concern that CNT/CNF may behave like asbestos, there needs to be a specific emphasis on pleural–lymphatic translocation and clearance pathways involving lymphatic stomata of the parietal pleura (Goodglick and Kane 1996; Donaldson et al. 2010). Thus, harvesting thoracic bifurcational lymph nodes as sentinels for clearance of lung-deposited CNT, and superior mediastinal lymph nodes and diaphragm as sentinels for clearance from the pleural space (Parungo et al. 2005), needs to be part of the study design. Indeed, Bernstein et al. (2011) reported that just a 5-d inhalation exposure of rats to a high concentration of amosite and chrysotile asbestos was sufficient to demonstrate significant inflammatory, granulomatous, and fibrotic responses in lung and pleura, including translocation to the pleura for amosite, whereas this was not observed with the low-biopersistent chrysotile. In contrast, while pleural translocation of aspiration-delivered well-dispersed MWCNT was found (Mercer et al. 2010), and single MWCNT at pleural sites and diaphragm of rats following inhalation exposure were observed (Mercer et al. 2013a,b), translocation of inhaled complex agglomerates of MWCNT to the pleural space has still to be demonstrated and remains a research gap to be filled. Another important tissue to include is the bone marrow, which was found as a site for significant uptake of NP (Bazile et al. 1992; Ballou et al. 2004; Cagle et al. 1999; Gibaud et al. 1994; 1996; 1998; Rinderknecht et al. 2007).

To determine retained lung burdens and CNT/CNF translocated to extrapulmonary secondary organs and target sites, sensitive analytical methods are necessary to reliably quantify even low tissue levels of elemental carbon (EC) of retained/translocated CNT/CNF. Early methods developed for measuring retained lung burdens in rats of diesel particles following 22–32 wk of inhalation to high concentrations of diesel exhaust used KOH/ethanol digestion of dried lungs, followed by sonication of the water-resuspended pellet, and optical density reading (Rudd and Strom 1981). This method was sufficient to measure the expected high lung burdens of 2–10 mg. NIOSH (2003) published a standard method to determine carbon from diesel exhaust on filter samples using a thermal optical method involving two stages with stepped-up temperature, first in helium and then in an He/O_2 mixture. This allowed separate measurement of organic carbon (OC) and EC. Diesel concentrations ranging between 6 and 630 $\mu g/m^3$ ambient air could be measured, but the method was not applied to tissue samples. Mercer et al. (2013a) used a three-step process to determine lung burdens of MWCNT after exposure of mice. Dried

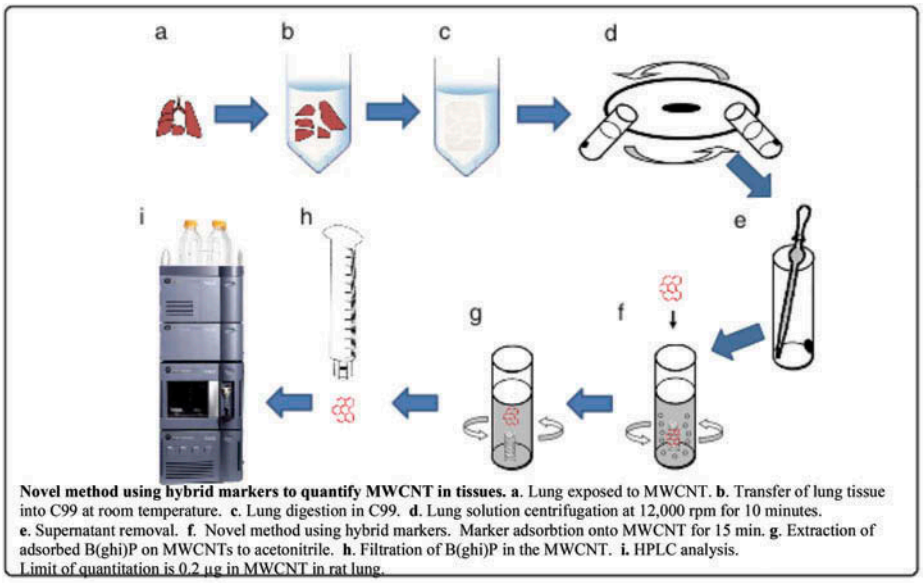

Novel method using hybrid markers to quantify MWCNT in tissues. a. Lung exposed to MWCNT. **b**. Transfer of lung tissue into C99 at room temperature. **c**. Lung digestion in C99. **d**. Lung solution centrifugation at 12,000 rpm for 10 minutes. **e**. Supernatant removal. **f**. Novel method using hybrid markers. Marker adsorbtion onto MWCNT for 15 min. **g**. Extraction of adsorbed B(ghi)P on MWCNTs to acetonitrile. **h**. Filtration of B(ghi)P in the MWCNT. **i**. HPLC analysis. Limit of quantitation is 0.2 μg in MWCNT in rat lung.

Modified from: Ohnishi et al., 2013 *(with permission)*

FIGURE 8.

lungs were digested in KOH/methanol, then in HNO_3/methanol, followed by resuspension in dH_2O with NP-40. Optical density in a spectrophotometer was read after sonication. Lung burdens of 3.125 μg/ml (sample size 100 μl) (Dale Porter personal communication, 2015) MWCNT were detected. Doudrick et al. (2013) developed a programmed thermal analysis (PTA) method to quantify CNT in lung tissue. After examining eight different tissue digestion methods, they noted that a two-step extraction/digestion method was optimal, consisting of solvable (mixture of 2.5% NaOH, 2.5–10% *N,N*-dimethyldodecylamine *N*-oxide, 2.5–10% polyethylene glycol trimethylnonyl ester) and proteinase K. Two types of MWCN were used, with weak thermal stability (high defect density) and strong thermal stability (low defect density). Similar to the *NIOSH Manual of Analytical Methods* (NMAM) (2003) method, PTA involved two heating steps: the first in 100% helium to remove any remaining OC from tissue, and the second in 90% He/10% O_2 to develop the CNT thermogram and quantify the carbon content after conversion to methane and detection by flame ionization detection (FID). Overall, recovery of MWCNT in spiked lung samples was 98% for lung burdens estimated between 1 and 10 μg in rats.

Ohnishi et al. (2013) established a different approach using a novel method to measure with high sensitivity retained lung burden of MWCNT-7 (Mitsui) following inhalation and IT instillation exposure of rats. Their concept involved adsorption of a PAH marker onto MWCNT followed by HPLC detection after desorption of the marker (Figure 8). Preparatory steps involved overnight digestion of rat lungs in C99-K200 (lab bleach), which was significantly improved by prior formalin fixation of the tissue; centrifugation at 10,500 × g, addition of Tween 80 mixture (9.6% phosphate buffered saline with 0.1% Tween 80), and centrifugation followed by brief concentrated sulfuric acid for complete digestion of undissolved tissue components; centrifugation and washing in dH_2O and addition of the hybrid marker benzo[ghi] perylene (B[ghi]P) for adsorption to MWCNT; centrifugation and extraction of marker to acetonitrile; and filtration and quantitative examination of eluate by high-performance liquid chromatography (HPLC). Recovery of spiked lung samples was 92.5%, and the limit of quantitation 0.2 μg in the lung. This is the most sensitive quantitative method reported so far and is an important contribution to nanotoxicology, providing the scientific community with a tool to establish

essential dose-response relationships of carbonaceous NM.

As stated earlier, it is desirable to consider realistic human exposure conditions when designing rodent inhalation studies with CNT/CNF. Relevant exposure levels and measuring respective lung burdens need to be included to obtain exposure-dose-response relationships. The analysis of the results needs to take into account dose metrics and response metrics when performing dosimetric extrapolation to humans for hazard identification and risk assessment purposes. For example, deposited and retained CNT/CNF doses in the lung can be expressed per unit alveolar or tracheobronchial surface or per unit lung tissue volume or gram lung tissue to normalize doses, which will allow extrapolation between humans and rats or mice. The selection of this dose metric is associated with the mode of action; it needs to be closely related to effects at the target site within the respiratory tract (i.e., epithelial vs. interstitial). Care needs to be taken in the selection of the region associated with the toxicological response, as dose per epithelial surface area will highly depend on the total retained amount and total surface area of the selected region.

In addition to dose metric, exposure metrics to characterize inhalation of particles are important. Exposure concentrations expressed as mass per cubic meter or number per cubic meter or also surface area per cubic meter were all used. Although for spherical NP in a well-dispersed state (singlets) these relationships can readily be determined, this is difficult for the less uniform and rather complex structures and tangles of CNT/CNF, except for the mass/surface area correlation. Thus, knowing this relation, expressing exposure as micrograms per cubic meter and determining deposited and retained mass allows one to convert a tissue mass dose to particle surface area dose. Additional model development is required to estimate tissue dose from retained dose on the surface of the airways.

In general, the use of tissue dose depends on CNT/CNF clearance rate into the interstitial space, including dissolution rate of contaminants/impurities, and possible interaction of CNT/CNF with interstitial cells. Data with poorly soluble particles indicate that a far greater portion of deposited particles in the lung migrates to the interstitium in primates than in rat (Nikula et al. 1997; 2001), which is supported by findings in coal mine workers and humans exposed to radioactive aerosols (Kuempel et al. 2001; Gregoratto, Bailey, and Marsh 2011). However, there is some evidence that—likely due to the hydrophobic nature of CNT—interstitialization of SWCNT and MWCNT may be substantial in rodents (Mercer et al. 2008; 2011). Further studies with CNT and CNF are required to describe biokinetics fully.

When expressing the deposited dose per unit surface area (cm^2) of airway epithelia, the inflation state of the lung needs to be considered: for example, functional residual capacity (FRC) versus total lung capacity (TLC). For example, values for the human alveolar surface vary widely, from approximately 60 m^2 (EPA 2004) to 140 m^2 (Gehr, Bachofen, and Weibel 1978). This range of published values reflects different inflation states of the lung when prepared for morphometric analyses, from FRC to TLC. A critical analysis and comparison of literature data by Miller et al. (2011) resulted in more definite and authoritative values for tracheobronchial and alveolar surface areas of human and rat lungs at FRC (Table 4).

Normal breathing starts at FRC such that the epithelial surface area available for deposition of inhaled particles is FRC plus the opening of additional surface by the tidal volume. Considering the tidal cycling of inhalation and exhalation during breathing, the approximate average epithelial surface area for particle deposition is determined by FRC + ½TV, which

TABLE 4. Surface Areas of Respiratory Tract Regions at FRC

	Rat		Human	
	cm^2	*% of total*	*cm^2*	*% of total*
Nasal	***18.5***	***0.75***	***210***	***0.03***
Trach-bronch	***24***	***1.00***	***4149***	***0.65***
Alveolar	***2422***	***98.25***	***634620***	***99.32***

Keyhani et al., 1997; Kimbell et al., 1997; Miller et al., 2011. (Keyhani, Scherer, and Mozell 1997; Kimbell et al. 1997; Miller et al. 2011).

is close to the surface of FRC, but lower than at TLC. Thus, lung inflation state at FRC is the more appropriate for dosimetric considerations and comparisons; it ranges from about 35 to 45% of TLC for different species. Table 4 shows values for the upper respiratory tract reported by Keyhani, Scherer, and Mozell (1997) and Kimbell et al. (1997). It is important for dosimetric comparison of experimental results of different rat inhalation studies and for purposes of dosimetric extrapolations to humans that researchers base assessments on the same well-justified and accepted values. Table 4 shows that for both species the alveolar region has essentially the same (98.3–99.3%) relative surface area, whereas there is a large difference between species for the less than 1% overall surface area of the nasal area.

Diverse methods to evaluate the biodistribution of CNT following different routes of administration have been used. These include TEM, radioactive and stable isotope labeling, Raman spectroscopy, near-infrared (NIR) spectroscopy, x-ray and other fluorescence, and metal impurity analysis. Liu et al. (2010b), after reviewing these methods and discussing their advantages and disadvantages, concluded that analytical methods for quantitation need to be improved and that optimization of biodistribution methods is urgently needed. The in vivo stability of any label has to be carefully confirmed. Other methods include thermo-optical analysis (Hyung et al. 2007; Peterson and Richards 1999; NIOSH Method 5040: NIOSH 2013; Watson, Chow, and Chen 2005; Westerhoff, Doudrick, and Herckes 2012; Doudrick et al. 2013) and turbidity measurement of retained carbonaceous material after tissue digestion (Rudd and Strom 1981). The most sensitive method appears to be the use of a hybrid marker, described by Ohnishi et al. (2013).

A minimum number of pulmonary endpoints—in addition to lung weight—measured at various time points postexposure needs to include an evaluation of inflammation, lung damage, granulomatous lesions, and interstitial fibrosis. Inflammation and damage may be evaluated by analysis of fluid obtained by BALF. Lung lavage after euthanasia may be performed in situ (lavaging via tracheal cannula without opening thorax), after opening the thorax in situ (lung expands more easily) or after excising the lungs and trachea *en bloc* and lavaging outside (on wetted gauze with gentle massaging of the lungs). Three to five repeated lavages using physiological saline or PBS are usually performed. The excised lung lavage results in significantly greater numbers of lavaged cells, probably due to retrieving more cells from the lung periphery. Lung cell damage may be determined by measuring LDH activity in the acellular fluid obtained from the first or combined first and second lavage aliquot. Alveolar air–blood barrier damage/integrity may be measured as the protein or albumin level in this acellular BALF. Selected cytokine and chemokine (IL–1, tumor necrosis factor [TNF] α, macrophage inflammatory protein [MIP]-1, etc.) levels in the first acellular BALF might also be measured as markers of inflammation. In addition, TGF-β levels in the first acellular BALF would be useful as an indicator of fibrogenic stimulation. Total BALF cells and cell differentials, in particular neutrophil counts, would be a sensitive indicator of pulmonary inflammation. Oxidant stress may be monitored by measuring total antioxidant levels in lung tissue. These assays are described in mouse and rat models after exposure to CNT (Lam et al. 2004; Warheit et al. 2004; Shvedova et al. 2005; Porter et al. 2010).

Histopathological analysis, using both light and electron microscopy, also needs to be conducted. Analyses needs to include a qualitative evaluation of the deposition sites of CNT/CNF agglomerates and more dispersed structures, pathological evaluation of granulomatous lesions (onset, distribution, and persistence), and a quantification of interstitial fibrosis (collagen) in Sirius red-stained lung tissue determining onset, distribution, and progression. Examples of such histopathological quantification for CNT were described by Mercer et al. (2008) for SWCNT and Mercer et al. (2010; 2011) for MWCNT.

Cell proliferation in response to CNT/CNF exposure is a useful indicator of hyperplasia for a potential pre-neoplastic response and may be quantified using the BrDU method (Warheit et al. 2004; DeLorme et al. 2012). In addition, histopathological analysis for bronchiole and alveolar epithelial and mesothelial hyperplasia and hypertrophy is of value (Porter et al. 2010).

Acute pulmonary exposure to high doses of CNT were found to produce adverse cardiovascular effects, including (1) oxidant stress in aortic and cardiac tissue, (2) an increase in aortic plaque lesions in ApoE-/-mice (Li et al. 2007b), and (3) inhibition of the ability of coronary arterioles of rats to respond normally to dilators (Stapleton et al. 2011; 2012). Therefore, systemic response to pulmonary CNT/CNF exposure may be monitored by histological evaluation of aortic plaque formation in ApoE-/- (atherosclerotic sensitive) mice and by monitoring the responsiveness of the rat tail artery to vasomodulating factors (Krajnak et al. 2009). In addition, systemic inflammatory response to pulmonary exposure to CNT/CNF may be monitored by measuring the ability of peripheral blood PMN leukocytes to produce reactive oxygen species (ROS) in response to ex vivo stimulation (Nurkiewicz et al. 2006) or determining blood mRNA expression or protein for selected inflammatory markers (Erdely et al. 2009). Blood fibrinogen and measurement of platelet activation may be used as markers for potential thrombogenic effects (Khandoga et al. 2004). While some of these measurements require specific methodological expertise and cannot easily be incorporated into a 90-d inhalation study, other endpoints determining acute-phase systemic responses from analysis of blood samples (e.g., fibrinogen; IL-6; CRP) may readily be incorporated into the design of acute, subchronic, and chronic studies. The timing of blood sample biomarker assays needs to be carefully considered, as some biomarkers may be expressed transiently.

There may be value in conducting genomic or proteomic analyses on lung tissue samples to obtain mechanistic information concerning pathways involved in pulmonary responses. This depends on the study objective; it would be useful though to save specific organs for later analysis. For example, lungs, bronchus-associated lymphatic tissue, lymph nodes, and other identified target tissues/organs could be rapidly removed and frozen at –80°C.

Evaluation

Although dosing of the respiratory tract with CNT/CNF can easily be achieved by bolus-type delivery of liquid suspension, or insufflation as powder, directly into the trachea, this cannot mimic physiological inhalation exposures in terms of disposition within the respiratory tract and with respect to the normally low inhaled deposition rate in the lung. Therefore, inhalation exposures of lab animals are most appropriate for toxicity testing. Selecting a method for the generation of CNT/CNF aerosols that closely resembles exposures that workers/consumers may experience requires a careful evaluation of aerosol generator technology, CNT/CNF aerosol characterization, and dosimetric issues. As indicated, a key consideration of an experimental exposure-dose-response design is to include doses and distribution in the respiratory tract of experimental animals that are predicted to be present in exposed humans.

The detailed discussion of inhalability and respirability in this review should provide guidance in this respect. This enables one not only to establish exposure-response relationships—which are often not easy to interpret—but to develop more comprehensive exposure-dose-response data. A critical evaluation of exposure-dose-response information from rodent inhalation studies may serve as a basis for risk assessment by considering different endpoints for pulmonary and secondary organ effects as well as systemic effects.

In addition to the analysis of exposure-dose responses, information about biokinetics provides essential information to the overall assessment of potential adverse effects of CNT/CNF. However, as previously discussed, sensitive methods to quantify low levels of CNT/CNF in tissue still need to be developed and refined.

TABLE 5. Acute to Chronic Inhalation Exposures of Rodents to CNT/CNF for Toxicity Testing. (rat as preferred species; 4–6 hrs/day, 5 d/wk; whole-body)

Acute/Subacute (14–28 days)	Subchronic (90 days)	Chronic (2 years)
• to obtain hazard ID and ranking (pos/neg control?) • may be preceded by i.t. instillation or 1 day inhalation with range of doses to estimate inhaled concentration with MPPD model • assure and test rat respirable aerosol with range of concentr. • if available use workplace or consumer exposure data to inform aerosol generation • to determine concentration for 90-day; (range-finding) • to collect biokinetic data for portal of entry, and possibly identification of secondary target organs, incl. pleura, and fetus • to provide guidance for dose levels for mechanistic in vitro testing, incl. secondary organs • post-exposure observation period desirable (∼2 months)	• to derive NOAEL • use minimum 3 conc, including known or expected human exposure levels; both sexes optional • if no effect at 50mg/m^3 rodent respirable aerosol, then no need to do chronic study* • to identify hazard: total resp.tract; pleura, cardiovascular, CNS, bone marrow • identify target organs • to select conc, for chronic study • detailed biokinetics: retention, clearance, organ accumulation, • predicting long-term effects? • to perform risk assessment by extrapolation to human via dosimetric extrapolation • post-exposure observation period for longer-term effects to assess progression-regression (∼3 months)	• to determine long latency effects (cancer); life shortening; extrapulmonary target organs • 3 conc; based on 90-day or range-finding study results; include human exposure level; high dose: MTD; low dose: no significant effect • to assess total respiratory tract, pleura and systemic effects, nose to alveoli; cardiovascular, CNS, bone marrow, others (reproductive?) • to determine detailed biokinetics: resp.tract retention, clearance, organ accumulation • to perform extrapolation to human for risk assessment • post-exposure observation period up to a total study duration of 30 months (if survival of ≥20%)

*This suggestion is based on the fact that such high concentrations will never be reached in a repeat exposure scenario, and it would be a waste of animals (ethical) and resources ($), (Bernstein et al. 2005) to design a chronic workplace study. It should even be considered to move this suggestion to the acute/subacute category and not follow up with a subchronic study if an appropriate postexposure (∼60 d) observation period is included. Even shorter-term (5 d) inhalation studies with CNT/CNF less than 10 mg/m^3 or a single 6-hr. inhalation at 30 mg/m^3 have induced significant effects (Ma-Hock et al. 2009; Ryman-Rasmussen et al. 2009a; b; Stapleton et al. 2012; Shvedova et al. 2008). Thus, a cutoff at 50 mg/m^3 in a subchronic study is very conservative.

In the absence of such data, visualization of CNT/CNF in lung and secondary organs by light and electron microscopy together with markers of exposure, such as pleural plaque formation or molecular biology-based effects, provides qualitative or descriptive proof for the existence of biokinetic pathways.

DISCUSSION

Types and Purpose of Inhalation Toxicity Testing

Assessing the potential of CNT/CNF exposure to induce adverse responses in the respiratory tract and in secondary organs requires the design and use of inhalation exposures. While dosing of the respiratory tract by noninhalation methods may be useful for purposes of toxicity ranking, inhalation avoids potential problems associated with bolus-type delivery or with pretreatment of the pristine CNT/CNF. Thus, while one goal of mimicking human exposure to CNT/CNF aerosols is achieved by administering them to rodents by inhalation, the appropriate methodology with respect to characterizing airborne properties of CNT/CNF also needs to be considered in order to reproduce the equivalent for rodent exposures.

The durations of experimental inhalation studies may range from acute short one-time to 28-d exposures to chronic repeat daily exposures for up to 2 yr. The purpose and some design and methodological details of these different exposures are summarized in Table 5. These range from using results of short-term studies to establish long-term study concentrations via data for accumulation, retention, and clearance kinetics; to identification of potential short- and long-term hazards in the respiratory tract, extrapulmonary tissues, and organs; to determination of a NOAEL; to collection of biokinetic data; and to risk assessment and dosimetric extrapolation.

General Guidelines for Inhalation Toxicity Testing

Guidelines have been issued by the U.S. EPA and OECD describing general requirements for testing chemicals by inhalation, including animal selection, concentration level selection, repeat exposure durations, exposure chambers and exposure conditions, data evaluation, quality control, data reporting, and many other details (EPA 2000; OECD 2009a; 2009b). Both guidelines focus on 90-d subchronic inhalation studies and both suggest nose-only exposures as the preferred method over whole-body, to minimize secondary oral exposure due to preening of the fur deposits. However, the stress induced by long-term nose-only exposure in restraining tubes is significant and affects the animals' growth and physiology (discussed earlier, Types of Inhalation). An earlier EPA guideline (EPA 2001) that applies to chronic toxicity/carcinogenicity testing of fibrous particles allowed for either nose-only or whole-body exposure.

Although these guidelines do not specifically address nanotechnology-related testing requirements, they are useful in terms of providing general recommendations for performing a subchronic 90-d inhalation study. For example, the EPA (2001) test guidelines provided valuable guidance that are applicable for testing NP, including concentrations, selections, lung burden analysis, and BALF analysis. As another example, the introduction to the OECD (2009a) guideline states:

> Subchronic inhalation toxicity studies are primarily used to derive regulatory concentrations for assessing worker risk in occupational settings. They are also used to assess human residential, transportation, and environmental risk. This guideline enables the characterization of adverse effects following repeated daily inhalation exposure to a test article for 90 days (approximately 10% of the lifespan of a rat). The data derived from subchronic inhalation toxicity studies can be used for quantitative risk assessments and for the selection of concentrations for chronic studies. This Test Guideline is not specifically intended for the testing of nanomaterials.

The OECD (2009a) Summary reads:

> This revised Test Guideline 413 (TG 413) has been designed to fully characterize test article toxicity by the inhalation route for a subchronic duration (90 days), and to provide robust data for quantitative inhalation risk assessments. Groups of 10 male and 10 female rodents are exposed 6 hours per day during a 90 day (13 week) period to a) the test article at three or more concentration levels, b) filtered air (negative control), and/or c) the vehicle (vehicle control). Animals are generally exposed 5 days per week, but exposure for 7 days per week is also allowed. Males and females are always tested, but they may be exposed at different concentration levels if it is known that one sex is more susceptible to a given test article. This guideline allows the study director the flexibility to include satellite (reversibility) groups, interim sacrifices, bronchoalveolar lavage (BALF), neurologic tests, and additional clinical pathology and histopathological evaluations in order to better characterize the toxicity of a test article.

Some specific requirements listed in OECD (2009a) include the target concentrations selected need to identify target organ(s) and demonstrate a clear concentration response:

- The high concentration level should result in toxic effects but not produce lingering signs or lethality that would prevent a meaningful evaluation.
- The intermediate concentration level(s) should be spaced to produce a gradation of toxic effects between that of the low and high concentration.
- The low concentration level should produce little or no evidence of toxicity and

> A satellite (reversibility) study may be used to observe reversibility, persistence, or delayed occurrence of toxicity for a post-treatment period of an appropriate length, but no less than 14 days. Satellite (reversibility) groups consist of 10 males and 10 females exposed contemporaneously with the experimental animals in the main study. Satellite (reversibility) study groups should be exposed to the test article at the highest concentration level and there should be concurrent air and/or vehicle controls as needed.

Another guidance document relates to acute inhalation toxicity testing of chemicals in general (OECD 2009b). General recommendations are presented, addressing the principle of the test, monitoring of exposure conditions including inhalation chamber design, and statistical analysis of data. One crude endpoint for this acute test is mortality (LC_{50}), although nonlethal points are also considered. The preferred

TABLE 6. Percent Deposition of Inhaled Particles of Unit Density ($\rho = 1$ g/cm^3) in Extrathoracic, Tracheobronchial, and Alveolar Regions of Rodents

		Mouse				Rat			
MMAD	(GSD)	ET	TB	Alv	Total Lung	ET	TB	Alv	Total Lung
4 μm	(1)	51.75	1.34	0.79	2.13	70.3	0.14	0.13	0.27
4 μm	(2)	42.94	1.71	1.56	3.27	61.4	0.69	1.28	1.97
4 μm	(3)	35.86	1.70	1.83	3.53	49.79	1.14	2.50	3.64
3 μm	(1)	55.34	2.93	2.26	5.19	75.92	0.55	0.75	1.3
3 μm	(2)	45.74	1.83	1.81	3.64	59.45	1.15	2.38	3.53
3 μm	(3)	37.28	1.60	1.90	3.50	43.58	1.17	3.02	4.19
2 μm	(1)	53.26	3.49	3.37	6.86	70.45	2.06	3.80	5.86
2 μm	(2)	46.25	2.54	2.55	5.09	50.11	1.24	3.10	4.34
2 μm	(3)	39.16	1.85	2.23	4.08	39.14	0.99	3.23	4.22
1 μm	(1)	39.16	2.77	3.43	6.20	21.87	2.00	5.68	7.68
1 μm	(2)	38.41	3.02	3.78	6.80	32.98	1.89	5.53	7.42
1 μm	(3)	36.35	3.48	4.37	7.85	38.14	1.62	5.38	7.00

MPPD Model 2.90.3
+ Inhalability Adjustment
Rat: Asymmetrical Multiple Path
Mouse: Balb-C
Default settings (nasal breathing; FRC; tidal volume; breathing frequency; no pause)

exposure mode again is nose-only, although for special objectives and longer duration studies whole-body chamber exposures may be given preference. Recommendations for aerosol size are given as MMAD between 1 and 4 μm and GSD 1.5–3.

As discussed earlier (Types of Inhalation), nose-only exposures may not be advisable for exposures to NP aerosols because of the associated significant stress resulting in retarded body weight gain and other stress-related effects. Further, CNT ingested due to fur preening appear to be cleared from the gut quickly without significant toxicity (Matsumoto et al. 2012). CNT/CNF inhalation studies should not be conducted with an MMAD of 4 μm, since this is close to the upper limit of the thoracic fraction for rodents (Figure 2). Specific guidelines for nanomaterials should consider workplace exposure conditions and include inhalability and respirability differences between humans and rodents. Some of these items are already addressed in the first nanomaterial-specific guidance issued by OECD (OECD 2012). Thus, lower MMAD and particularly CMD up to several hundred nanometers—depending on actual workplace data—need to be included in future nano-specific guidelines, including aerosols of CNT/CNF.

A specific recommendation for optimal aerosol sizes for rodents would be an MMAD up to 2 μm with a geometric standard deviation up to 3. Table 6 lists deposition efficiencies for rats and mice for MMAD from 1 μm to 3 μm, and geometric standard deviations from 1 to 3. The low deposition efficiency of 3-μm particles becomes obvious, considering that seemingly small differences in deposition fractions result in large differences of retained lung burdens during a subchronic or chronic exposure; retained lung burdens would be even less for 4-μm MMAD particles, which would not be ideal for exposing rodents. Instrumentation to determine median aerodynamic diameters (low pressure and regular impactors) and count median diameters (diffusion or electrical mobility particle size spectrometers) of the aerosols is used. Rats are the preferred species for inhalation exposures to poorly soluble particles because of their greater sensitivity to detect fibrotic and carcinogenic responses relative to mice (ILSI 2000).

Nanotechnology-Specific Guidelines

Presently no guidelines specific for CNT/CNF inhalation testing have been issued; however, several newer guidelines that focus on nanotechnology should briefly

be mentioned for interested readers because of their close connection to the topic of this document.

ISO Standard 10808 (ISO 2010a) "specifies requirements for, and gives guidance on, the characterization of airborne nanoparticles in inhalation chambers for the purpose of inhalation toxicity studies in terms of particle mass, size distribution, number concentration and composition." It includes definitions of physical characteristics of nanoparticles and emphasizes the importance of precise characterization of the test material for establishing a quantitative relationship between the observed toxicological outcome and the dose metrics used. The physical and chemical properties include median and mean size, size distributions, number and mass concentrations, composition, surface area, electrical charge, surface characterization, hygroscopicity, and shape. Obviously, shape becomes very important for CNT/CNF but is not further discussed in the guidance document. Agglomeration and aggregation state also need to be added, as should be purity and contaminants.

ISO 10808 further describes measuring systems for airborne nanosized particles, describes general and specific monitoring methods, and discusses assessment of results. Measurements of number-based size distributions by DMA is suggested as the only method to fulfill all of the requirements for continuous monitoring and accuracy of size and concentration in the animals' breathing zone with high resolution that permits conversion from number-based distribution to surface-area-based or volume-based distribution. However, an important caveat is highlighted in the document for nonspherical particles by cautioning that DMA-derived particle size measurement might result in significant error and, therefore, that DMA application for nonspherical particles is not recommended.

With regard to mass-concentration measurements, gravimetric measurements of material collected on membrane filters, beta attenuation mass monitor (BAM), tapered element oscillating microbalance (TEOM), and piezoelectric microbalance are listed. Estimation of mass by DMA is also mentioned for NP when particle density is known (Ku and De La Mora 2009). However, it is cautioned again that for nonspherical particles DMA-based mass estimates might produce errors, and significant errors in calculated mass concentration may result if particle density is inaccurate or unknown.

Maynard et al. (2006) and Ku et al. (2006) used tandem mobility–mass analysis consisting of a DMA and aerosol particle mass analyzer (APM) to characterize shape and structure of SWCNT and of CNF. However, while certain morphological features correlated with mass can be assessed, this method is not suitable for routine analyses. In particular, the DMA–APM system is useful for well-defined fibers/spheres, but not for larger, irregular complex structures and tangles.

Specific recommendations regarding characterization of experimental CNT/CNF aerosols are not given in ISO 10808. Gravimetric sampling for mass concentration data is a reliable, though discontinuous, method. The meaning of DMA and SMPS for continuous real-time measurement of the electrical mobility diameter of CNT/CNF is not clarified, as there is no agreement how to interpret the data (Ku et al. 2007). As alternative, a micro-orifice uniform deposit impactor (MOUDI) provides an MMAD and the GSD for size distributions down to 0.1 μm; if used as a low pressure impactor, or nano-MOUDI, aerodynamic size distributions to approximately 10 nm can be determined, although in a discontinuous mode (see Figure 9). The different shapes, structures, and agglomerate sizes are collected based on the aerodynamic properties of the CNT/CNF aerosols. These data are useful for dosimetric extrapolation modeling.

ISO/FDIS10801 (ISO 2010b) is specific for generation of silver NP through an evaporation (heating of solid silver)–condensation method and reiterates general principles of NP properties, their measurements, monitoring, and exposure system operations.

Two ISO technical reports (TR) relate to health and safety assessment at the workplace relevant to nanotechnologies. ISO/TR 27628 (ISO 2007)—workplace atmospheres/ultrafine nanoparticle and nanostructured aerosols/

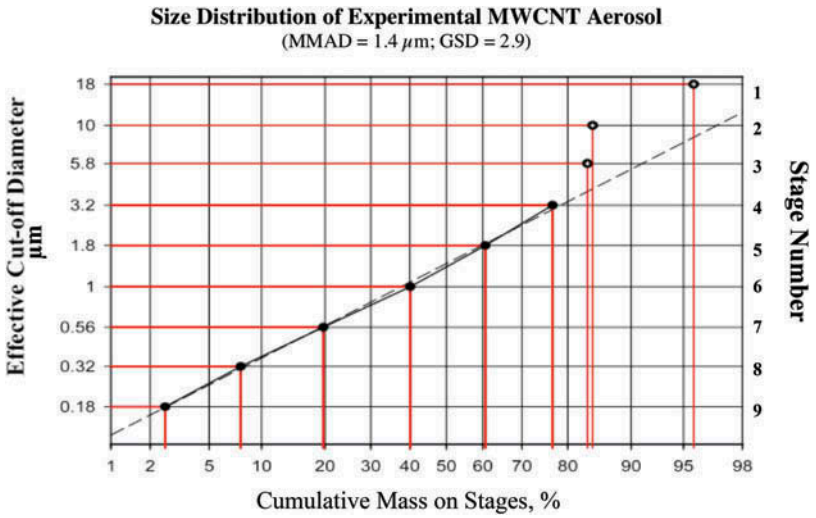

FIGURE 9. MWCNT aerosol size distribution in rodent inhalation study.

MWCNT aerosol size distribution as determined by a nano-MOUDI through weighing of deposits on the individual stages. The aerosol was generated with an acoustic aerosol generation system (Fig. 6) and collected with a 13-stage nano-MOUDI (NanoMoudi-II™ Model 125A, MSP Corp., Shoreview, MN) for 10 minutes at a flow rate of 10 l/min. Lower stages (10–13) were removed because deposits could not be reliably weighed; they contained less than 2% of the total mass. Larger structures with aerodynamic sizes >5 μm contribute much of the total mass concentration of the aerosol, but not to the deposition in the lower respiratory tract of rodents. Thus, describing a CNT/CNF aerosol exposure only by its total airborne mass concentration can be highly misleading when used as comparison to a human exposure concentration. Concepts of dosimetric rodent to human extrapolation discussed in this document have to be taken into consideration.

Placing a cyclone separator in line before the aerosol enters the inhalation chamber may eliminate the non-inhalable tangles. On the other hand, if such larger structures are still inhalable by humans and if they are present at the workplace, it could be considered to use intratracheal inhalation *(Oberdörster et al., 1997)* in rats to circumvent the upper respiratory tract. However, intratracheal inhalation requires anesthesia of rats and is not recommended for day-to- day repeat exposures.

inhalation exposure characterization and assessment—contains sections on source and formation of occupational nano-aerosols, and strategies for their exposure characterization and exposure assessment, including measurement of airborne size distribution by electrical mobility analysis (SMPS) and by aerodynamic inertial impaction. Problems associated with the interpretation of SMPS data when sampling nanofibers and nanotubes are pointed out. These are due to the ill-defined electrical charging of such structures, as has been described in the OECD documents summarized earlier.

Supplementing Current Guidelines

Several issues of importance for risk assessment purposes have not been addressed in currently existing testing guidelines. Some have been alluded to previously, but are included here again with some additional details.

Particle Size Distributions for Worst-Case Inhalation Testing As pointed out earlier in Table 6, optimal particle sizes for inhalation exposure of rodents to dose the alveolar region of the rodent lung should not exceed an MMAD of 2 μm with a GSD up to 3. It would in fact be ideal if experimental exposure atmospheres were correlated to the aerosols to which humans are exposed under real-world occupational or environmental conditions. However, most often these aerosols are of larger, agglomerated sizes with MMAD that are significantly larger, approaching the limits of rodent respirability. Micronization of the agglomerated structures as conducted by Pauluhn (2010) for exposing rats to MWCNT may be one solution to make the aerosol rodent respirable. As indicated by Pauluhn (2010), care has to be taken

that the method of micronization does not alter other physicochemical properties, which in many cases may be difficult to achieve. Still, the objective of a general testing strategy should be to expose the experimental animals to materials that are similar to the pristine materials to which humans are exposed.

To verify appropriate dosing, sensitive analytical methods for quantifying retained doses of CNT/CNF in rodent lungs need to be available (Doudrick et al. 2013; Ohnishi et al. 2013) so that exposure-dose-response relationships can be established (Figure 4). A minimum of three concentrations (plus zero control) should be planned, with the highest at the maximum aerosol concentration (MAC) to deliver the maximum tolerated dose (MTD), and the lowest concentration, if possible, being at the NOAEL (Vu et al. 1996; Morrow et al. 1996; Oberdörster 1997). The MAC should induce significant toxicity without substantially altering the normal life span of the animals, whereas the lowest concentration should not induce toxicity, and some signs of toxicity should be induced at an appropriately spaced intermediate concentration. Measuring retained lung burdens following inhalation exposure of any duration should be mandatory, to be determined in the postexposure recovery phase to define retention and clearance kinetics.

With regard to defining an MFTD for PSP of low cytotoxicity, Muhle et al. (1990) followed suggestions by Morrow (1986) and proposed to use a maximum functionally tolerated dose (MFTD) for these types of particles. Muhle et al. (1990) defined it—based on Morrow (1986)—as "the maximum lung burden above which macrophage-mediated lung clearance is significantly impaired," and suggested as a reasonable criterion a two- to fourfold increase in the alveolar retention half time of the tested or suitable surrogate particulate material. However, one has to be careful in applying this concept of MFTD indiscriminately to any particulate nanomaterial without confirmation that the material to be tested indeed is a PSP material. For example, exposure to crystalline silica and amphibole asbestos—known human carcinogens—also induces significant retardation of alveolar retention halftimes for particles, easily exceeding an assumed MFTD based on volumetric dust overloading of the lung. Although the MFTD concept still is meaningful for such highly reactive persistent particles, it may well be that other endpoints of toxicity are more sensitive, showing significant adverse effects (toxicity) before alveolar macrophage mediated clearance function is affected. Thus, before uncritically focusing solely on this concept of MFTD for nanomaterials, other sensitive endpoints also need to be considered.

Benchmark and Reference Materials The availability of benchmark and reference materials will facilitate the interpretation of results of rodent inhalation studies. *Reference* materials are defined as "sufficiently homogeneous and stable with respect to one or more specified properties . . . [and] established to be fit for its intended use in a measurement process" (ISO 2006). *Benchmark* materials should be well characterized physicochemically and toxicologically for a specific response endpoint and serve as a point of reference for comparing dose-response relationships for use in risk assessment (Oberdörster et al. 2005b; Kuempel et al. 2012). Although, reference and benchmark materials may serve different purposes, ideally, a toxicologically well characterized benchmark material should also be metrologically characterized as reference or certified reference material.

Examples of traceable certified reference materials for use in metrology of nanomaterials that are available at the National Institute for Standards and Technology (NIST) include gold (10, 30, 60 nm), polystyrene (60, 100 nm), TiO_2, and SWCNT (NIST 2012). No MWCNT reference is yet available. Officially sanctioned benchmark materials for purposes of toxicological comparative hazard and risk assessment have not been established. However, Figure 4 shows an example of comparing responses observed in 3-mo rat inhalation studies with CNT and CNF, using as benchmark the data of a previously performed 3-mo rat inhalation study with particles for a rather benign material (CB, negative benchmark control). Ideally, a highly toxic material (e.g., crystalline SiO_2, asbestos) could

be selected as a positive benchmark. However, it was not possible to identify a subchronic rat inhalation study with appropriate endpoints (lung lavage data, lung weight, multidose). If possible, rats would be exposed to positive and/or negative control at the same time; however, given the extraordinary high demand on labor and costs, simultaneous exposures are impractical and not recommended, so the search for previous appropriately performed inhalation studies is suggested. Preferably, benchmark materials should be of similar type and inhalation exposures be of the same duration as used for the material to be tested, but this is impossible for MWCNT given the lack of other prior multidose subchronic MWCNT or CNF inhalation studies.

Postexposure Observation Adding a postexposure recovery or observation period is essential for any type of inhalation exposure, whether subacute, subchronic, or chronic. This not only enables one to obtain information on clearance of the retained lung burden, but also provides evidence of progression or regression of effects observed at the end of exposure. The duration of the postexposure recovery should be at least 1–2 mo for shorter exposures, and approximately 3 mo for subchronic exposures, and longer for chronic 2-yr exposures. The clearance kinetics of different retained lung burdens provide valuable information as to whether the alveolar macrophage clearance function for particles has been affected dose-dependently. Thus, a postexposure period of 60–70 d—which is the physiological retention half time for PSP of low cytotoxicity in rats—needs to be considered as minimum duration for the shorter exposures, and longer recovery times for subchronic and chronic studies. Knowledge about progression of fibrotic or other health effects or their potential revision over this time period is helpful for planning subsequent studies and for risk assessment process. Pauluhn (2010) added a 6-mo postexposure observation period to the 3-mo MWCNT rat inhalation study to determine T½ in the different exposure groups (Table 3).

Monitoring Exposure Atmospheres Use of static size-selective samplers using inertial cascade impactors is discussed in some detail in ISO/TR 27628 (ISO 2007). Potential problems due to overloading (altering impactor characteristics) and bouncing (skewing particle size distribution) are identified. Of importance for nano-aerosols including CNT/CNF, the use of low pressure impactors (nano-MOUDI) is acknowledged, yet longer sampling times for the expected low mass in the 10- to 100-nm particle sizes are required with the potential of overloading the upper stages (>0.5–1 μm). An example of a lab-generated MWCNT aerosol for toxicity testing is shown in Figure 9. Size selective pre-separators may be necessary to avoid upper-stage overloading.

The monitoring and characterization by available instruments discussed in ISO TR27628 for monitoring nano-aerosol exposure are summarized in a table in this document according to mass, number and surface area as endpoints. This table is updated in a second workplace related ISO documentation, ISO/TR12885 (ISO 2008), which is directed at the protection of workers. A major aspect in this ISO guidance document is sampling of particles at the workplace and their characterization. Four tasks are listed to accomplish this: (1) assessment of personal exposure for compliance with regulations, (2) determination of personal exposure for linking with potential adverse health effects in epidemiological studies, (3) identification of major emission sources for establishing targeted control plan, and (4) assessment of efficiency of control systems deployed.

An additional purpose for workplace sampling and characterization that is not listed in the document, but indirectly serves to protect workers' health and to prevent adverse effects, is providing information on the design of relevant animal inhalation studies to assess potential acute and long-term toxicity and the correlation with exposure metrics and dose metrics. In the already-mentioned table of ISO TR 12885, the metrics of mass, number, and surface area are separately grouped as both directly measured and calculated by specific

TABLE 7. Instruments and techniques for characterizing nano-aerosol exposure (modified from ISO TR12885)

Metric	Devices	Remarks	CNT Monitoring *(M) and Quantitation (Q)
Mass directly	Membrane filter sampling	Requires size selective inlet cutoff device to collect only structures <100 nm. However, most aerosols generated from nanomaterials contain larger agglomerates and aggregates so a size limitation may not be meaningful. Gravimetric and chemical analyses can be used. Major problem: separation of background.	Yes(M + Q) (average/integration over longer time)
	Size selective static sampler	The only devices offering a cut point around 100 nm are cascade impactors (Berne-type low pressure impactors, or Microorifice impactors). Allows gravimetric and chemical analysis of samples on stages below 100 nm	Yes (M + Q) (average/integration over longer time)
	TEOM*	Sensitive real-time monitors such as the Tapered Element Oscillating Microbalance (TEOM) might be useable to measure nanoaerosol mass concentration on-line, with a suitable size selective inlet.	Yes (M + Q)
Mass by calculation	ELPI™	Real lime size selective (aerodynamic diameter) detection of active surface-area concentration giving aerosol size distribution. Mass concentration of aerosols can be calculated, only if particle charge and density are assumed or known. Sue selected samples might be further analyzed off-line (as above).	Yes (M) No(Q)
	DMAS	Real-time size-selective (mobility diameter) detection of number concentration, giving aerosol size distribution. Mass concentration of aerosols can be calculated, only if particle shape and density are known or assumed.	Yes (M) No (Q)
Number directly	CPC	CPCs provide real-time number concentration measurements between their particle diameter detection limits. Without a nanoparticle preseparator, they are not specific to the nanometre size range. P-Trak has diffusion screen to limit top size to 1 μm.	Yes (M) No(Q)
Number directly	DMAS	Real-time size-selective (mobility diameter) detection of number concentration, giving number-based size distribution.	Yes (M) No (Q)
	Electron Microscopy	Offline analysis of electron microscope samples can provide information on size-specific aerosol number concentration	Yes (M + Q) and morphology
Mass by calculation	ELPI™	Real-time size-selective (aerodynamic diameter) detection of active surface-area concentration, giving aerosol size distribution, Data might be interpreted in terms of number concentration. Size-selected samples might be further analyzed off-line.	Yes (M) No (Q)
	Diffusion Charger	Real-time measurement of aerosol active surface area. Active surface area does not scale directly with geometric surface area for particles larger than 100 nm. Note that not all commercially available diffusion chargers have a response that scales with particle active surface area for particles smaller than 100 nm. Diffusion chargers are only specific to nanoparticles if used with an appropriate inlet preseparator.	No (M+Q)
Surface-area directly	ELPI™	Real-time size-selective (aerodynamic diameter) detection of active surface-area concentration. Active surface area does not scale directly with geometric surface area for particles larger than 100 nm.	No (M + Q)
	Electron Microscopy	Off-line analysis of electron microscope samples can provide information on particle surface area with respect to size. TEM analysis provides direct information on the projected area of collected particles, which might be related to geometric area for some particle shapes.	Yes (M + Q)

instruments. This table is reproduced here with an addition for applicability to CNT/CNF aerosols (Table 7).

Chapter 5 of ISO TR 12885, entitled "Exposure assessment to nanomaterials," is a useful contribution to our discussion of characterizing CNT/CNF aerosols. This chapter not only provides valuable suggestions for exposure assessment at workplaces, which is necessary complementary information for performing risk assessment together with results of well-designed animal studies, but the aerosol measurement methods discussed in ISO TR12885 can also be applied to characterizing exposures of animal inhalation studies with CNT/CNF. Table 7 expands the table of that ISO document and is expanded to include additional information on the applicability of measurement methods to CNT/CNF aerosols. Future developments of an ideal universal real-time monitoring device that simultaneously measures all three exposure metrics (mass, number, surface area) as well as aerodynamic and mobility behavior may be envisioned (Maynard and Aitken 2007), but its realization is unlikely, at least within the next decade.

Evaluation of Carcinogenicity and Toxicity

The International Agency for Research on Cancer (IARC) convened a Monograph meeting in October 2014, to evaluate—among other compounds—evidence for labeling CNT with respect to carcinogenicity (Grosse et al. 2014). Based on the data of mesothelioma induction by MWCNT-7 in several studies in mice and rats, the Working Group concluded that there is sufficient evidence of carcinogenicity for MWCNT in animals, limited evidence for two other types of MWCNT, and inadequate evidence for SWCNT. Given that there was inadequate evidence in humans and sufficient evidence in two animal species, MWCNT-7 were classified as "possibly carcinogenic to humans" (Group 2B), and other MWCNT and SWCNT as "not classifiable as to their carcinogenicity to humans" (Group 3). Thus, the IARC Working Group acknowledged that differences in biological activities between distinct MWCNT need to be considered for carcinogen classification, given also that mechanistic evidence for carcinogenicity is not strong for any specific CNT. Since the IARC (2014) carcinogenicity classification for MWCNT is presently based on bolus-type ip injection studies in rodents, the outcome of a 2-yr multidose rat inhalation study with MWCNT-7 with respect to their carcinogenicity will be crucial for a final classification of these MWCNT as either a Group 1 or Group 2A or 2B carcinogen. The 2-yr inhalation study has been completed, and results will be published in the near future (Fukushima et al. personal communication).

Results of three of the subchronic inhalation studies in rats with MWCNT and CNF (Table 3) have been used to derive occupational exposure levels (OEL) for workplace exposure based on different methods of extrapolation modeling of a NOAEL or LOAEL of toxicity observed in the rat studies. NIOSH (2013) derived a Recommended Exposure Level of 2 $\mu g/m^3$ and 1 $\mu g/m^3$ for MWCNT and CNF using a Benchmark Dose (BMD) approach; Aschberger et al. (2010) used the approach based on guidance by Registration, Evaluation, Authorization and Restriction of Chemicals (REACH) in Europe to derive OEL of 2 $\mu g/m^3$ and 1 $\mu g/m^3$ for two different MWCNT. In contrast to these extremely low values, Pauluhn (2010), using dosimetric extrapolation and the volumetric overload concept, derived specifically for the MWCNT Baytubes an OEL of 50 $\mu g/m^3$. Results of a 2-yr rat inhalation study with MWCNT are forthcoming (Fukushima et al. personal communication) and will be essential for deriving more definitely an OEL.

RECOMMENDATION/CONCLUSION

General

- Inhalation is the preferred method to obtain data necessary for risk assessment of pulmonary exposure to CNT/CNF. Intratracheal instillation or pharyngeal aspiration may be useful exposure techniques for hazard characterization and for screening various types of CNT/CNF for relative toxicity.

However, effects due to bolus delivery (very high dose rate) need to be considered and—if dispersants are used to suspend CNT/CNF in a liquid—responses and biokinetics may be altered.

- The rat is the preferred rodent species. Rats have been found in studies with fine particles to be more sensitive regarding fibrosis and lung tumor responses than mice. In addition, the availability of larger tissues is of advantage (e.g., lavage of only the right lung and save the left lung for histology/histochemistry). Rodent respirability (Table 6) has to be considered to optimize deposition in the lower respiratory tract (MMAD $\leq$ 2 μm). One may increase sensitivity to observe lung cancer or mesothelioma with KO mouse models, which would provide information concerning mechanisms of action. In general, mesothelioma induction by inhaled fibrous particles in rats is a rare event, and hamsters would be the preferred species for this endpoint (McConnell et al. 1999).
- Whole-body exposure is less stressful and thus preferred over nose-only exposure, in particular for 90-d and longer inhalation studies.
- At present, 90-d inhalation studies are preferred (Bernstein et al. 2005; see objectives in Table 5), with CNT/CNF aerosol characterization according to OECD/EPA general guidelines for performing a subchronic study. In general, OECD test guidelines, guidance, and good laboratory practices for subchronic inhalation studies are applicable; however, modification noted here should be considered. Physicochemical properties of the as-produced and as-administered material should be characterized (Table 8).
- Use a minimum of three concentrations that include a NOAEL and an MTD. Determination of retained lung burden is essential in order to express results based on dose-response data rather than only as exposure-response relationship. Risk assessment prefers at least one dose that gives a positive response (e.g., MTD). However, use of a dose for this purpose far exceeding the MTD may be of little practical value and leads to erroneous conclusions.
- Inclusion of a postexposure observation/recovery period is highly desirable. This would be specifically important for the highest concentration to determine regression, persistence, or progression of effects, and to determine retention/clearance kinetics in primary and secondary organs.
- A 28-d inhalation exposure may provide sufficient information with added postexposure observation/recovery time. Shorter repeat exposures (5–10 d) designed to achieve the same retained lung burdens as in a 90-d study by using higher concentrations need to consider the potential impact of significant differences in dose rate.
- Precede the 90-d inhalation study with an acute 1- to 10-d inhalation study with 3 or more concentrations in order to identify effects; estimate exposure concentrations for subchronic 90-d study; and verify aerosol characteristics and evenness of chamber distribution and general tolerance of the animals to exposure. (*Inhalation study may be preceded by dose-response study with intratracheal instillation (rats), oropharyngeal aspiration (mice), to identify types of effects.)*

Sample Preparation of CNT/CNF for Inhalation

Use pristine material as experienced by human inhalation exposures; no treatment with dispersant or sonication to mimic human exposure, but consider rodent/human differences in respirability. Aerosolization from liquid suspension needs to consider likely impact of alteration of pristine CNT/CNF. Micronization of non-rat-respirable larger agglomerates needs to assure that no alteration of CNT or CNF surfaces is introduced.

Aerosol Generation

- Generators: Dry powder generators are highly preferred. Sufficient agitation is required to achieve CNT/CNF aerosols that would be representative of the size distribution of CNT/CNF structures found at human exposure sites. Need to avoid changing CNT/CNF morphology (cutting,

TABLE 8. Recommendation for exposure characterization of sampled and airborne CNT/CNF (modified from Oberdörster et al., 2005)

	Human exposure		Rodent Exposure	
Characterization Type	Aerosol	Supplied material	Aerosol	Filter samples
Size distribution (primary particles)	E	D	E	D
Agglomeration/aggregation state	E	D	E	D*
Density	D	E	D	N
Shape	E	E	E	E
Surface area	O	E	D	D*
Concentration, mass and number	E	–	E	E
Composition	E	E	E	E
Surface chemistry	O	E	D	D
Surface contamination	D	E	D	E
Surface charge – suspension/solution	O	O	D	E
Surface charge – powder	D	O	D	E
Crystal structure	D	E	D	E
Particle physicochemical structure	D	E	D	E
Solubility	N	E	N	E
Porosity	N	E	N	N
Method of production	E	E	E	E
Preparation process	E	E	E	E
Heterogeneity	D	E	E	E
Prior storage of material	E	E	E	E

E: These characterizations arc considered to be essential and to be available for each characterization at least once.

D: These characterizations are considered to provide valuable information, but are not recommended as essential due to constraints associated with complexity, cost and method availability.

O: These characterizations are considered to provide valuable but non-essential information.

N: These characterizations are not considered to be essential for all studies.

*The CNT/CNF property is assumed to be the same as in the supplied material and therefore no need to repeat measurement. If the CNT/CNF material has been altered from that supplied (e.g., micronization), then the new properties as used in the rodent assay have to be determined.

shearing, breaking) and producing CNT/CNF contamination (addition of metals) from a generator device. If a liquid suspension is used, consider alteration of surface properties of the pristine material due to dispersants.

- It is key to mimic human exposure in terms of aerosol characteristics and concentrations. Therefore, it is essential to obtain available information about such human exposure at workplaces and to consumers. However, to allow for adequate penetration of CNTs and CNFs into the lower respiratory tract, the generated aerosol of singlets, agglomerated structures, or aggregated structures should be administered to rodents with an MMAD of less than or equal to 2 μm, and GSD not exceeding 3.
- If no human exposure data are available, generate a rodent-respirable CNT/CNF aerosol (mix of individual structures and agglomerated versus well-dispersed forms). In order to optimize the composition of such mix, knowledge about effects of preferentially single CNT/CNF structures and of preferentially tangles of CNT/CNF would be helpful (see Research Gaps).
- Consider including the use of positive (asbestos) and negative (CB) benchmark controls where feasible. Otherwise, considering the high cost of nanomaterial inhalation studies, data on new CNT/CNF should be anchored to preexisting studies with appropriate benchmark materials. (See Research Gaps for identifying reference CNT/CNF.)

CNT Aerosol Characterization/Monitoring

Evaluate size distribution, mass, number concentration, agglomeration/aggregation state (see later description), density, and other

physicochemical characteristics, such as surface properties, impurities, length, diameter, dissolution, and leaching (in vivo and in vitro) related to biodurability/biopersistence. Table 8 lists recommendations for characterization of CNT/CNF aerosols occurring for human exposures (workplace, consumer) and experimental animal exposures. They are identified by their essentiality for CNT/CNF based on the general recommendations on nanomaterial characterization by participants of a 2005 ILSI Workshop (Oberdörster et al. 2005b).

Endpoints

- As listed in the OECD and EPA 90-d inhalation guidelines, one should monitor conventional standard endpoints listed there. Of particular importance are lung weight changes as integrating indicator of adverse effects.

In addition, the following should be considered as

a. Mandatory:
   - Pulmonary endpoints should include lung lavage (BALF) analysis for lung damage (cellular, biochemical, cytokines) related to inflammation and oxidative stress.
   - Retained lung burden at end of exposure and in postexposure period to establish exposure-dose-response relationships and clearance kinetics as essential data for purposes of risk assessment.
   - Histopathology (see existing guidelines) should include specific staining for fibrosis and analysis of granulomatous lesions, cell proliferation and pleural response.
b. Optional, evaluation of:
   - Cardiovascular effects (heart rate, blood pressure, microvascular effects, levels of clotting factors in the blood).
   - Systemic effects (acute-phase proteins to assess systemic inflammation, e.g., fibrinogen, CRP, IL-6).
   - CNS effects (markers of inflammation and damage; behavioral tests).
   - Bone-marrow effects and effects in other sensitive organs.

- Dosimetry/biokinetics: Evaluation of deposition, translocation, accumulation, elimination/clearance (e.g., lung; pleura; liver; spleen; heart; CNS; bone marrow) and for determining pulmonary retention T½ should be included as an important goal in the study design. This requires sensitive analytical methods for detecting retained CNT/CNF in the primary and secondary targets. Analysis of CNT/CNF retention separately for BALF cells, supernatant, and lung tissue and lymph nodes (bifurcational vs. supramediastinal) is desirable.

Instrumentation

The usefulness and limitations of instruments for measuring size, mass, and number concentration needs to be understood (Table 7):

- Mass, gravimetric (filter; mass only; averaging over time): nano-MOUDI (aerodynamic size distribution and mass, see Figure 9, averaging over time); TEOM (real-time monitoring mass only); APS (optical short time, size, number, and mass, but only above approximately 300 nm).
- Number: CPC (real-time, no size information; okay for monitoring stability); SMPS; DMAS (size distribution with unknown relevancy; caveats).
- Morphology, shape: TEM; SEM; scanning transmission electron microscopy (STEM).
- Surface area: BET.

Data Analysis

Could include:

- Interpretation of aerosol characterization data.
- Evaluation of exposure-dose-response dose response, including the NOAEL and postexposure time course (retention; persistence/resolution of effects).
- Considering the need for a risk assessment if the NOAEL is at a high exposure concentration of rodent-respirable aerosol (>50 mg/m^3) and results demonstrate high

lung burden (>2 mg/g) in a 28-d or even 90-d study (including 90-d recovery period).
- Dosimetric extrapolation to humans (dose/alveolar epithelial surface area) of deposited dose (only short-term; no retention data needed) and retained dose (preferable, but retention T½ required).

Research Gaps/Needs

A number of publications have pointed out potential risks of nanomaterials as discussed at the beginning of this document. After reports described mesothelioma-inducing asbestos-like effects of MWCNT in 2008/2009, concerns increased and CNT/CNF-specific reviews (Donaldson et al. 2006; 2010) and documents (NIOSH Intelligence Bulletin, 2013) emphasized the need for preventive measures, avoiding exposure, and called for more research to understand the risk of CNT/CNF exposure. In fact, the NIOSH Intelligence Bulletin (2013) derived a recommended exposure level for CNT and for CNF of 1 $\mu g/m^3$.

The ultimate goal is to develop a scientifically well supported realistic risk assessment of CNT/CNF inhalation exposure. Are all CNT/CNF to be treated the same in terms of their potential or potency of causing fibrosis, cancer, and diverse systemic adverse effects? Most likely there may be differences in bioactivity between SWCNT and MWCNT and CNF, as well as differences within each group (raw vs. purified CNT/CNF, functionalization, length or width, agglomerated *vs*. dispersed).

There is an urgent need to address this using inhalation as the most prominent route of exposure, and carrying out appropriately designed and executed studies is key. Although IT instillation or pharyngeal aspiration studies may be useful in ranking the relative bioactivity of various CNT/CNF, they cannot replace inhalation studies. A future goal is to move from reliance on in vivo studies toward acceptance of alternative testing strategies including predictive validated in vitro screening tests. This should be a high priority, requiring highly focused research efforts and sufficient funding.

The following list of research needs was generated to fill data gaps for improving the design, analyses, interpretation, and extrapolation of results of inhalation studies in order to refine our ability to perform meaningful risk assessments in the absence of human epidemiological data. Addressing these research needs will lead to the development of new concepts for assessing the biokinetics and toxicity of inhaled CNT/CNF and for the understanding of results from acute and chronic inhalation studies:

- Determine accumulation and clearance kinetics: T½ and translocation to secondary target organs (pleura; CNS; bone marrow).
- Compare results of inhalation exposure of individual versus heavily agglomerated CNT/CNF: Is response different?
- Define inhalability and respirability of highly variable CNT/CNF aerosol shapes and incorporate into existing predictive deposition models.
- Determine the suitability of a 28-d inhalation study plus postexposure period to replace 90-d subchronic study.
- Perform chronic inhalation study (1 yr or longer + long postexposure period) to determine tumorigenic (rat, lung tumor) and mesotheliogenic (hamster mesothelioma) potential of MWCNT that tested positive in ip studies.
- Measure equivalent diameters in various instruments that simulate CNT/CNF deposition in the lung, such as impactor (impaction diameter), diffusion battery (diffusion diameter), elutriator (sedimentation diameter). *(These diameters are needed to assess the CNT/CNF dose to the lung.)*
- Determine in vivo translocation to pleura of inhaled CNT/CNF tangles versus inhaled single CNT/CNF, considering also rigidity and flexibility, as well as length and diameter.
- Develop and optimize sensitive detection/quantification methods in tissue for deposited/translocated CNT/CNF.
- Develop a validated method to determine effective density of CNT/CNF aerosol.

- Identify reference material for CNT/CNF (positive and negative controls).
- Compare effects of liquid aerosol (+ surfactant) versus dry aerosol at the same deposited dose.
- Evaluate inhalation exposure-dose-response data with dose as mass, number, and surface area: impact of dose metric?
- Compare/correlate acute and long-term effects and biokinetics of instilled (single/repeat dosing) versus inhaled CNT/CNF.
- Correlate in vivo with in vitro response to develop and validate simple predictive high-throughput assays, as part of a tiered testing approach incorporating in vitro (cell-free and cellular) and in vivo (acute, repeat) studies emphasizing exposure-dose-response analysis.
- Develop a universal monitoring instrument for combined measurement of aerosol exposure characteristics for mass, number, surface area, volume distribution, and morphology (Wang et al. 2011).
- Determine exposure data during CNT/CNF life cycle.
- Determine in vivo (lung, secondary tissues) adsorption of proteins and change in associated particle surface properties and the impact on kinetics and effects in vivo.
- Identify underlying mechanisms of toxicity and its dependence on dose.
- Investigate stability of agglomerates depositing in the lung: Does lung surfactant and/or tissue motion disperse CNT/CNF? Dispersion is likely to facilitate interstitial uptake.
- Investigate species differences in biological sensitivity to CNT/CNF between rodents and humans.

ACKNOWLEDGMENTS

Portions of this work were funded by the U.S. Environmental Protection Agency, Office of Pollution Prevention and Toxics (OPPT) under EPA contract EP-W-09-27 (GO, BA), supported in part by NIEHS Grant P30 ESO1247 (GO), and the National Science Foundation EPSCoR Research Infrastructure Improvement Cooperative Agreement #1003907 (VC). The authors wish to thank Mrs. Judy Havalack for outstanding editorial assistance in the preparation of this article.

DISCLAIMER

Views expressed in this document are those of the authors and do not necessarily reflect EPA or NIOSH policy.

REFERENCES

ACGIH. 2010. *2010 TLVs® and BEIs®, Threshold limit values for chemical substances and physical agents & biological exposure indices*. ACGIH Publications, Cincinnati, OH.

Ahn, K.-H., S.-M. Kim, and I. J. Yu. 2011. Multi-walled carbon nanotube (MWCNT) dispersion and aerosolization with hot water atomization without addition of any surfactant. *Safety and Health at Work* 2:65–69. doi:10.5491/SHAW.2011.2.1.65.

Aiso, S., K. Yamazaki, Y. Umeda, M. Asakura, T. Kasai, M. Takaya, T. Toya, S. Koda, K. Nagano, H. Arito, and S. Fukushima. 2010. Pulmonary toxicity of intratracheally instilled multiwall carbon nanotubes in male Fischer 344 rats. *Industrial Health* 48:783–95. doi:10.2486/indhealth.MS1129.

Aitken, R. J., P. E. J. Baldwin, G. C. Beaumont, L. C. Kenny, and A. D. Maynard. 1999. Aerosol inhalability in low air movement environments. *Journal of Aerosol Science* 30:613–26. doi:10.1016/S0021-8502(98)00762-9.

Allen, B. L., P. D. Kichambare, P. Gou, I. I. Vlasova, A. A. Kapralov, N. Konduru, V. E. Kagan, and A. Star. 2008. Biodegradation of single-walled carbon nanotubes through enzymatic catalysis. *Nano Letters* 8: 3899–903. doi:10.1021/nl802315h.

Allen, B. L., G. P. Kotchey, Y. Chen, N. V. K. Yanamala, J. Klein-Seetharaman, V. E. Kagan, and A. Star. 2009. Mechanistic investigations of horseradish peroxidase-catalyzed degradation of single-walled carbon nanotubes. *Journal of the American Chemical Society* 131:17194–205. doi:10.1021/ja9083623.

Asbach, C., H. Kaminski, D. Von Barany, T. A. J. Kuhlbusch, C. Monz, N. Dziurowitz, J. Pelzer, K. Vossen, K. Berlin, S. Dietrich, U. Götz, H.-J. Kiesling, R. Schierl, and D. Dahmann. 2012. Comparability of portable nanoparticle exposure monitors. *Annals of Occupational Hygiene* 56:606–21.

Aschberger, K., H. J. Johnston, V. Stone, R. J. Aitken, S. M. Hankin, S. A. K. Peters, C. L. Tran, and F. M. Christensen. 2010. Review of carbon nanotubes toxicity and exposure—Appraisal of human health risk assessment based on open literature. *Critical Reviews in Toxicology* 40:759–90. doi:10.3109/10408444.2010.506638.

Asgharian, B., W. Hofmann, and R. Bergmann. 2001. Particle deposition in a multiple-path model of the human lung. *Aerosol Science and Technology* 34:332–39. doi:10.1080/02786820119122.

Asgharian, B., J. T. Kelly, and E. W. Tewksbury. 2003. Respiratory deposition and inhalability of monodisperse aerosols in Long-Evans rats. *Toxicological Sciences* 71:104–11. doi:10.1093/toxsci/71.1.104.

Asgharian, B., and O.T. Price. 2006. Airflow Distribution in the Human Lung and its Influence on Particle Deposition, *Inhalation Toxicology* 18:795–801.

Asgharian, B., and O. T. Price 2008. A predictive model of inhaled nanofibers/nanotubes deposition in the human lung. Final report submitted to CDC/NIOSH.

Baisch, B. L., N. M. Corson, P. Wade-Mercer, R. Gelein, A. J. Kennell, G. Oberdörster, and A. Elder. 2014. Equivalent titanium dioxide nanoparticle deposition by intratracheal instillation and whole body inhalation: The effect of dose rate on acute respiratory tract inflammation. *Particle Fibre Toxicology* 11:5.

Ballou, B., B. C. Lagerholm, L. A. Ernst, M. P. Bruchez, and A. S. Waggoner. 2004. Non-invasive imaging of quantum dots in mice. *Bioconjugate Chemistry* 15:79–86. doi:10.1021/bc034153y.

Baron, P. A., G. J. Deye, B. T. Chen, D. Schwegler-Berry, A. A. Shvedova, and V. Castranova. 2008. Aerosolization of single-walled carbon nanotubes for an inhalation study. *Inhalation Toxicology* 20:751–60. doi:10.1080/08958370801975303.

Baumgartner, H., and C. R. E. Coggins. 1980. Description of a continuous smoking inhalation machine for exposing small animals to tobacco smoke. *Beiträge zur Tabakforschung International* 10:169–74.

Bazile, D., C. Ropert, P. Huve, T. Verrecchia, M. Mariard, A. Frydman, M. Veillard, and G. Spenlehauer. 1992. Body distribution of fully biodegradable [^{14}C]-poly(lactic acid) nanoparticles coated with albumin after parenteral administration to rats. *Biomaterials* 13:1093–102. doi:10.1016/0142-9612(92)90142-B.

Bernstein, D., V. Castranova, K. Donaldson, B. Fubini, J. Hadley, T. Hesterberg, A. Kane, D. Lai, E. E. McConnell, H. Muhle, G. Oberdorster, S. Olin, and D. B. Warheit. 2005. Testing of fibrous particles: Short-term assays and strategies. ILSI report. *Inhalation Toxicology* 17:497–537. doi:10.1080/08958370591001121.

Bernstein, D. M., and R. Drew. 1980. Experimental approaches for exposure to sized glass fibers. *Environmental Health Perspectives* 34:47–57. doi:10.1289/ehp.803447.

Bernstein, D. M., R. A. Rogers, R. Sepulveda, K. Donaldson, D. Schuler, S. Gaering, P. Kunzendorf, J. Chevalier, and S. E. Holm. 2011. Quantification of the pathological response and fate in the lung and pleura of chrysotile in combination with fine particles compared to amosite-asbestos following short-term inhalation exposure. *Inhalation Toxicology* 23:372–91. doi:10.3109/08958378.2011.575413.

Bernstein, D. M., P. Thevenaz, H. Fleissner, R. Anderson, T. W. Hesterberg and R. Mast. 1995. Evaluation of the oncogenic potential of man-made vitreous fibres: the inhalation model. *Ann Occup Hyg* 39(5): 661–672.

Berry, R. D., and F. Froude 1989. An investigation of wind conditions in the workplace to assess their effect on the quantity of dust inhaled. HSE Internal Report IR/L/DS/

89/3, Health and Safety Executive, London, UK.

Birch, M. E., B.-K. Ku, D. E. Evans, and T. A. Ruda-Eberenz. 2011. Exposure and emissions monitoring during carbon nanofiber production—Part I: Elemental carbon and iron-soot aerosols. *Annals of Occupational Hygiene* 55:1016–36. doi:10.1093/annhyg/mer073.

Bolton, R. E., J. H. Vincent, A. D. Jones, J. Addison, and S. T. Beckett. 1983. An overload hypothesis for pulmonary clearance of UICC amosite fibres inhaled by rats. *British Journal of Industrial Medicine* 40:264–72.

Bonner, J. C., R. M. Silva, A. J. Taylor, J. M. Brown, S. C. Hilderbrand, V. Castranova, D. W. Porter, A. Elder, G. Oberdörster, J. Harkema, L. A. Bramble, T. J. Kavanagh, D. Botta, A. Nel, and K. E. Pinkerton. 2013. interlaboratory evaluation of rodent pulmonary responses to engineered nanomaterials: The NIEHS Nano GO Consortium. *Environmental Health Perspectives* 121:676–82. doi:10.1289/ehp.1205693.

Borm, P. J. A., F. Kelly, N. Kunzli, R. P. F. Schins, and K. Donaldson. 2006. Oxidant generation by particulate matter: From biologically effective dose to a promising, novel metric. *Occupational and Environmental Medicine* 64(2): 73–74. doi:10.1136/oem.2006.029090

Brain, J. D., D. E. Knudson, S. P. Sorokin, and M. A. Davis. 1976. Pulmonary distribution of particles given by intratracheal instillation or by aerosol inhalation. *Environmental Research* 11:13–33. doi:10.1016/0013-9351(76)90107-9.

Breysse, P. N., and D. L. Swift. 1990. Inhalability of large particles into the human nasal passage: In vivo studies in still air. *Aerosol Science and Technology* 13:459–64. doi:10.1080/02786829008959460.

Broaddus, V. C., J. I. Everitt, B. Black, and A. B. Kane. 2011. Non-neoplastic and neoplastic pleural endpoints following fiber exposure. *Journal of Toxicology and Environmental Health, Part B* 14:153–78. doi:10.1080/10937404.2011.556049.

Brown, J. S. 2005. Particle inhalability at low wind speeds. *Inhalation Toxicology* 17:831–37. doi:10.1080/08958370500241296.

Brunauer, S., P. H. Emmett, and E. Teller. 1938. *Adsorption of gases in multimolecular layers J. Amer. Chem. Soc.*, 60:309 Contribution From the Bureau of Chemsitry and Soils and George Washington University.

Cagle, D. W., S. J. Kennel, S. Mirzadeh, J. M. Alford, and L. J. Wilson. 1999. In vivo studies of fullerene-based materials using endohedral metallofullerene radiotracers. *Proceedings of the National Academy of Sciences of the United States of America* 96:5182–87. doi:10.1073/pnas.96.9.5182.

Cannon, W. C., E. F. Blanton, and K. E. McDonald. 1983. The flow-past chamber: An improved nose-only exposure system for rodents. *American Industrial Hygiene Association Journal* 44:923–28. doi:10.1080/15298668391405959.

Carrero-Sánchez, J. C., A. L. Elías, R. Mancilla, G. Arrellín, H. Terrones, J. P. Laclette, and M. Terrones. 2006. Biocompatibility and toxicological studies of carbon nanotubes doped with nitrogen. *NanoLetters* 6:1609–16. doi:10.1021/nl060548p.

CEN ISO/TS 27687. 2008. *Nanotechnologies—Terminology and definitions for nano-objects—Nanoparticle, nanofiber and nanoplate*. International Organization for Standardization, Geneva, Switzerland.

Coggins, C. R. E., P. H. Ayres, A. T. Mosberg, J. W. Sagart, and A. W. Hayes. 1993. Comparative inhalation study in rats using cigarettes containing tobacco expanded with chlorofluorocarbon-11 (CFC-11) or hydrochlorofluorocarbon-123 (HCFC-123). *Inhalation Toxicology* 5:97–115. doi:10.3109/08958379309034496.

Coggins, C. R. E., J. S. Edmiston, A. M. Jerome, T. B. Langston, E. J. Senaa, D. C. Smith, and M. J. Oldham. 2011. A comprehensive evaluation of the toxicology of cigarette ingredients: Essential oils and resins. *Inhalation Toxicology* 23(S1): 41–69. doi:10.3109/08958378.2010.543188

Coppeta, L., J. Legramante, A. Galante, A. J. Bergamashi, E. Bergamashi, A. Margrini, and A. Pietroiusti. 2007. Interaction between carbon nanotubes and cardiovascular autonomic nervous system regulation: Proposal of an animal model and preliminary findings. *Giornale Italiano di Medicina del Lavoro Ergonomics* 5:465–67.

Dahm, M. M., D. E. Evans, M. K. Schubauer-Berigan, M. E. Birch, and J. A. Deddens. 2013. Occupational exposure assessment in carbon nanotube and nanofiber primary and secondary manufacturers: Mobile direct-reading sampling. *Annals of Occupational Hygiene* 57:328–44. doi:10.1093/annhyg/mes079.

Dahm, M. M., D. E. Evans, M. K. Schubauer-Berigan, M. E. Birch, and J. E. Fernback. 2012. Occupational exposure assessment in carbon nanotube and nanofiber primary and secondary manufacturers. *Annals of Occupational Hygiene* 56:542–56.

De Volder, M. F. L., S. H. Tawfick, R. H. Baughman, and A. J. Hart. 2013. Carbon nanotubes: Present and future commercial applications. *Science* 339:535–39. doi:10.1126/science.1222453.

DeLorme, M. P., Y. Muro, T. Arai, D. A. Banas, S. R. Frame, K. L. Reed, and D. B. Warheit. 2012. Ninety-day inhalation toxicity study with a vapor grown carbon nanofiber in rats. *Toxicological Sciences* 128:449–60. doi:10.1093/toxsci/kfs172.

Dick, C. A. J., D. M. Brown, K. Donaldson, and V. Stone. 2003. The role of free radicals in the toxic and inflammatory effects of four different ultrafine particle types. *Inhalation Toxicology* 15:39–52. doi:10.1080/08958370304454.

DIN EN 725–9 2006–05(E). 2006. Deutsches Institut fur Normung E.V. Advanced technical ceramics—Method of test for ceramic powders—Part 9: Determination of untapped bulk density. DAkkS (Deutsche Akkreditierungsstelle). Accessed July 15, 2015. http://www.beuth.de/en/standard/din-en-725-9/88827999.

Donaldson, K., R. Aitken, L. Tran, V. Stone, R. Duffin, G. Forrest, and A. Alexander. 2006. Carbon nanotubes: A review of their properties in relation to pulmonary toxicology and workplace safety. *Toxicological Sciences* 92:5–22. doi:10.1093/toxsci/kfj130.

Donaldson, K., P. H. Beswick, and P. S. Gilmour. 1996. Free radical activity associated with the surface of particles: A unifying factor in determining biological activity? *Toxicology Letters* 88:293–98. doi:10.1016/0378-4274(96)03752-6.

Donaldson, K., F. A. Murphy, R. Duffin, and C. A. Poland. 2010. Asbestos, carbon nanotubes and the pleural mesothelium: A review and the hypothesis regarding the role of long fibre retention in the parietal pleura, inflammation and mesothelioma. *Particle and Fibre Toxicology* 7:5.

Donaldson, K., A. Schinwald, F. Murphy, W.-S. Cho, R. Duffin, L. Tran, and C. Poland. 2013. The biologically effective dose in inhalation nanotoxicology. *Accounts of Chemical Research* 46:723–32. doi:10.1021/ar300092y.

Dorries, A. M., and P. A. Valberg. 1992. Heterogeneity of phagocytosis for inhaled versus instilled material. *American Review of Respiratory Disease* 146:831–37. doi:10.1164/ajrccm/146.4.831.

Doudrick, K., N. Corson, G. Oberdörster, A. C. Eder, P. Herckes, R. U. Halden, and P. Westerhoff. 2013. Extraction and quantification of carbon nanotubes in biological matrices with application to rat lung tissue. *ACS Nano* 02 September 2013. http://pubs.acs.org 7:8849–56. doi:10.1021/nn403302s.

Driscoll, K., D. Costa, G. Hatch, R. Henderson, G. Oberdörster, H. Salem, and R. Schlesinger. 2000. Intratracheal instillation as an exposure technique for the evaluation of respiratory tract toxicity: Uses and limitations. *Toxicological Sciences* 55:24–35. doi:10.1093/toxsci/55.1.24.

Duffin, R., L. Tran, D. Brown, V. Stone, and K. Donaldson. 2007. Proinflammogenic effects of low-toxicity and metal nanoparticles in vivo and in vitro: Highlighting the role of particle surface area and surface reactivity. *Inhalation Toxicology* 19:849–56. doi:10.1080/08958370701479323.

Dutta, D., S. K. Sundaram, J. G. Teeguarden, B. J. Riley, L. S. Fifield, J. M. Jacobs, S. R. Addleman, G. A. Kaysen, B. M. Moudgil, and T. J. Weber. 2007. Adsorbed proteins influence the biological activity and molecular targeting of nanomaterials. *Toxicological Sciences* 100:303–15. doi:10.1093/toxsci/kfm217.

Elder, A., R. Gelein, J. N. Finkelstein, K. E. Driscoll, J. Harkema, and G. Oberdörster. 2005. Effects of subchronically inhaled carbon black in three species. I. Retention kinetics, lung inflammation, and histopathology. *Toxicological Sciences* 88:614–29. doi:10.1093/toxsci/kfi327.

Elder, A., R. Gelein, V. Silva, T. Feikert, L. Opanashuk, J. Carter, R. Potter, A. Maynard, Y. Ito, J. Finkelstein, and G. Oberdörster. 2006. Translocation of inhaled ultrafine manganese oxide particles to the central nervous system. *Environmental Health Perspectives* 114:1172–78. doi:10.1289/ehp.9030.

Elías, A. L., J. C. Carrero-Sánchez, H. Terrones, M. Endo, J. P. Laclette, and M. Terrones. 2007. Viability studies of pure carbon- and nitrogen-doped nanotubes with *Entamoeba histolytica:* From amoebicidal to biocompatible structures. *Small* 3:1723–29. doi:10.1002/(ISSN)1613-6829.

EPA. 1998. Health effects test guidelines, OPPTS870.3465 90-day inhalation toxicity. EPA 712-C-98-204, August.

EPA. 2000. *OPPTS 870. 3465, US EPA health effects test guidelines, 90-day inhalation toxicity*. EPA 712-C-98-204. Washington, DC: Environmental Protection Agency.

EPA. 2001. *OPPTS 870. 8355,US EPA health effects test guidelines, combined chronic toxicity/carcinogenicity testing of repirable fibrous particles*. EPA 712-C01-352, July Washington, DC: Environmental Protection Agency.

EPA. 2004. *Air quality criteria for particulate matter*. EPA/600/P-99/002aF; EPA/600/P-99/002bF, October. Washington, DC: Environmental Protection Agency.

Erdely, A., T. Hulderman, R. Salmen, A. Liston, P. C. Zeidler-Erdely, D. Schwegler-Berry, V. Castranova, S. Koyama, Y.-A. Kim, M. Endo, and P. P. Simeonova. 2009. Cross-talk between lung and systemic circulation during carbon nanotube respiratory exposure. *Potential Biomarkers Nano Letters* 9: 36–43.

Esch, R. K., L. Han, K. K. Foarde, and D. S. Ensor. 2010. Endotoxin contamination of engineered nanomaterials. *Nanotoxicology* 4:73–83. doi:10.3109/17435390903428851.

Evans, D. E., B. K. Ku, M. E. Birch, and K. H. Dunn. 2010. Aerosol monitoring during carbon nanofiber production: Mobile direct-reading sampling. *Annals of Occupational Hygiene* 54:514–31. doi:10.1093/annhyg/meq015.

Fawcett, T. W., S. L. Sylvester, K. D. Sarge, R. I. Morimoto, and N. J. Holbrook. 1994. Effects of neurohormonal stress and aging on the activation of mammalian heat shock factor 1. *Journal of Biological Chemistry* 269:32272–78.

Fenoglio, I., G. Greco, M. Tomatis, J. Muller, E. Raymundo-Piñero, F. Béguin, A. Fonseca, J. B. Nagy, D. Lison, and B. Fubini. 2008. Structural defects play a major role in the acute lung toxicity of multiwall carbon nanotubes: Physicochemical aspects. *Chemical Research in Toxicology* 21:1690–97. doi:10.1021/tx800100s.

Frampton, M. W., J. C. Stewart, G. Oberdörster, P. E. Morrow, D. Chalupa, A. P. Pietropaoli, L. M. Frasier, D. M. Speers, C. Cox, L.-S. Huang, and M. J. Utell. 2006. Inhalation of ultrafine particles alters blood leukocyte expression of adhesion molecules in humans. *Environmental Health Perspectives* 114:51–58. doi:10.1289/ehp.7962.

Fubini, B., M. Ghiazza, and I. Fenoglio. 2010. Physico-chemical features of engineered nanoparticles relevant to their toxicity. *Nanotoxicology* 4:347–63. doi:10.3109/17435390.2010.509519.

Fujitani, Y., A. Furuyama, and S. Hirano. 2009. Generation of airborne multi-walled carbon nanotubes for inhalation studies. *Aerosol Science and Technology* 43:881–90. doi:10.1080/02786820903002423.

Gasser, M., B. Rothen-Rutishauser, H. F. Krug, P. Gehr, M. Nelle, B. Yan, and P. Wick. 2010. The adsorption of biomolecules to multi-walled carbon nanotubes is influenced by bothpulmonary surfactant lipids and surface chemistry. *Journal of Nanobiotechnology* 8:31.

Gasser, M., P. Wick, M. J. D. Clift, F. Blank, L. Diener, Y. Yan, P. Gehr, H. F. Krug, and B. Rothen-Rutishauser. 2012. Pulmonary surfactant coating of multi-walled carbon nanotubes (MWCNT) influences their oxidative andpro-inflammatory potential in vitro. *Particle and Fibre Toxicology* 9:17.

Gehr, P., M. Bachofen, and E. R. Weibel. 1978. The normal human lung: Ultrastructure and morphometric estimation of diffusion capacity. *Respiration Physiology* 32:121–40. doi:10.1016/0034-5687(78)90104-4.

Gibaud, S., J. P. Andreux, C. Weingarten, M. Renard, and P. Couvreur. 1994. Increased bone marrow toxicity of doxorubicin bound to nanoparticles. *European Journal of Cancer* 30:820–26. doi:10.1016/0959-8049(94)90299-2.

Gibaud, S., M. Demoy, J. P. Andreux, C. Weingarten, B. Gouritin, and P. Couvreur. 1996. Cells involved in the capture of nanoparticles in hematopoietic organs. *Journal of Pharmaceutical Sciences* 85:944–50. doi:10.1021/js960032d.

Gibaud, S., C. Rousseau, C. Weingarten, R. Favier, L. Douay, J. P. Andreux, and P. Couvreur. 1998. Polyalkylcyanoacrylate nanoparticles as carriers for granulocyte-colony stimulating factor (G-CSF). *Journal of Controlled Release* 52:131–39. doi:10.1016/S0168-3659(97)00194-6.

Goodglick, A., and A. B. Kane 1996. The role of fiber length in crocidolite abestos toxicity in vitro and in vivo. VIIth International Pneumoconioses Conference Pittsburgh, Pennsylvania.

Gordon, C. J. 1993. *Temperature regulation in laboratory rodents*. New York, NY: Cambridge University Press.

Gregoratto, D., M. R. Bailey, and J. W. Marsh. 2011. Particle clearance in the alveolar-interstitial region of the human lungs: Model validation. *Radiation Protection Dosimetry* 144:353–56. doi:10.1093/rpd/ncq314.

Grosse, Y., K. Z. Guyton, B. Lauby-Secretan, F. El Ghissassi, V. Bouvard, L. Benbrahim-Tallaa, N. Guha, C. Scoccianti, H. Mattock, and K. Straif, on behalf of the IARC Monograph Working Group. 2014. Carcinogenicity of fluoro-edenite, silicon carbide fibres and whiskers, and carbon nanotubes. *Lancet/Oncology* 15: 1427–28.

Guo, N. L., Y.-W. Wan, J. Denvir, D. W. Porter, M. Pacurari, M. G. Wolfarth, V. Castranova, and Y. Qian. 2012. Multiwalled carbon nanotube-induced gene signatures in the mouse lung: Potential predictive value for human lung cancer risk and prognosis. *Journal of Toxicology and Environmental Health, Part A* 75:1129–53. doi:10.1080/15287394.2012.699852.

Han, J. H., E. J. Lee, J. H. Lee, K. P. So, Y. H. Lee, G. N. Bae, S. Lee, J. H. Ji, M. H. Cho, and I. J. Yu. 2008. Monitoring multiwalled carbon nanotube exposure in carbon nanotube research facility. *Inhalation Toxicology* 20:741–49. doi:10.1080/08958370801942238.

Han, S. G., R. Andrews, and C. G. Gairola. 2010. Acute pulmonary response of mice to multi-wall carbon nanotubes. *Inhalation Toxicology* 22:340–47. doi:10.3109/08958370903359984.

Han, S. G., D. Howatt, A. Daugherty, and G. Gairola. 2015. Pulmonary and atherogenic effects of multi-walled carbon nanotubes (MWCNT) in apolipoprotein-E-deficient mice. *Journal of Toxicology and Environmental Health, Part A* 78:244–53. doi:10.1080/15287394.2014.958421.

Haniu, H., N. Saito, Y. Matsuda, Y.-A. Kim, K. C. Park, T. Tsukahara, Y. Usui, K. Aoki, M. Shimizu, N. Ogihara, K. Hara, S. Takanashi, M. Okamoto, N. Ishigaki, K. Nakamura, and H. Kato. 2011.

Effect of dispersants of multi-walled carbon nanotubes on cellular uptake and biological responses. *International Journal of Nanomedicine* 6:3295–307.

Harris, P. J. F.. 2005. New perspectives on the structure of graphitic carbons. *Critical Reviews in Solid State and Materials Sciences* 30:235–53. doi:10.1080/10408430500406265.

Hemenway, D. R., M. P. Absher, L. Trombley, and P. M. Vacek. 1990. Comparative clearance of quartz and cristobalite from the lung. *American Industrial Hygiene Association Journal* 51:363–69. doi:10.1080/15298669091369790.

Hesseltine, G. R., R. K. Wolff, R. L. Hanson, R. O. McClellan, and J. L. Mauderly. 1985. Comparison of lung burdens of inhaled particles of rats exposed during the day or night. *Journal of Toxicology and Environmental Health* 16:323–29. doi:10.1080/15287398509530744.

Hinds, W. C., N. J. Kennedy, and K. Tatyan. 1998. Inhalability of large particles for mouth and nose breathing. *Journal of Aerosol Science* 29(suppl. 1): S277–S278. doi:10.1016/S0021-8502(98)00416-9

Hsieh, S.-F., D. Bello, D. F. Schmidt, A. K. Pal, and E. J. Rogers. 2012. Biological oxidative damage by carbon nanotubes: Fingerprint or footprint? *Nanotoxicology* 6:61–76. doi:10.3109/17435390.2011.553689.

Hsu, D.-J., and D. L. Swift. 1999. The measurements of human inhalability of ultralarge aerosols in calm air using mannikinS. *Journal of Aerosol Science* 30:1331–43. doi:10.1016/S0021-8502(99)00022-1.

Hyung, H., J. D. Fortner, J. B. Hughes, and J.-H. Kim. 2007. Natural organic matter stabilizes carbon nanotubes in the aqueous phase. *Environment Science & Technology* 41:179–84. doi:10.1021/es061817g.

Ichihara, G., V. Castranova, A. Tanioka, and K. Miyazawa. 2008. Letter to editor, Induction of mesothelioma in p53 +/- mouse by intraperitoneal application of multi-walled carbon nanotube. *Journal of Toxicological Sciences* 33:381–82. doi:10.2131/jts.33.381.

International Life Sciences Institute. 2000. The relevance of the rat lung response to particle overload for human risk assessment: A workshop consensus report. *Inhalation Toxicology* 12:1–17. doi:10.1080/08958370050029725.

International Organization for Standardization. 2005a. ISO 15901-1. Pore size distribution and porosity of solid materials by mercury porosimetry and gas adsorption. Part 1: Mercury porosimetry. Accessed July 15, 2015. htttp://www.iso.org/iso/home

International Organization for Standardization. 2005b. ISO/IEC 17025. General requirements for the competence of testing and calibration laboratories.

International Organization for Standardization. 2006. *ISO guide 35: 2006: Reference materials—General and statistical principles for certification*. Geneva, Switzerland: International Organization for Standardization.

International Organization for Standardization. 2007. ISO/TR 27628. Workplace atmospheresUltrafine, nanoparticle and nano-structured aerosols—Inhalation exposure characterization and assessment.

International Organization for Standardization. 2008. ISO/TR12885. Technical Report: Nanotechnologies—Health and safety practices in occupational settings relevant to nanotechnologies.

International Organization for Standardization. 2009. ISO 15900. Determination of particle size distribution—Differential electrical mobility analysis for aerosol particles.

International Organization for Standardization. 2010a. ISO Standard 10808. ISO/TC229—Nanotechnologies—Characterization of nanoparticles in inhalation exposure chambers for inhalation toxicity testing.

International Organization for Standardization. 2010b. ISO/FDIS10801. Nanotechnologies—Generation of metal nanoparticles for inhalation toxicity testing using the evaporation/condensation method.

Jarabek, A. M., B. Asgharian, and F. J. Miller. 2005. Dosimetric adjustments for interspecies extrapolation of inhaled poorly soluble particles (PSP). *Inhalation Toxicology* 17:317–34. doi:10.1080/08958370590929394.

Jiang, J., G. Oberdörster, and P. Biswas. 2009. Characterization of size, surface charge, and agglomeration state of nanoparticle dispersions for toxicological studies. *Journal of Nanoparticle Research* 11:77–89. doi:10.1007/s11051-008-9446-4.

Johnson, D. R., M. M. Methner, A. J. Kennedy, and J. A. Steevens. 2010. Potential for occupational exposure to engineered carbon-based nanomaterials in environmental laboratory studies. *Environmental Health Perspectives* 118:44–54.

Kagan, V. E., Y. Y. Tyurin, V. A. Tyurin, N. V. Konduru, A. I. Potapovich, A. Osipov, E. R. Kisin, D. Schwegler-Berry, R. Mercer, V. Castranova, and A. A. Shvedova. 2006. Direct and indirect effects of single walled carbon nanotubes on RAW 264.7 macrophages: Role of iron. *Toxicology Letters* 165:88–100. doi:10.1016/j.toxlet.2006.02.001.

Kan, H., Z. X. Wu, S.-H. Young, T.-H. Chen, J. L. Cumpston, F. Chen, M. L. Kashon, and V. Castranova. 2012. Pulmonary exposure of rats to ultrafine titanium dioxide enhances cardiac protein phosphorylation and substance P synthesis in nodose ganglia. *Nanotoxicology* 6:736–45. doi:10.3109/17435390.2011.611915.

Kasai, T., K. Gotoh, T. Nishizawa, T. Sasaki, T. Katagiri, Y. Umeda, T. Toya, and S. Fukushima. 2014. Development of a new multi-walled carbon nanotube (MWCNT) aerosol generation and exposure system and confirmation of suitability for conducting a single-exposure inhalation study of MWCNT in rats. *Nanotoxicology* 8:169–78. doi:10.3109/17435390.2013.766277.

Kasai, T., Y. Umeda, M. Ohnishi, H. Kondo, T. Takeuchi, S. Aiso, T. Nishizawa, M. Matsumoto, and S. Fukushima. 2015. Thirteen-week study of toxicity of fiber-like multi-walled carbon nanotubes with whole-body inhalation exposure in rats. *Nanotoxicology* 9:413–22.

Kennedy, N. J., and W. C. Hinds. 2002. Inhalability of large solid particles. *Journal of Aerosol Science* 33:237–55. doi:10.1016/S0021-8502(01)00168-9.

Keskinen, J., K. Pietarinen, and M. Lehtimäki. 1992. Electrical low pressure impactor. *Journal of Aerosol Science* 23:353–60. doi:10.1016/0021-8502(92)90004-F.

Keyhani, K., P. W. Scherer, and M. M. Mozell. 1997. A numerical model of nasal odorant transport for the analysis of human olfaction. *Journal of Theoretical Biology* 186:279–301. doi:10.1006/jtbi.1996.0347.

Khandoga, A., A. Stampfl, S. Takenaka, H. Schulz, R. Radykewicz, W. Kreyling, and F. Krombach. 2004. Ultrafine particles exert prothrombotic but not inflammatory effects on the hepatic microcirculation in healthy mice in vivo. *Circulation* 109:1320–25. doi:10.1161/01.CIR.0000118524.62298.E8.

Kido, T., M. Tsunoda, T. Kasai, T. Sasaki, Y. Umeda, H. Senoh, H. Yanagisawa, M. Asakura, Y. Aizawa, and S. Fukushima. 2014. The increases in relative mRNA expressions of inflammatory cytokines and chemokines in splenic macrophages from rats exposed to multi-walled carbon nanotubes by whole-body inhalation for 13 weeks. *Inhalation Toxicology* 26:750–58. doi:10.3109/08958378.2014.953275.

Kim, J.-E., H.-T. Lim, A. Minai-Tehrani, J.-T. Kwon, J.-Y. Shin, C.-G. Woo, M. Choi, J. Baek, D. H. Jeong, Y.-C. Ha, C.-H. Chae, K.-S. Song, K.-H. Ahn, J.-H. Lee, H.-J. Sung, I.-J. Yu, G. R. Beck, and M.-H. Cho. 2010a. Toxicity and clearance of intratracheally administered multiwalled carbon nanotubes from murine lung. *Journal of Toxicology and Environmental Health, Part A* 73:1530–43. doi:10.1080/15287394.2010.511578.

Kim, S. C., D.-R. Chen, C. Qi, R. M. Gelein, J. N. Finkelstein, A. Elder, K. Bentley, G. Oberdörster, and D. H. Y. Pui. 2010b. A nanoparticle dispersion method for in vitro and in vivo nanotoxicity study.

Nanotoxicology 4:42–51. doi:10.3109/17435390903374019.

Kim, Y. A., T. Hayashi, M. Endo, and M. Dresselhaus. 2013. Carbon nanofibers. In *Springer handbook of nanomaterials*, R. Vajtai ed., 233–62. Berlin, Germany: Springer-Verlag.

Kimbell, J. S., M. N. Godo, E. A. Gross, D. R. Joyner, R. B. Richardson, and K. T. Morgan. 1997. Computer simulation of inspiratory airflow in all regions of the F344 rat nasal passages. *Toxicology and Applied Pharmacology* 145:388–98. doi:10.1006/taap.1997.8206.

Kingston, C., R. Zepp, A. Andrady, D. Boverhof, R. Fehir, D. Hawkins, J. Roberts, P. Sayre, B. Shelton, Y. Sultan, V. Vejins, and W. Wohlleben. 2014. Release characteristics of selected carbon nanotube polymer composites. *Carbon* 68:33–57. doi:10.1016/j.carbon.2013.11.042.

Knuckles, T. L., J. Yi, D. G. Frazer, H. D. Leonard, B. T. Chen, V. Castranova, and T. R. Nurkiewicz. 2012. Nanoparticle inhalation alters systemic arteriolar vasoreactivity through sympathetic and cyclooxygenase-mediated pathways. *Nanotoxicology* 6:724–35. doi:10.3109/17435390.2011.606926.

Kobayashi, N., M. Naya, M. Ema, S. Endoh, J. Maru, K. Mizuno, and J. Nakanishi. 2010. Biological response and morphological assessment of individually dispersed multi-wall carbon nanotubes in the lung after intratracheal instillation in rats. *Toxicology* 276:143–53. doi:10.1016/j.tox.2010.07.021.

Koblinger, L. 1985. Analysis of human lung morphometric data for stochastic aerosol deposition calculations. *Physics in Medicine and Biology* 30:541–56. doi:10.1088/0031-9155/30/6/004.

Kotchey, G. P., Y. Zhao, V. E. Kagan, and A. Star. 2013. Peroxidase-mediated biodegradation of carbon nanotubes in vitro and in vivo. *Advanced Drug Delivery Reviews* 65:1921–32. doi:10.1016/j.addr.2013.07.007.

Krajnak, K., S. Waugh, C. Johnson, R. Miller, and M. Kiedrowski. 2009. Vibration disrupts vascular function in a model of metabolic syndrome. *Industrial Health* 47:533–42. doi:10.2486/indhealth.47.533.

Kreyling, W. G., M. Semmler-Behnke, J. Seitz, W. Scymczak, A. Wenk, P. Mayer, S. Takenaka, and G. Oberdörster. 2009. Size dependence of the translocation of inhaled iridium and carbon nanoparticle aggregates from the lung of rats to the blood and secondary target organs. *Inhalation Toxicology* 21 (S1):55–60. doi:10.1080/08958370902942517

Ku, B. K., and J. F. De La Mora. 2009. Relation between electrical mobility, mass, and size for nanodrops 1–6.5 nm in diameter in air. *Aerosol Science and Technology* 43:241–49. doi:10.1080/02786820802590510.

Ku, B. K., M. S. Emery, A. D. Maynard, M. R. Stolzenburg, and P. H. McMurry. 2006. In situ structure characterization of airborne carbon nanofibres by a tandem mobility–mass analysis. *Nanotechnology* 17:3613–21. doi:10.1088/0957-4484/17/14/042.

Ku, B. K., A. D. Maynard, P. A. Baron, and G. J. Deye. 2007. Observation and measurement of anomalous responses in a differential mobility analyzer caused by ultrafine fibrous carbon aerosols. *Journal of Electrostatics* 65:542–48. doi:10.1016/j.elstat.2006.10.012.

Kuempel, E. D., V. Castranova, C. L. Geraci, and P. A. Schulte. 2012. Development of risk-based nanomaterial groups for occupational exposure control. *Journal of Nanoparticle Research* 14:15. doi:10.1007/s11051-012-1029-8.

Kuempel, E. D., E. J. O'Flaherty, L. T. Stayner, R. J. Smith, F. H. Y. Green, and V. Vallyathan. 2001. A biomathematical model of particle clearance and retention in the lungs of coal miners. I. Model development. *Regulatory Toxicology and Pharmacology* 34:69–87. doi:10.1006/rtph.2001.1479.

Lam, G.-W., J. T. James, R. McCluskey, and R. L. Hunter. 2004. Pulmonary toxicity of single-wall carbon nanotubes in mice 7 and 90 days

after intratracheal instillation. *Toxicological Sciences* 77:125–34.

LeBlanc, A. J., J. L. Cumpston, B. T. Chen, D. Frazer, V. Castranova, and T. R. Nurkiewicz. 2009. Nanoparticle inhalation impairs endothelium-dependent vasodilation in subepicardial arterioles. *Journal of Toxicology and Environmental Health, Part A* 72:1576–84. doi:10.1080/15287390903232467.

Lee, K. P., H. J. Trochimowcz, and C. F. Reinhardt 1985. Pulmonary response of rats exposed to titanium dioxide (TiO_2) by inhalation for two years. *Toxicology and Applied Pharmacology* 79: 179–192.

Lee, J. H., S.-B. Lee, G. N. Bae, K. S. Jeon, J. U. Yoon, J. H. Ji, J. H. Sun, B. G. Lee, J. H. Lee, J. S. Yang, H. Y. Kim, C. S. Kang, and I. J. Yu. 2010. Exposure assessment of carbon nanotube manufacturing workplaces. *Inhalation Toxicology* 22:369–81. doi:10.3109/08958370903367359.

Legramante, J. M., F. Valentini, A. Magrini, G. Palleschi, S. Sacco, I. Iavicoli, M. Pallante, D. Moscone, A. Galante, E. Bergamaschi, A. Bergamaschi, and A. Pietroiusti. 2009. Cardiac autonomic regulation after lung exposure to carbon nanotubes. *Human & Experimental Toxicology* 28:369–75. doi:10.1177/0960327109105150.

Li, J.-G., W.-X. Li, J.-Y. Xu, X.-Q. Cai, R.-L. Liu, Y.-J. Li, Q.-F. Zhao, and Q.-N. Li. 2007a. Comparative study of pathological lesions induced by multiwalled carbon nanotubes in lungs of mice by intratracheal instillation and inhalation. *Environmental Toxicology* 22:415–21. doi:10.1002/(ISSN)1522-7278.

Li, R., X. Wang, Z. Ji, B. Sun, H. Zhang, C. H. Chang, S. Lin, H. Meng, Y.-P. Liao, M. Wang, Z. Li, A. A. Hwang, T.-B. Song, R. Xu, Y. Yang, J. I. Zink, A. Nel, and T. Xia. 2013. Surface charge and cellular processing of covalently functionalized multiwall carbon nanotubes determine pulmonary toxicity. *ACS Nano* 7:2352–68. doi:10.1021/nn305567s.

Li, Z., T. Hulderman, R. Salmen, R. Chapman, S. S. Leonard, A. Shvedova, M. I. Luster, and P. P. Simeonova. 2007b. Cardiovascular effects of pulmonary exposure to single-wall carbon nanotubes. *Environmental Health Perspectives* 115:377–88. doi:10.1289/ehp.9688.

Liang, G., L. Yin, J. Zhang, R. Liu, T. Zhang, B. Ye, and Y. Pu. 2010. Effects of subchronic exposure to multi-walled carbon nanotubes on mice. *Journal of Toxicology and Environmental Health, Part A* 73:463–70. doi:10.1080/15287390903523378.

Liu, A., K. Sun, J. Yang, and D. Zhao. 2008. Toxicological effects of multi-wall carbon nanotubes in rats. *Journal of Nanoparticle Research* 10:1303–07. doi:10.1007/s11051-008-9369-0.

Liu, J.-H., S.-T. Yang, H. Wang, and Y. Liu. 2010b. Advances in biodistribution study and tracing methodology of carbon nanotubes. *Journal of Nanoscience and Nanotechnology* 10:8469–81. doi:10.1166/jnn.2010.2689.

Liu, Q., X. Ma, and M. R. Zachariah. 2012. Combined on-line differential mobility and particle mass analysis for determination of size resolved particle density and microstructure evolution. *Microporous and Mesoporous Materials* 153:210–16.

Liu, X., R. H. Hurt, and A. B. Kane. 2010a. Biodurability of single-walled carbon nanotubes depends on surface functionalization. *Carbon* 48:1961–69.

Ma-Hock, L., S. Burkhardt, V. Strauss, A. O. Gamer, K. Wiench, B. Van Ravenzwaay, and R. Landsiedel. 2009b. Development of a short-term inhalation test in the rat using nano-titanium dioxide as a model substance. *Inhalation Toxicology* 21:102–18.

Ma-Hock, L., S. Trenmann, V. Strauss, S. Brill, F. Luizi, M. Mertler, K. Wiench, A. O. Gamer, B. Van Ravenzwaay, and R. Landsiedel. 2009a. Inhalation toxicity of multiwall carbon nanotubes in rats exposed for 3 months. *Toxicological Sciences* 112:468–81.

Mangum, J. B., E. A. Turpin, A. Antao-Menezes, M. F. Cesta, E. Bermudez, and J. C. Bonner. 2006. Single-walled carbon nanotubes (SWCNT)-induced interstitial fibrosis in the lungs of rats is associated with increased levels of PDGF mRNA and the formation

of unique intercellular carbon structures that bridge alveolar macrophages in situ. *Particle and Fibre Toxicology* 3:15. doi:10.1186/1743-8977-3-15.

Matsumoto, M., H. Serizawa, M. Sunaga, H. Kato, M. Takahashi, M. Hirata-Koizumi, A. Ono, E. Kamata, and A. Hirose. 2012. No toxicological effects on acute and repeated oral gavage doses of single-wall or multi-wall carbon nanotube in rats. *Journal of Toxicological Sciences* 37: 463–74.

Mauderly, J. L. 1986. Respiration of F344 rats in nose-only inhalation exposure tubes. *Journal of Applied Toxicology* 6:25–30.

Maynard, A. D., and R. J. Aitken. 2007. Assessing exposure to airborne nanomaterials: Current abilities and future requirements. *Nanotoxicology* 1:26–41.

Maynard, A. D., P. A. Baron, M. Foley, A. A. Shvedova, E. R. Kisin and V. Castranova. 2004. Exposure to carbon nanotube material: Aerosol release during the handling of unrefined single-walled carbon nanotube material. J. *Toxicology & Environmental Health, Part A* 67:87–107.

Maynard, A. D., P. A. Baron, M. Foley, A. A. Shvedova, E. R. Kisin, and V. Castranova. 2009. Exposure to carbon nanotube material during the handling of unrefined single walled carbon nanotube material. *Journal of Toxicology and Environmental Health A* 67:87–107.

Maynard, A. D., B. K. Ku, M. Emery, M. R. Stolzenburg, and P. H. McMurry. 2006. Measuring particle size-dependent physiochemical structure in airborne single walled carbon nanotube agglomerates. *Journal of Nanoparticle Research* 9 :865–92.

McConnell, E. E., C. Axten, T. W. Hesterberg, J. Chevalier, J. Miiller, J. Everitt, G. Oberdörster, G. R. Chase, P. Thevenaz, and P. Kotin. 1999. Studies on the inhalation toxicology of two fiberglasses and amosite asbestos in the Syrian golden hamster. Part II. Results of chronic exposure. *Inhalation Toxicology* 11:785–835.

McKinney, W., B. Chen, and D. Frazer. 2009. Computer controlled multi-walled carbon nanotube inhalation exposure system. *Inhalation Toxicology* 21:1053–61.

Meier, R., K. Clark, and M. Riediker. 2013. Comparative testing of a miniature diffusion size classifier to assess airborne ultrafine particles under field conditions. *Aerosol Science and Technology* 47:22–28.

Ménache, M. G., F. J. Miller, and O. G. Raabe. 1995. Particle inhalability curves for humans and small laboratory animals. *Annals of Occupational Hygiene* 39:317–28.

Mercer, R. R., A. F. Hubbs, J. F. Scabilloni, L. Wang, L. Battelli, D. Schwegler-Berry, V. Castranova, and D. W. Porter. 2010a. Distribution and persistence of pleural penetrations by multi-walled carbon nanotubes. *Particle and Fibre Toxicology* 7:28.

Mercer, R. R., A. F. Hubbs, J. F. Scabilloni, L. Wang, L. A. Battelli, S. Friend, V. Castranova, and D. W. Porter. 2011. Pulmonary fibrotic response to aspiration of multi-walled carbon nanotubes. *Particle and Fibre Toxicology* 8:21.

Mercer, R. R., J. Scabilloni, L. Wang, E. Kisin, A. R. Murray, D. Schwegler-Berry, A. A. Shvedova, and V. Castranova. 2008. Alteration of deposition pattern and pulmonary response as a result of improved dispersion of aspirated single walled carbon nanotubes in a mouse model. *American Journal of Physiology: Lung Cellular and Molecular Physiology* 294: L87–L97.

Mercer, R. R., J. F. Scabilloni, A. F. Hubbs, L. A. Battelli, W. McKinney, S. Friend, M. G. Wolfarth, M. Andrew, V. Castranova, and D. W. Porter. 2013a. Distribution and fibrotic response following inhalation exposure to multi-walled carbon nanotubes. *Particle and Fibre Toxicology* 10:33.

Mercer, R. R., J. F. Scabilloni, A. F. Hubbs, L. Wang, L. A. Battelli, W. McKinney, V. Castranova, and D. W. Porter. 2013b. Extrapulmonary transport of MWCNT following inhalation exposure. *Particle and Fibre Toxicology* 10:38.

Mercer, R. R., J. F. Scabilloni, L. Wang, L. A. Battelli, and V. Castranova. 2009. Use of labeled single walled carbon nanotubes to study translocation from the lungs. *Toxicologist* 108:A2192.

Mercer, R. R., J. F. Scabilloni, L. Wang, L. A. Battelli, and V. Castranova. 2010. Use of labeled single walled carbon modulates arteriolar sympathetic constriction: Role of nitric oxide, prostanoids, and α-adrenergic receptors. *Toxicologist* 114:A1728.

Methner, M., L. Hodson, A. Dames, and C. Geraci. 2010. Nanoparticle Emission Assessment Technique (NEAT) for the identification and measurement of potential inhalation exposure to engineered nanomaterials—Part B: Results from 12 field studies. *Journal of Occupational and Environmental Hygiene* 7:163–76.

Miller, F. J., B. Asgharian, J. D. Schroeter, O. Price, R. A. Corley, D. R. Einstein, R. E. Jacob, T. C. Cox, S. Kabilan, and T. Bentley. 2014. Respiratory tract lung geometry and dosimetry model for male Sprague-Dawley rats. *Inhalation Toxicology* 26: 524–44.

Miller, F. J., S. W. Kaczmar, R. Danzeisen, and O. R. Moss. 2013. Estimating lung burdens based on individual particle density estimated form scanning electron microscopy and cascade impactor samples. *Inhalation Toxicology* 25:813–27.

Miller, F. J., J. S. Kimbell, R. J. Preston, J. H. Overton, E. A. Gross, and R. B. Conolly. 2011. The fractions of respiratory tract cells at risk in formaldehyde carcinogenesis. *Inhalation Toxicology* 23: 689–706.

Mitchell, L. A., J. Gao, R. V. Wal, A. Gigliotti, S. W. Burchiel, and J. D. McDonald. 2007. Pulmonary and systemic immune response to inhaled multiwalled carbon nanotubes. *Toxicological Sciences* 100: 203–14.

Moalli, P. A., J. L. MacDonald, L. A. Goodglick, and A. B. Kane. 1987. Acute injury and regeneration of the mesothelium in response to asbestos fibers. *American Journal of Pathology* 128:426–45.

Morello, M., C. L. Krone, S. Dickerson, E. Howerth, W. A. Germishuizen, Y. L. Wong, D. Edwards, B. R. Bloom, and M. K. Hondalus. 2009. Dry-powder pulmonary insufflation in the mouse for application to vaccine or drug studies. *Tuberculosis* 89:371–77.

Morrow, P. E. 1986. The setting of particulate exposure levels for chronic inhalation toxicity studies. *Journal of the American College of Toxicology* 5:533–44.

Morrow, P. E. 1988. Possible mechanisms to explain dust overloading of the lungs. *Fundamental and Applied Toxicology* 10:369–84.

Morrow, P. E., J. K. Haseman, C. H. Hobbs, K. E. Driscoll, V. Vu, and G. Oberdörster. 1996. Workshop overview—The maximum tolerated dose for inhalation bioassays: Toxicity vs. overload. *Fundamental and Applied Toxicology* 29:155–67.

Moss, O. R., R. A. James, and B. Asgharian. 2006. Influence of exhaled air on inhalation exposure delivered through a directed-flow nose-only exposure system. *Inhalation Toxicology* 18:45–51.

Muhle, H., B. Bellmann, O. Creutzenberg, R. Fuhst, W. Koch, U. Mohr, S. Takenaka, P. Morrow, R. Kilpper, J. MacKenzie, and R. Mermelstein. 1990. Subchronic inhalation study of toner in rats. *Inhalation Toxicology* 2:341–60.

Muller, J., F. Huaux, N. Moreau, P. Misson, J.-F. Heilier, M. Delos, M. Arras, A. Fonseca, J. B. Nagy, and D. Lison. 2005. Respiratory toxicity of multi-wall carbon nanotubes. *Toxicology and Applied Pharmacology* 207:221–31.

Muller, J., M. Delos, N. Panin, V. Rabolli, F. Huaux, and D. Lison. 2009. Absence of carcinogenic response to multiwall carbon nanotubes in a 2-year bioassay in the peritoneal cavity of the rat. *Toxicological Sciences* 110: 442–47.

Murphy, F. A., C. A. Poland, R. Duffin, K. T. Al-Jamal, H. Ali-Boucetta, A. Nunes, F. Byrna, A. Prina-Mello, Y. Volkov, S. Li, S. J. Mathor, A. Bianco, M. Prato, A. MacNea, W. A. Wallace, K. Kosturelos, and K. Donaldson.

2011. Length-dependent retension of carbon nanotubes in the pleural space of mice initiates sustained inflammation and progressive fibrosis on the parietal pleura. *American Journal of Pathology* 178:2587–600.

Murray, A. R., E. R. Kisin, A. V. Tkach, N. Yanamala, R. Mercer, S. H. Young, B. Fadeel, V. E. Kagan, and A. A. Shvedova. 2012. Factoring-in agglomeration of carbon nanotubes and nanofibers for better prediction of their toxicity versus asbestos. *Particle and Fibre Toxicology* 9:10.

Myojo, T., T. Oyabu, K. Nishi, C. Kadoya, I. Tanaka, M. Ono-Ogaswara, H. Sakae, and T. Shirai. 2009. Aerosol generation and measurement of multi-wall carbon nanotubes. *Journal of Nanoparticle Research* 11:91–99.

Nagai, H., Y. Okazaki, S. H. Chew, N. Misawa, Y. Yamashita, S. Akatsuka, T. Ishihara, K. Yamashita, Y. Yoshikawa, H. Yasui, L. Jiang, H. Ohara, T. Takahashi, G. Ichihara, K. Kostarelos, Y. Miyata, H. Shinohara, and S. Toyokuni. 2011. Diameter and rigidity of multiwalled carbon nanotubes are critical factors in mesothelial injury and carcinogenesis. *Proceedings of the National Academy of Sciences of the United States of America* 108:1330–38.

Nanomaterial Registry. 2014. Accessed August 15, 2014. https://www.nanomaterialregistry.org/about/MinimalInformationStandards.asppx.

Narciso, S. P., E. Nadziejko, L. C. Chen, T. Gordon, and C. Nadziejko. 2003. Adaptation to stress induced by restraining rats and mice in nose-only inhalation holders. *Inhalation Toxicology* 15:1133–43.

National Institute for Occupational Safety and Health. 2003. Elemental carbon (diesel particulate)—Method 5040. *NIOSH manual of analytical methods*, 4th ed., 2003 issue 3. NIOSH.

National Institute for Occupational Safety and Health. 2012. General safe practices for working with engineered nanomaterials in research laboratories. Accessed August 15, 2014. http://www.cdc.gov/niosh/doc/2012.147/.

National Institute for Occupational Safety and Health. 2013. *Current Intelligence Bulletin 65: Occupational exposure to carbon nanotubes and nanofibers*. NIOSH/CDC/Department of Health and Human Services. Atlanta: NIOSH/CDC.

National Institute of Standards and Technology. 2012. Presentation, BERM-13 meeting, Vienna, Austria, June 2012: Development of nanoscale reference materials at NIST, presented by Stephen Wise (NIST).

Nel, A. E., L. Mädler, D. Velegol, T. Xuia, E. M. V. Hoek, P. Somasundaran, F. Klaessig, V. Castranova, and M. Thompson. 2009. Understanding biophysicochemical interactions at the nano-bio interface. *Nature Materials* 8:543–57.

Nikula, K. J., K. J. Avila, W. C. Griffith, and J. L. Mauderly. 1997. Lung tissue responses and sites of particle retention differ between rats and cynomolgus monkeys exposed chronically to diesel exhaust and coat dust. *Fundamental and Applied Toxicology* 37:37–53.

Nikula, K. J., V. Vallyathan, F. H. Green, and F. F. Hahn. 2001. Influence of exposure concentration or dose on the distribution of particulate material in rat and human lungs. *Environmental Health Perspectives* 109:311–18.

Nowak, B., R. David, H. Fissan, H. Morris, J. Shatkin, M. Stintz, R. Zepp, and D. Brower. 2013. Potential release scenarios for carbon nanotubes used in composites. *Environment International* 59:1–11.

Nurkiewicz, T. R., D. W. Porter, M. Barger, L. Millecchia, K. M. Rao, P. J. Marvar, A. F. Hubbs, and V. Castranova. 2006. Systemic microvascular dysfunction and inflammation after pulmonary particulate matter exposure. *Environmental Health Perspectives* 114:412–19.

Nurkiewicz, T. R., D. W. Porter, A. F. Hubbs, J. L. Cumpston, B. T. Chen, D. G. Frazer, and V. Castranova. 2008. Nanoparticle inhalation augments particle-dependent systemic microvascular dysfunction. *Particle and Fibre Toxicology* 5:1.

Nurkiewicz, T. R., D. W. Porter, A. F. Hubbs, S. Stone, B. T. Chen, D. G. Frazer, M. A. Boegehold, and V. Castranova. 2009. Pulmonary nanoparticle exposure disrupts systemic microvascular nitric oxide signaling. *Toxicological Sciences* 110:191–203.

Oberdörster, G. 1989. Dosimetric principles for extrapolating results of rat inhalation studies to humans, using nickel as an example. *Health Physics* 57 (suppl. 1): 213–20.

Oberdörster, G. 1997. Pulmonary carcinogenicity of inhaled particles and the maximum tolerated dose. *Environmental Health Perspectives* 195(suppl. 5): 1347–56.

Oberdörster, G. 2012. Correspondence: Nanotoxicology: *In vitro–in vivo* dosimetry. *Environmental Health Perspectives* 120:A13.

Oberdörster, G., C. Cox, and R. Gelein. 1997. Intratracheal instillation versus intratracheal inhalation of tracer particles for measuring lung clearance function. *Experimental Lung Research* 23:17–34.

Oberdörster, G., J. Ferin, and B. E. Lehnert. 1994a. Correlation between particle size, in vivo particle persistence, and lung injury. *Environmental Health Perspectives* 102(suppl. 5): 173–79.

Oberdörster, G., J. Ferin, S. C. Soderholm, R. Gelein, C. Cox, R. Baggs, and P. E. Morrow. 1994b. Increased pulmonary toxicity of inhaled ultrafine particles: Due to lung overload alone? *Annals of Occupational Hygiene* 38(suppl. 1): 295–302.

Oberdörster, G., A. Maynard, K. Donaldson, V. Castranova, J. Fitzpatrick, K. D. Ausman, J. Carter, B. Karn, W. Kreyling, D. Lai, S. Olin, N. Monteiro-Riviere, D. Warheit, and H. Yang, A.A.R.F.I.R. Foundation. 2005b. Principles for characterizing the potential human health effects from exposure to nanomaterials: Elements of a screening strategy. *Particle and Fibre Toxicology* 2:8.

Oberdörster, G., E. Oberdörster, and J. Oberdörster. 2005a. Invited review: Nanotoxicology: An emerging discipline evolving from studies of ultrafine particles. *Environmental Health Perspectives* 113:823–39.

Oberdörster, G., Z. Sharp, V. Atudorei, A. Elder, R. Gelein, W. Kreyling, and C. Cox. 2004. Translocation of inhaled ultrafine particles to the brain. *Inhalation Toxicology* 16: 437–45.

Organization for Economic Cooperation and Development. 2009a. OECD Guideline for the testing of chemicals, section 4: Health effects. Test no. 413: Subchronic inhalation toxicity: 90-Day study. Test Guideline 413 (TG 413), adopted 7 September.

Organization for Economic Cooperation and Development. 2009b. Organization for Economic Cooperation and Development. 2009. Environment, health and safety publications, series on testing and assessment, no. 39: Guidance document on acute inhalation toxicity testing. ENV/JM/MONO 28. 21 July.

Organization for Economic Cooperation and Development. 2010. OECD Environment, health and safety publications—Series on the safety of manufactured nanomaterials, no. 14: Guidance manual for the testing of manufactured nanomaterials: OECD's sponsorship programme.

Organization for Economic Cooperation and Development. 2012. OECD Environment, health and safety publications—Series on the safety of manufactured nanomaterials, no. 36. Guidance on sample preparaiton and dosimetry for the safety testing of manufactured nanomaterials.

Ohnishi, M., H. Yajima, T. Kasai, Y. Umeda, M. Yamamoto, S. Yamamoto, H. Okuda, M. Suzuki, T. Nishizawa, and S. Fukushima. 2013. Novel method using hybrid markers: Development of an approach for pulmonary measurement of multi-walled carbon nanotubes. *Journal of Occupational Medicine and Toxicology* 8:30.

Oyabu, T., T. Myojo, Y. Morimoto, A. Ogami, M. Hirohashi, M. Yamamoto, M. Todoroki, Y. Mizuguchi, M. Hashiba, B. W. Lee, M. Shimada, W. N. Wang, K. Uchida, S. Endoh, N. Kobayashi, K. Yamamoto, K. Fujita, K. Mizuno, M. Inada, T. Nakazato, J. Nakanishi, and I. Tanaka.

2011. Biopersistence of inhaled MWCNT in rat lungs in a 4-week well-characterized exposure. *Inhalation Toxicology* 23: 784–91.

Pare, W. P., and G. B. Glavin. 1986. Restraint stress in biomedical research: A review. *Neuroscience and Biobehavioral Reviews* 10:339–70.

Park, K., D. B. Kittelson, M. R. Zachariah, and P. H. McMurry. 2004. Measurement of inherent material denisty of nanoparitcle agglomerates. *Journal of Nanoparticle Research* 6:267–72.

Parungo, C. P., Y. L. Colson, S. M. Kim, S. Kim, L. H. Cohn, M. G. Bawendi, and J. V. Frangioni. 2005. Sentinel lymph node mapping of the pleural space. *Chest* 127:1799–804.

Pauluhn, J. 2009. Comparative pulmonary response to inhaled nanostructures: Considerations on test design and endpoints. *Inhalation Toxicology* 21(suppl 1): 40–54.

Pauluhn, J. 2010. Subchronic 13-week inhalation exposure of rats to multiwalled carbon nanotubes: Toxic effects are determined by density of agglomerate structures, not fibrillar structure. *Toxicological Sciences* 113:226–42.

Pauluhn, J., and U. Mohr. 1999. Repeated 4-week inhalation exposure of rats: Effect of low-, intermediate, and high-humidity chamber atmospheres. *Experimental and Toxicologic Pathology* 51:178–87.

Pauluhn, J., and M. Rosenbruch. 2015. Lung burdens and kinetics of multi-walled carbon nanotubes (Baytubes) are highly dependent on the disaggregation of aerosolized MWCNT. *Nanotoxicology* 9:242–52.

Pauluhn, J., and A. Thiel. 2007. A simple approach to validation of directed-flow nose-only inhalation chambers. *Journal of Applied Toxicology* 27:160–67.

Peigney, A., C. Laurent, E. Flahaut, R. R. Bacsa, and A. Rousset. 2001. Specific surface area of carbon nanotubes and bundles of carbon nanotubes. *Carbon* 39:507–14.

Peterson, M. R., and M. H. Richards 1999. Thermal-optical-transmittance analysis for organic, elemental, carbonate, total carbon, and OCX2 in PM2.5 by the EPA/NIOSH Method—#83. Accessed August 15, 2014. www.rti.org/pubs/OC-EC_Paper_83_3b.pdf.

Phalen, R. F. 2009. *Inhalation studies, foundations and techniques*, 2nd ed. New York, NY: Informa Healthcare.

Poland, C. A., R. Duffin, I. Kinloch, A. Maynard, W. A. Wallace, A. Seaton, V. Stone, S. Brown, W. MacNee, and K. Donaldson. 2008. Carbon nanotubes introduced into the abdominal cavity of mice show asbestos-like pathogenicity in a pilot study. *Nature Nanotechnology* 3:423–28.

Porter, D., K. Sriram, M. Wolfarth, A. Jefferson, D. Schwegler-Berry, M. Andrew, and V. Castranova. 2008. A biocompatible medium for nanoparticle dispersion. *Nanotoxicology* 2:144–54.

Porter, D. W., A. Hubbs, R. Mercer, N. Wu, M. G. Wolfarth, K. Sriram, S. Leonard, L. Battelli, D. Schwegler-Berry, S. Friend, M. Andrew, B. T. Chen, S. Tsuruoka, M. Endo, and V. Castranova. 2010. Mouse pulmonary dose-and time course-response induced by exposure to multi-walled carbon nanotubes. *Toxicology* 269:136–47.

Pritchard, J. N., A. Holmes, J. C. Evans, N. Evans, R. J. Evans, and A. Morgan. 1985. The distribution of dust in the rat lung following administration by inhalation and by single intratracheal instillation. *Environmental Research* 36:268–97.

Raabe, O. G., H.-C. Yeh, G. M. Schum, and R. F. Phalen 1976. Tracheobronchial geometry: Human, dog, rat, hamster, LF-53. Albuquerque, NM: Lovelace Foundation.

Rafique, M. M. A., and J. Iqbal. 2011. Production of carbon nanotubes by different routes - A review. *Journal of Encapsulation and Adsorption Sciences* 1:29–34.

Rinderknecht, A., A. Elder, R. Prud'homme, M. Gindy, J. Harkema, and G. Oberdörster. 2007. Surface functionalization affects the role of nanoparticle disposition. *American Journal of Respiratory and Critical Care Medicine* 175:A246.

Rittinghausen, S., A. Hackbarth, O. Creutzenberg, H. Ernst, U. Heinrich, A. Leonhardt, and D. Schaudien. 2014.

The carcinogenic effect of various multi-walled carbon nanotubes (MWCNTs) after intraperitoneal injection in rats. *Particle and Fibre Toxicology* 11:59.

Rothenberg, S. J., R. M. Parker, R. G. York, G. E. Dearlove, and M. M. Martin. 2000. Lack of effects of nose-only inhalation exposure on testicular toxicity in male rats. *Toxicological Sciences* 53:127–34.

Rudd, C. J., and K. A. Strom. 1981. A spectrophotometric method for the quantitation of diesel exhaust particles in guinea pig lung. *Journal of Applied Toxicology* 1: 83–87.

Rudolf, G., J. Gebhart, J. Heyder, C. F. Schiller, and W. Stahlhofen. 1986. An empirical formula describing aerosol deposition in man for any particle size. *Journal of Aerosol Science* 17:350–55.

Rudolf, G., R. Kobrich, and W. Stahlhofen. 1990. Modelling and algebraic formulation of regional aerosol deposition in man. *Journal Aerosol Sciences* 21(suppl. 1): S403–S406.

Rushton, E. K., J. Jiang, S. S. Leonard, S. Eberly, V. Castranova, P. Biswas, A. Elder, X. Han, R. Gelein, J. Finkelstein, and G. Oberdörster. 2010. Concept of assessing nanoparticle hazards considering nanoparticle dosemetric and chemical/biological response-metrics. *Journal of Toxicology and Environmental Health, Part A* 73:445–61.

Ryman-Rasmussen, J. P., M. F. Cesta, A. R. Brody, J. K. Shipley-Phillips, J. I. Everitt, E. W. Tewksbury, O. R. Moss, B. A. Wang, D. E. Dodd, M. E. Anderson, and J. C. Bonner. 2009b. Inhaled carbon nanotubes reach the subpleural tissue in mice. *Nature Nanotechnology* 4:747–51.

Ryman-Rasmussen, J. P., E. W. Tewksbury, O. R. Moss, M. F. Cesta, B. A. Wong, and J. C. Bonner. 2009a. Inhaled multiwalled carbon nanotubes potentiate airway fibrosis in murine allergic asthma. *American Journal of Respiratory Cell and Molecular Biology* 40:349–58.

Sager, T. M., D. W. Porter, V. A. Robinson, W. G. Lindsley, D. E. Schwegler-Berry, and V. Castranova. 2007. Improved method to disperse nanoparticles for in vitro and in vivo investigation of toxicity. *Nanotoxicology* 1:118–29.

Sager, T. M., M. W. Wolfarth, M. Andrew, A. Hubbs, S. Friend, T. Chen, D. W. Porter, N. Wu, F. Yang, R. F. Hamilton, and A. Holian. 2014. Effect of multi-walled carbon nanotube surface modification on bioactivity in the C57BL/6 mouse model. *Nanotoxicology* 8:317–27.

Sakamoto, Y., D. Nakae, N. Fukumori, K. Tayama, A. Maekawa, K. Imai, A. Hirose, T. Nishimura, N. Ohashi, and A. Ogata. 2009. Induction of mesothelioma by a single intrascrotal administration of multi-wall carbon nanotube in intact male Fischer 344 rats. *Journal of Toxicological Sciences* 34: 65–76.

Salvador-Morales, C., E. V. Basiuk, V. A. Basiuk, M. L. H. Green, and R. B. Sim. 2008. Effects of covalent functionalization on the biocompatibility characteristics of multi-walled carbon nanotubes. *Journal of Nanoscience and Nanotechnology* 8:2347–56.

Sargent, L., D. W. Porter, L. M. Staska, A. F. Hubbs, D. T. Lowry, L. Battelli, K. J. Siegrist, M. L. Kashon, R. R. Mercer, A. K. Bauer, B. T. Chen, J. L. Salisbury, D. Frazer, W. McKinney, M. Andrew, S. Tsuruoka, M. Endo, K. Fluharty, V. Castranova, and S. H. Reynolds. 2014. Promotion of lung adenocarcinoma following inhalation exposure to multi-walled carbon nanotubes. *Particle and Fibre Toxicology* 11:3.

Scherer, P. W., L. H. Shendalman, and N. M. Greene. 1972. Simultaneous diffusion and convection in single breath lung washout. *Bulletin of Mathematical Biophysics* 34:393–412.

Schleh, C., W. Kreyling and C. M. Lehr. 2013. Pulmonary sufactant is indispensable in order to simulate the in vivo situation. *Part Fibre Toxicol* **10**: 6.

Scuri, M., B. T. Chen, V. Castranova, J. S. Reynolds, V. J. Johnson, L. Samsell, C. Walton, and G. Piedimonte. 2010. Effects of titanium dioxide nanoparticle exposure on neuroimune responses in rat airways. *Journal*

of Toxicology and Environmental Health, Part A 73:1353–69.

Shimada, M., W.-N. Wang, K. Okuyama, T. Myojo, T. Oyabu, Y. Morimoto, I. Tanaka, S. Endoh, K. Uchida, K. Ehara, H. Sakurai, K. Yamamoto, and J. Nakanishi. 2009. Development and evaluation of an aerosol generation and supplying system for inhalation experiment of manufactured nanoparticles. *Environmental Science & Technology* 43:5529–34.

Shvedova, A. A., E. Kisin, A. R. Murray, V. J. Johnson, O. Gorelik, S. Arepali, A. F. Hubbs, R. R. Mercer, P. Keohavong, N. Sussman, J. Jin, S. Stone, B. T. Chen, G. Deye, A. Maynard, V. Castranova, P. A. Baron, and V. E. Kagan. 2008. Inhalation, versus aspiration of single walled carbon nanotubes in C57BL/6 mice: Inflammation, fibrosis, oxidative stress and mutagenesis. *American Journal of Physiology: Lung Cellular and Molecular Physiology* 295:L552–L565.

Shvedova, A. A., E. R. Kisin, R. Mercer, A. R. Murray, V. J. Johnson, A. I. Potapovich, Y. Y. Tyurina, O. Gorelik, S. Arepulli, D. Schwegler-Berry, A. F. Hubbs, J. Antonini, D. E. Evans, B.-K. Ku, D. Ramsey, A. Maynard, V. E. Kagan, V. Castranova, and P. Buron. 2005. Unusual inflammatory and fibrogenic pulmonary responses to single walled carbon nanotubes in mice. *American Journal of Physiology: Lung Cellular and Molecular Physiology* 289:L698– L708.

Shvedova, A. A., A. Tkach, E. R. Kisin, A. R. Murray, N. Yanamala, A. Hubbs, P. Keohavong, L. P. Sycheva, V. E. Kagan, and V. Castranova. 2014. Long-term effects of carbon containing engineered nanomaterials and asbestos in the lung: One year post exposure comparisons. *American Journal of Physiology: Lung Cellular and Molecular Physiology* 306:L170–L182.

Shvedova, A. A., A. V. Tkach, E. R. Kisin, T. Khaliullin, S. Stanley, D. W. Gutkin, A. Star, Y. Chen, G. V. Shurin, V. E. Kagan, and M. R. Shurin. 2013. Carbon nanotubes enhance metastatic growth of lung carcinoma via up-regulation of myeloid-derived suppressor cells. *Small* 9:1691–95.

Singh, C., T. Quested, C. B. Boothroyd, P. Thomas, I. A. Kinloch, A. I. Abou-Kandil, and A. H. Windle. 2002. Synthesis and characterization of carbon nanofibers produced by the floating catalyst method. *Journal of Physical Chemistry. B* 106:10915–22.

Sisan, T. B., and S. Lichter. 2014. Solitons transport water through narrow carbon nanotubes. *Physical Review Letters* 112:044501–05.

Sistonen, L., K. D. Sarge, B. Phillips, K. Abravaya, and R. I. Morimoto. 1992. Activation of heat shock factor 2 during hemin-induced differentiation of human erythroleukemia cells. *Molecular and Cellular Biology* 12:4104–11.18

Slikker, W., Jr., M. E. Andersen, M. S. Bogdanffy, J. S. Bus, S. D. Cohen, R. B. Conolly, D. M. David, N. G. Doerrer, D. C. Dorman, D. W. Gaylor, D. Hattis, J. M. Rogers, S. R. Woodrow, J. A. Swenberg, and K. Wallace. 2004. Dose-dependent transitions in mechanisms of toxicity: Case studies. *Toxicology and Applied Pharmacology* 201:203–25.

Sriram, K., D. W. Porter, A. M. Jefferson, G. X. Lin, M. G. Wolfarth, B. T. Chen, W. McKinney, D. G. Frazer, and V. Castranova. 2009. Neuro inflammation and blood–brain barrier changes following exposure to engineered nanomaterials. *Toxicologist* 108:A2197.

Stahlhofen, W., G. Rudolf, and A. C. James. 1989. Intercomparison of experimental regional aerosol deposition data. *Journal of Aerosol Medicine* 2:285–308.

Stapleton, P. A., V. Minarchick, A. Cumpston, W. McKinney, B. T. Chen, D. Frazer, V. Castranova, and T. R. Nurkiewicz. 2011. Time-course of improved coronary arteriolar endothelium-dependent dilation after multi-walled carbon nanotube inhalation. *Toxicologist* 120:A194.

Stapleton, P. A., V. C. Minarchick, A. M. Cumpston, W. McKinney, B. T. Chen, T. M. Sager, D. G. Frazer, R. R. Mercer, J. Scabilloni, M. E. Andrew, V. Castranova, and T. R. Nurkiewicz. 2012. Impairment of coronary arteriolar endothelium-dependent

dilation after multi-walled carbon nanotube inhalation: A time-course study. *International Journal of Molecular Sciences* 13:13781–803.

Stinn, W., A. Teredesai, E. Anskeit, K. Rustemeier, G. Schepers, P. Schgnell, H.-J. Haussmann, R. A. Carchman, C. R. E. Coggins, and W. Reininghaus. 2005. Chronic nose-only inhalation study in rats, comparing room-aged sidestream cigarette smoke and diesel engine exhaust. *Inhalation Toxicology* 17:549–76.

Stoeger, T., C. Reinhard, S. Takenaka, A. Schroeppel, E. Karg, B. Ritter, J. Heyder, and H. Schulz. 2006. Instillation of six different ultrafine carbon particles indicates a surface area threshold dose for acute lung inflammation in mice. *Environmental Health Perspectives* 114:328–33.

Tabet, L., C. Bussy, A. Setyan, A. Simon-Deckers, M. J. Rossi, J. Boczkowski, and S. Lanone. 2011. Coating carbon nanotubes with a polystyrene-based polymer protects against pulmonary toxicity. *Particle and Fibre Toxicology* 8:3.

Takagi, A., A. Hirose, M. Futakuchi, H. Tsuda, and J. Kanno. 2012. Dose-dependent mesothelioma induction by intraperitoneal administration of multi-wall carbon nanotubes in p53 heterozygous mice. *Cancer Science* 103:1440–44.

Takagi, A., A. Hirose, T. Nishimura, W. Fukumori, A. Ogata, and N. Ohashi. 2008. Induction of mesothelioma in p53 +/- mouse by intraperitoneal application of multi-walled carbon nanotube. *Journal of Toxicological Sciences* 33: 105–16.

Taquahashi, Y., Y. Ogawa, A. Takagi, M. Tsuji, K. Morita, and J. Kanno. 2013. An improved dispersion method of multi-wall carbon nanotube for inhalation toxicity studies of experimental animals. *Journal of Toxicological Sciences* 38:619–28.

Thomson, E. M., A. Williams, C. L. Yauk, and R. Vincent. 2009. Impact of nose-only exposure system on pulmonary gene expression. *Inhalation Toxicology* 21(S1): 74–82.

Timbrell, V., T. Ashcroft, B. Goldstein, F. Heyworth, L. O. Meurman, R. E. G. Randall, J. A. Reynolds, K. B. Shilkin, and D. Whitaker. 1988. Relationships between retained amphibole fibres and fibrosis in human lung tissue specimens. In: Inhaled Particles VI. *Annals of Occupational Hygiene* 32(suppl. 1): 323–40.

Tran, C. L., D. Buchanan, R. T. Cullen, A. Searl, A. D. Jones, and K. Donaldson. 2000a. Inhalation of poorly soluble particles. II. Influence of particle surface area on inflammation and clearance. *Inhalation Toxicology* 12:1113–26.

Tran, C. L., D. Buchanan, B. G. Miller, and A. D. Jones. 2000b. Mathematical modeling to predict the responses to poorly soluble particles in rat lungs. *Inhalation Toxicology* 12 (Suppl. 3):403–09.

Treumann, S., L. Ma-Hock, S. Gröters, R. Landsiedel, and B. Van Ravenzwaay. 2013. Additional histopathologic examination of the lungs from a 3-month inhalation toxicity study with multiwall carbon nanotubes in rats. *Toxicological Sciences* 134:103–10.

Tsai, S. J., M. Hofmann, M. Hallock, E. Ada, J. Kong, and M. Ellenbecker. 2009. Characterization and evaluation of nanoparticle release during the synthesis of single-walled and multiwalled carbon nanotubes by chemical vapor deposition. *Environmental Science & Technology* 43:6017–23.

Tsuruoka, S., K. Takeuchi, K. Koyama, T. Noguchi, M. Endo, F. Tristan, M. Terrones, H. Matsumoto, N. Saito, Y. Usui, D. W. Porter, and V. Castranova. 2013. ROS evaluation for a series of CNT and their derivatives using an ESR method with DMPO. *Journal of Physics: Conference Series* 429:012029.IOP Publishing

Tyl, R. W., L. Ballantyne, C. Fisher, D. L. Fait, T. A. Savine, I. M. Pritts, and D. E. Dodd. 1994. Evaluation of expousre to water aerosol or air by nose-only or whole-body inhation procedures for CD-1 mice in developmental toxicity studies. *Fundamental and Applied Toxicology* 23:251–60.

Udelsman, R., M. J. Blake, C. A. Stagg, D.-G. Li, D. J. Putney, and N. J. Holbrook. 1993. Vascular heat shock protein expression in response to stress. *Journal of Clinical Investigation* 91:465–73.

Umeda, Y., T. Kasai, M. Saito, H. Kondo, T. Toya, S. Aiso, H. Okuda, T. Nishizawa, and S. Fukushima. 2013. Two-week toxicity of multi-walled carbon nanotubes by whole-body inhalation exposure in rats. *Journal of Toxicology and Pathology* 26: 131–40.

Utembe W., K. Potgieter, A. B. Stefaniak, J. M. Gulumian. 2015. Dissolution and biodurability: Important parameters needed for risk assessment of nanomaterials. *Particle and Fibre Toxicology* 12:11. doi:10.1186/s12989-015-0088-2.

Van Eijl, S., R. Van Oorschot, B. Olivier, F. P. Nijkamp, and N. Bloksma. 2006. Stress and hypothermia in mice in a nose-only cigarette smoke exposure system. *Inhalation Toxicology* 18:911–18.

Vu, V., C. Barrett, J. Roycroft, L. Schuman, D. Dankovic, P. Baron, T. Martonen, W. Pepelko, and D. Lai. 1996. Chronic inhalation toxicity and carcinogenicity testing of respirable fibrous particles. *Regulatory Toxicology and Pharmacology* 24: 202–12.

Wang, J., C. Asbach, H. Fissan, T. Hülser, T. A. J. Kuhlbusch, D. Thompson, and D. Y. H. Pui. 2011. How can nanobiotechnology oversight advance science and industry: Examples from environmental, health, and safety studies ofnanoparticles (nano-EHS). *Journal of Nanoparticle Research* 13:1373–87.

Wang J., Y.K Bahk, S-.C. Chen, D.Y.H. Pui. 2015. Characteristics of airborne fractal-like agglomerates of carbon nanotubes. *Carbon* 93: 441–450.

Warheit, D. B. 2008. How meaningful are the results of nanotoxicity studies in the absence of adequate material characterization? *Toxicological Sciences* 101:183–85.

Warheit, D. B., B. R. Laurence, K. L. Reed, D. H. Rouch, G. A. M. Reynolds, and T. R. Webb. 2004. Comparative pulmonary toxicity assessment of single-wall carbon nanotubes in rats. *Toxicological Sciences* 77:117–25.

Warheit, D. B., K. L. Reed, and M. P. DeLorme. 2013. Subchronic inhalation of carbon nanofibers: No apparent cross-talk between local pulmonary and cardiovascular/systemic responses. *Carbon* 62:165–76.

Watson, J. G., J. C. Chow, and L.-W. A. Chen. 2005. Summary of organic and elemental carbon/black carbon analysis methods and intercomparisons. *Aerosol and Air Quality Research* 5:65–102.

Weibel, E. R. 1963. *Morphometry of the human lung*. Berlin, Germany: Springer Verlag.

Westerhoff, P., K. Doudrick, and P. Herckes 2012. Detection of carbon nanotubes in environmental and biological matrices using programmed thermal analysis. American Chemical Society Annual Conference, , Philadelphia, PA, August 19–23.

WHO. 1981. *Methods of monitoring and evaluating airborne man-made mineral fibres*. Report on a WHO Consultation. EURO Reports and Studies 48, Copenhagen, Denmark, 29 April–1 May 1980.

Wong, B. 2007. Inhalation exposure systems: Design, methods and operation. *Toxicologic Pathology* 33:3–14.

Xu, J., D. B. Alexander, M. Futakuchi, T. Numano, K. Fukamachi, M. Suzui, T. Omori, J. Kanno, A. Hirose, and H. Tsuda. 2014. Size- and shape-dependent pleural translocation, deposition, fibrogenesis, and mesothelial proliferation by multiwalled carbon nanotubes. *Cancer Science* 105: 763–69.

Xu, J., M. Futakuchi, H. Shimizu, D. B. Alexander, K. Yanagihara, K. Fukamachi, M. Suzui, J. Kanno, A. Hirose, A. Ogata, Y. Sakamoto, D. Nakae, T. Omori, and H. Tsurda. 2012. Multi-walled carbon nanotubes translocate into the pleural cavity and induce visceral mesothelial proliferation in rats. *Cancer Science* 103:2045–50.

Yeh, H. C., and G. M. Schum. 1980. Models of human lung airways and their application to inhaled particle deposition. *Bulletin of Mathematical Biology* 42: 461–80.

Yeh, H. C., M. B. Snipes, A. E. Eidson, and C. H. Hobbs. 1990. Comparative evaluation of nose-only versus whole-body inhalation expsoures for rats - Aerosol characteristics and lung deposition. *Inhalation Toxicology* 2:205–21.

Yu, C. P.1978. Exact analysis of aerosol deposition during steady state breathing. *Powder Technology* 21:55–62.

Yu, K.-N., J. E. Kim, H. W. Seo, C. Chae, and M.-H. Cho. 2013. Differential toxic responses between pristine and functionalized multiwall naniotubes involve induction of autophagy accumualtion in murine lung. *Journal of Toxicology and Environmental Health, Part A* 76:1282–92.

Zhang, L., and C. P. Yu. 1993. Empirical equations for nasal deposition of inhaled particles in small laboratory animals and humans. *Aerosol Science and Technology* 19:51–56.

Zhao, J., and V. Castranova. 2011. Toxicology of nanomaterials used in nanomedicine. *Journal of Toxicology and Environmental Health B* 14:593–632.

Zhao, Y., B. L. Allen, and A. Star. 2011. Enzymatic degradation of multiwalled carbon nanotubes. *Journal of Physical Chemistry. A* 115:9536–44.

APPENDIX A: RESPIRATORY-TRACT FRACTIONS

Inhalability

To develop a model for CNT/CNF inhalability, one must first characterize airborne CNT/CNF. Unlike particles, which can be represented by their diameters, CNT/CNF are described by several characteristics dimensions called equivalent diameters. Equivalent diameters are identified with respect to the physical mechanism(s) controlling the transport of CNT/CNF in the respiratory tract. A reduction in inhalability will result when inhaled CNT/CNF are prevented from entering the extrathoracic passages due to their inertias. Therefore, inhalability of CNT/CNF depends on their equivalent diameter for impaction (or impaction diameter). The following model illustrations are with the assumption of CNT/CNF being present as single, straight fibers. Conditions (shape factor) will be different for complex structures of tangles, agglomerates, and aggregates. Once the shape of CNT/CNF is characterized, impaction diameter is obtained by equating the drag and inertial forces of CNT/CNF for an equivalent spherical particle. For example, by assuming that CNT/CNF are shaped as cylinders and are randomly oriented in the air, an expression for equivalent diameter for impaction (d_{ei}) may be found as (Asgharian and Price, 2006)

$$d_{ei} = d_f \sqrt{\frac{\rho\beta \ln\left(\beta + \sqrt{\beta^2 - 1}\right)}{\sqrt{\beta^2 - 1}}} \qquad (1)$$

where d_f, β, and ρ are the CNT/CNF diameter, aspect ratio, and mass density, respectively. Predictive models for the inhalability of particles may be extended to CNT/CNF by replacing particle diameter with equivalent impaction diameter. The majority of existing predictive models of particle inhalability are related to particle diameter (Ménache, Miller, and Raabe 1995; Brown 2005). However, particle inertia depends both on its diameter and traveling velocity. Asgharian, Kelly, and Tewksbury (2003) developed a semiempirical expression for rat inhalability based on measurements obtained from a series of brief nose-only inhalation studies in which rats were exposed to titanium dioxide particles. The following expression was proposed to calculate the inhalability:

$$IF(\phi, \theta, \phi) = \frac{1}{1 + \alpha d_{ei}^{\delta}(\phi, \theta, \phi) Q^{\gamma}} \qquad (2)$$

where Q is the inhalation flow rate. By fitting Eq. (2) to inhalability measurements in rats, coefficients α, δ, and γ were found to be 19.87, –1.5532, and –0.7466, respectively. In humans, coefficients α, δ, and γ were reported as 0.1361, 0.9906, and –0.8527 for oral breathing and 4.451×10^{-4}, 2.168, and 0.3778 for nasal breathing (Asgharian and Price, 2006). A plot of CNT/CNF inhalability versus equivalent diameter for impaction is given in

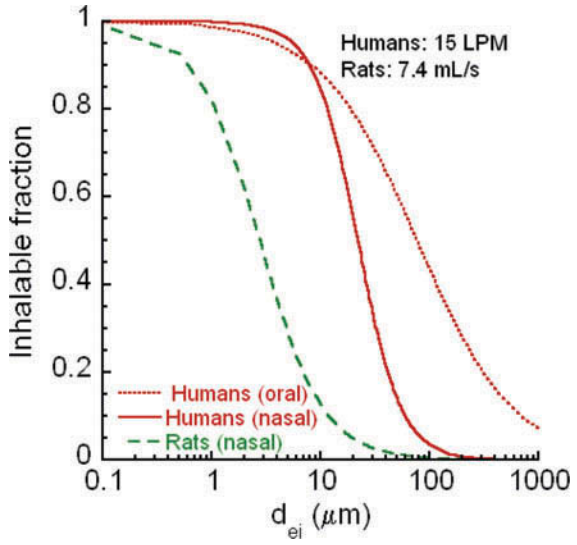

FIGURE A-1. CNT/CNF inhalability for humans and rats.

CNT/CNF inhalability for humans via oral and nasal, and rats nasal breathings. Equivalent impaction diameter in the figure includes shape and orientation effects. d_{ei} is found from Equation (1) for cylindrical shapes. Additional size measurements are needed to develop more realistic models of d_{ei} for CNT/CNF which, while being elongated, generally are not cylindrical.

Figure A-1. Breathing flow rates of 15 LPM and 7.4 ml/s were used in Eq. (2) for humans and rats, respectively. CNT/CNF inhalability is greater for humans than for rats and increases further during by oral breathing than nasal breathing. In humans, CNT/CNF of 10-μm impaction diameter or smaller CNT/CNF are 100% inhalable. Rats have a significantly lower inhalability than humans, with about 90% of 1-μm and 50% of 3-μm CNT/CNF being inhalable.

The shape of CNT/CNF affects their aerodynamic properties and thus transport and deposition in lung airways. The shape has been found to be complex and to vary quite considerably based on filter sample observations; however, it has not been characterized so far and thus cannot be described mathematically at the present time. The current version of MPPD assumes CNT/CNF to be shaped as cylinders. In addition, those CNT/CNF that are not straight may be described by equivalent diameters for impaction, sedimentation, and diffusion. Deposition of these particles can be estimated from the MPPD model for spherical particles. Thus, the fiber and spherical particle models of MPPD may be jointly used to predict deposition as first order of approximation. The degree of inaccuracy cannot be estimated until a mathematical model for different shape CNT/CNF are developed. The fiber version of the model will be made available in the near future. CNT/CNF sizes (1 and 3 μm) are for equivalent diameter for impaction in Eq. (2). This diameter can take on different dimensions as described in Eq. (1) to give the desired impaction diameters of 1 and 3 μm. Experimentally, impaction diameter can be measured by an impactor.

Thoracic Fraction

A fraction of inhaled materials is deposited in the extrathoracic airways, and the remaining inhaled materials that escape deposition are considered to be penetrable into the thoracic region. The thoracic fraction of CNT/CNF is the net effect of two filtering mechanisms: inhalability (IF) and removal efficiency in the head airways (η). Therefore, the thoracic fraction (TF) of CNT can be described by

$$TF = IF \times (1 - \eta) \tag{3}$$

Losses of inhalable CNT/CNF in the head airways are by inertial impaction. Hence, the same as for inhalability, CNT/CNF thoracic fraction will depend on equivalent diameter for impaction and inhalation flow rate. Loss efficiency expressions for CNT/CNF are obtained by replacing particle diameter with CNT/CNF impaction diameters. For humans, nasal and oral breathing deposition efficiencies may be given by (Rudolf, Kobrich, and Stahlhofen 1990; Rudolf et al. 1986; and Stahlhofen, Rudolf, and James 1989)

$$\eta_{H-n} = 1 - \frac{1}{1 + 3 \times 10^{-4} d_{ei}^2 Q} \tag{4}$$

$$\eta_{H-o} = 1 - \frac{1}{1 + 10^{-4} \left(d_{ei}^2 Q^{0.6} V_t^{-0.2}\right)^{1.4}} \tag{5}$$

where V_t is the tidal volume. Similarly, for rats, the following relationship was proposed by Zhang and Yu (1993):

$$\eta_{R-n} = \left[\frac{\left(d_{ei}^2 Q\right)^{2.553}}{10^5 + \left(d_{ei}^2 Q\right)^{2.553}} \right]^{0.627} \quad (6)$$

Respirable Fraction

Additional losses of CNT/CNF occur while passing through conducting airways of the lung, mainly by inertial impaction for micrometer and larger size CNT/CNF and Brownian diffusion of smaller CNT/CNF sizes. Consequently, the amount of CNT/CNF that reaches the alveolar region or the respirable fraction is lower than thoracic fraction. A lung deposition model such as MPPD is needed to calculate the total conducting airway losses based on available deposition efficiency expressions for impaction and diffusion losses. The respirable fraction of CNT/CNF is found by correcting TF for the total loss fraction of CNT/CNF in the conducting airways. The respirable fraction depends on CNT/CNF size and lung and breathing parameters.

APPENDIX B: EXTRAPOLATION

Extrapolation Based on Inhaled Dose

Inhaled dose refers to the amount of CNT/CNF that reaches different regions of the respiratory tract, and it should not serve as a basis for human risk estimates deduced from laboratory animal studies. Since the ability of CNT to reach various locations of the lung depends on the filtering efficiencies in the passing airways, one needs to calculate the inhalable, thoracic, and respirable fractions to use as the basis for interspecies extrapolations.

Extrapolation across lab testing and human exposure scenarios may involve two cases. The intention in case 1 is to set up an exposure atmosphere in the lab setting (animal inhalation studies) based on the human exposure scenario.

Thus, an equivalent CNT/CNF size and concentration will be sought for the exposure systems to deliver the same dose to humans and laboratory animals. Size equivalency in case 1 will be based on an equal inhaled dose metric of exposure (i.e., inhalable, thoracic, or respirable fractions). The opposite is to be achieved in case 2, where human equivalent concentration is sought for a given animal inhalation exposure concentration. Again, extrapolation across exposure scenarios will be based on the dose-metric of equal inhalable, thoracic, or respirable fraction. The same dose equivalent can also be considered as a goal for in vitro studies, either for conventional exposure via suspension in culture medium or via aerosol in an Air Liquid Interface (ALI) system. The medium concentration could be interpreted as the equivalent exposure atmosphere in the lung regions of interest.

Figure B-1 describes scenario 1, in which equivalent CNT/CNF sizes will be calculated for the design of an animal inhalation study. Given that the thoracic fraction depends on the size of CNT/CNF, there will be an equivalent CNT/CNF size in animal studies for each CNT/CNF size in the human exposure scenario. It is assumed in Figure B-1 that humans are exposed to 2.5-μm-diameter CNT/CNF. The equivalent CNT/CNF size in animals also depends on the breathing route in humans. The corresponding impaction diameters for animal studies are 0.4 μm and 1.6 μm for human oral breathing and nasal breathing, respectively. Minute ventilations of 15 LPM and 7.4 ml/s were assumed in the calculations. If the exposure environment is made of various size particles, calculations must be repeated for each size interval. Ideally, an equivalent exposure environment must be generated with equivalent CNT/CNF sizes and concentrations in each size interval.

For case 2, a similar approach to the preceding one may be applied if the airborne size of a rat inhalation study is to be used to determine the human inhaled size of CNT/CNF. However, since the CNT/CNF thoracic fraction is greater in humans than rats (Figure B-1), CNT/CNF size correction is not needed in case

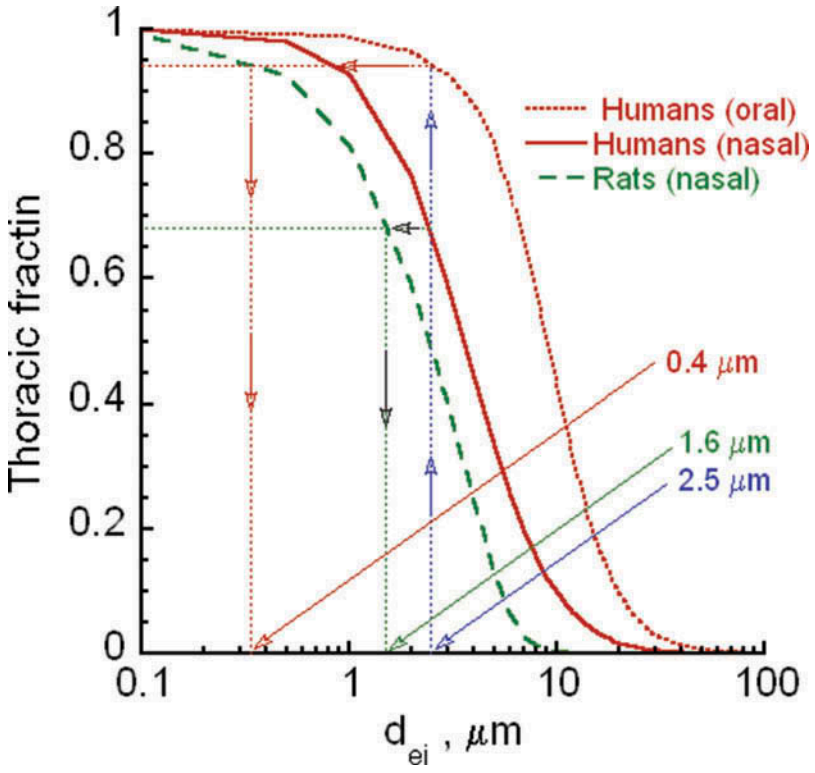

FIGURE B-1. CNT/CNF thoracic fractions for humans and rats.

CNT/CNF Thoracic fraction for different sizes for humans and rats at minute ventilations of 15 LPM and 7.4 mL/s, respectively.

2, for which toxicity assessment is based on observed laboratory outcomes. Human health risk is inferred based on in vivo results, which require estimation of human equivalent exposure (HEC) concentration for a given laboratory setting. For example, by assuming the same delivered dose for human exposure scenarios and rats in an inhalation study, the following relationship is obtained for the calculations of HEC:

$$\frac{HEC}{C_R} = \frac{TF_R(d_{ei})}{TF_H(d_{ei})} \times \frac{(\dot{V}_E)_R}{(\dot{V}_E)_H} \times \frac{\delta t_R}{\delta t_H} \qquad (7)$$

where C_R is the rat exposure concentration, reported from rodent inhalation studies, $\dot{V}_E$ is the minute ventilation, and δt is the exposure duration. Subscripts R and H refer to rats and humans, respectively. Figure B-2 presents the ratio of HEC/C_Rversus impaction diameter of CNT for equal exposure duration for humans and animals. Minute ventilations of 15 LPM and 7.4 ml/s were used in the calculations of Eq. (7). Exposure concentration ratio decreases with increasing impaction diameter of CNT/CNF. In addition, since the concentrations ratio is smaller than unity, HEC must be smaller than the exposure concentration in rats to yield the same delivered dose.

Extrapolation Based on Deposited Dose

While inhalable, thoracic, and respirable fractions are good indicators of the delivered dose to the lung, they do not directly correlate to the biological response because only a fraction of inhaled CNT/CNF is deposited on lung airway surfaces. The deposited dose is what triggers the biological response and must therefore be linked to it. Given that human

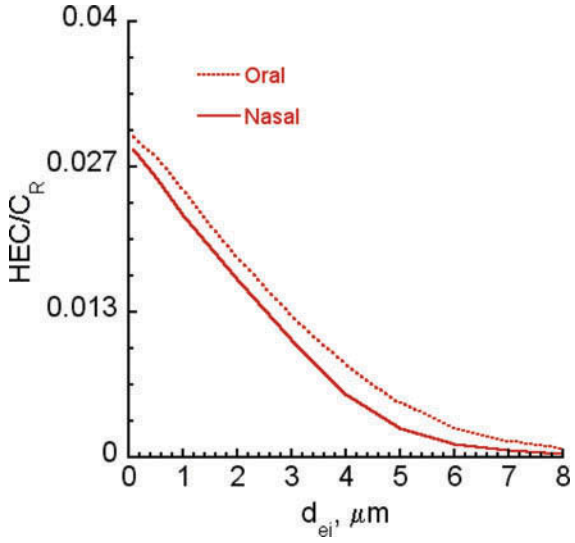

FIGURE B-2. Human to rat ratios for equal thoracic fractions.

Ratio of human equivalent concentration to rat exposure concentration based on equal thoracic fractions for minute ventilations of 15 LPM and 7.4 mL/s in humans and rats respectively.

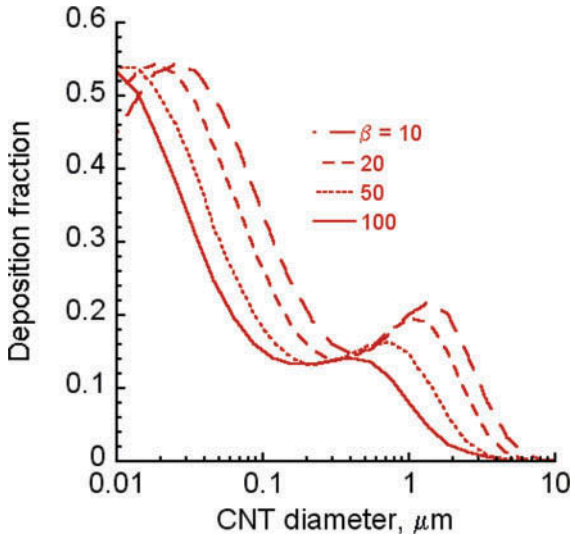

FIGURE B-3. CNT/CNF respiratory fractions for humans at different aspect ratios.

CNT/CNF deposition fraction in the human lung via nasal breathing for different aspect ratios. A minute ventilation of 7.5 LMP is used in the calculations.

exposure studies are not possible due to ethical concerns of possible adverse health effects and that there is a limitation to conducting animal studies from the standpoint of practicality and cost, lung dosimetry models have been developed to assess deposition of airborne materials in the lungs of humans and laboratory animals. These models allow direct prediction of both deposited and retained doses in the lungs of humans and animals and dosimetric extrapolation and comparison of such doses between animals and humans for cases 1 and 2.

Predictive models of inhaled aerosols in the lungs of humans and laboratory animals have been around for a few decades. First-generation deposition models were compartmental and limited in predictive capability. More realistic deposition models assumed the lung to be dynamic and to undergo expansion and contract during a breathing cycle. The lung geometry also resembled a trumpet in shape when symmetric lung geometry was assumed (Scherer, Shendalman, and Greene 1972; Yu 1978). These models have been validated for regional deposition fractions. The human lung has an asymmetric branching structure that affects both airflow and particle deposition. Asgharian, Hofmann, and Bergmann (2001) developed a multiple-path particle dosimetry model (MPPD) and used it to predict site-specific and regional deposition of particles in 10 stochastically generated lungs of human adults. The stochastic lungs were based on morphometric measurements of Raabe et al. (1976) and developed by Koblinger and Hofmann (1985). Significant dose variations among the lung structures were found, which indicated the significance of intersubject variability in the population.

Particle deposition models were extended to CNT/CNF by adjusting for shape and size effects of CNT/CNF (Asgharian and Price 2008 for cylindrical shapes). The deposition model consisted of four components. First is the extrathoracic component for calculating head losses of inhalable CNT/CNF so that the delivered dose to the lung could be obtained as already described . The next component was the lung geometry that enabled mechanistic calculations of CNT/CNF deposition in this geometry. Due to complexity of airway structure, multiscale dimensions of the lung, and the

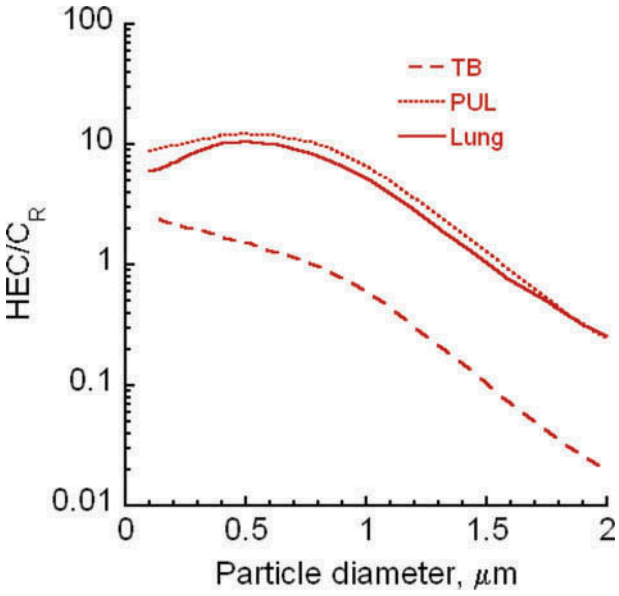

FIGURE B-4. HEC/CR ratios for CNT/CNF (100 nm—2 μm diameter) at aspect ratio of 10.

Ratio of HEC/C_R for different diameter CNT/CNF and aspect ratio of 10. Minute ventilations for humans and rats were 7.5 LPM and 0.241 LPM respectively.

large population of airways, a complete measurement of the entire airway tree was infeasible. Airway measurements typically included selecting a number of pathways extending from the trachea down to the alveolar airways and measuring airway dimensions and angles along these paths (Raabe et al. 1976). By assuming lung airways to be shaped as a cylinder and performing statistical analysis of airway parameters, various lung geometries were developed (Koblinger and Hofmann, 1985; Yeh and Schum 1980) and implemented in MPPD. Lung geometries in MPPD extended from a typical path geometry such as that proposed by Weibel (1963) to a complete asymmetric geometry (Koblinger 1985).

The third component of the deposition was the lung ventilation, which in effect was the mechanism of transport of CNT/CNF to various locations within the lung. The dose (and hence the effect) at any site in the lung depends on the amount of inhaled material that reaches there. Hence, lung ventilation directly impacts biological response. Various ventilation models based on lung compliance and airway resistance were developed and implemented in the deposition model. At normal low frequency breathing, lung lobar expansion is quasi-steady and linear among lobes. Hence, MPPD implemented a uniform airway expansion and contraction during a complete breathing cycle (Asgharian, Hofmann, and Bergmann 2001).

The last component of the deposition model entailed the application of the first principles to develop lung-specific conservation of mass and momentum equations for inhaled CNT/CNF. It was assumed that CNT/CNF concentration varied with lung depth and time and was constant across an airway cross-section. The movement of CNT/CNF in an expanding–contracting airway was described by the simplified, cross-sectional area averaged, convective-diffusion (general dynamic) equation:

$$\frac{\partial (AC)}{\partial t} + \frac{\partial (QC)}{\partial x} = \frac{\partial}{\partial x}\left(DA\frac{\partial C}{\partial x}\right) - \lambda AC. \quad (8)$$

where A is the total airway cross-sectional area and includes the contribution of the surrounding the airways in the pulmonary region, C is the CNT/CNF concentration, D is the apparent diffusion coefficient, Q is the flow rate through the airway, λC is the number of CNT/CNF lost to the airways by diffusion per unit time, per unit volume, and x and t are the distance into the lung and elapsed time, respectively. The apparent diffusion coefficient D is the sum of molecular diffusion coefficient and convective diffusion (dispersion) coefficient by dispersion.

Losses of uncharged particles in lung airways (λAC) are designated by the last term in Eq. (8). Losses occurred by major mechanisms of impaction, sedimentation, diffusion, and interception, which were time-invariant for a given aerosol size and lung and breathing parameters. It should be noted that while the functional form of Eq. (8) is the same for different shape particles, CNT/CNF specific shape and orientation effects were embedded in models for diffusion coefficient (D) and loss term (λAC) by different deposition mechanisms (Asgharian and Price 2008). Currently, the only deposition model for CNT/CNF is based on long, straight geometry. The model will

be extended to other shapes of CNT/CNF by accounting for geometry-specific effects, which alter orientation and hence transport and deposition in lung airways.

Prediction of CNT/CNF deposition in the lung provides the missing link between exposure and biological response. In humans, CNT/CNF losses are determined based on a given exposure scenario, which comprises exposure concentration, duration, and CNT/CNF size characteristics. Losses in the lung are then directly linked to the response if the target site is within the respiratory tract. For extrathoracic target sites, the deposition model is linked to a pharmacokinetic or pharmacodynamic model to establish exposure-dose-response relationships. Deposition fraction of elongated CNT/CNF in the lung is calculated at different aspect ratios (β) for various CNT/CNF diameters ranging from 0.01 to 10 μm for the case of nasal breathing (Figure B-3). The minute ventilation is 7.5 LPM. For diameters below 0.4 μm, lung deposition fraction increases with decreasing CNT/CNF diameter and aspect ratio. Given that CNT/CNF equivalent diameter depends on its diameter and aspect ratio, deposition of submicrometer-diameter CNT/CNF is inversely proportional to its size. For diameters greater than 0.4 μm, lung deposition should increase with size due to sedimentation and impaction effects. However, the nasal filtering effect reduces the amount entering the lung, and as a result, deposition first increases and then drops sharply to zero. It is also interesting to note that the influence of aspect ratio is minimized near a CNT/CNF diameter of 0.3 μm.

The predictions in Figure B-3 are based on the assumption that CNT/CNF are cylindrically shaped. However, collected CNT/CNF on the stages of nano-MOUDI showed highly irregular structures and were often tangled together. In fact, very few, if any, were straight. Nonetheless, the shapes were clearly elongated with large aspect ratios. Therefore, modeling CNT/CNF behavior in the air and deposition on airway surfaces based on cylindrical geometry is a fair representation in the absence of experimental data. The agglomerates take on various shapes, including compact (spherical), elongated (cylinders), and other (irregular) geometries. However, the majority is believed to be elongated based on observations and thus can be described by MPPD models for fibers.

In lab animals, predicted deposition can be extrapolated to human exposure scenarios to find the HEC for risk analysis. Lab exposure concentrations at which biological responses are observed may be used to estimate CNT/CNF deposition in the rat lung. A dose metric such as deposition per unit surface area that is relevant to the observed effect is selected and used to extrapolate animal exposure settings to human exposure scenarios. Under the assumption that the same dose (deposition per unit surface area) in humans and rats gives the same response, HEC is obtained from the following relationship (Jarabek, Asgharian, and Miller 2005):

$$\frac{HEC}{C_R} = \frac{\delta t_R}{\delta t_H} \times \frac{\left(\dot{V}_E\right)_R}{\left(\dot{V}_E\right)_H} \times \frac{(DF/SA)_R}{(DF/SA)_H} \qquad (9)$$

where DF is the CNT/CNF deposition fraction in the lung during one breathing cycle and SA is the surface area for the region of interest in the lung. Alternatively, deposition per unit lung weight can be selected as the dose metric if the response of concern involves the pulmonary interstitium rather than the epithelium, for example a fibrotic response. However, because this is a long-term effect knowledge about pulmonary retention kinetics in rats and humans needs to be available so that the HEC can be based on the retained rather than the deposited dose (Figure B-3). A longer term multidose inhalation study (subchronic) that includes a NOAEL should be the goal for dosimetric extrapolation to derive the HEC; the selection of a unit, surface area or mass of the lung as the basis depends on the effect seen at higher concentrations/doses. Preferably, surface area should primarily be selected unless there is strong evidence of mainly interstitial responses.

For human/rat and rat/human extrapolation modeling the requirements are:

Determining the CNT/CNF concentration best in the breathing zone of a worker, secondbest from area monitor.
Determining airborne particle size distribution.
Determining what size distribution for rodent exposure would mimic human exposure interms of deposited doses in specific regions of the respiratory tract.
Exposing rodents (preferably whole-body) to different concentrations to establish acute, subchronic, and chronic exposure-dose-response relationships, including exposureconcentrations that are predicted to result in rodent retained lung burdens (per unit epithelial surface, or per unit lung weight) that correspond to those in exposed workers.
Analyzing results to determine rodent NOAEL for extrapolating to humans.

The MPPD deposition model was used to calculate CNT/CNF deposition fraction in rats for a given exposure atmosphere (concentration and CNT/CNF size characteristics) and rat lung and breathing parameters (functional residual capacity, tidal volume, breathing frequency, and breathing interval times). A dose metric was calculated based on deposition fraction per unit surface area or mass of the region of interest in the lung (i.e., tracheobronchial, pulmonary, lobar, etc.). The dose metric was used as the basis to calculate HEC by iteration: Deposition fraction in the human lung was calculated for different exposure concentrations of CNT/CNF until the predicted deposited mass per unit surface area (or mass) in humans matched that in rats. Figure B-4 presents HEC/C_R calculations for different size CNT/CNF at an aspect ratio of 10 with minute ventilations of 7.5 LPM and 0.241 LPM for humans and rats, respectively. Equal short exposure duration is used in the calculations ($\delta t_R = \delta t_H$). The ratio was calculated based on tracheobronchial (TB) and pulmonary (PUL) regions as well as for the entire lung. The surface areas of all airways in each region were added together to find the total surface areas for the TB and PUL regions. The surface area in the PUL region did not include the alveoli surface areas, because it is not yet included in the present version of the model. For losses by diffusion in the pulmonary region at diameters below 0.5 μm, HEC rose with increasing CNT/CNF diameter. Otherwise, HEC decreased with increasing CNT/CNF diameter where losses were by sedimentation and impaction. Predicted HEC was similar for the PUL region and the entire lung because the majority of deposition occurred in the PUL region. In addition, HEC was smallest if it was based on the TB region. When the ratio was above 1, HEC was larger than rat exposure concentration and vice versa.

Depending on the extent of available data—both from experimental animal inhalation and from human exposure—the HEC can be estimated based on the deposited or also—even more useful—on the long-term retained dose as explained in Figure B-3. While Figure B-4 was based on equal acute exposure duration and deposition per surface area as the dose metric, a more relevant dose metric should be based on a lifelong exposure for both humans and rats. Since CNT/CNF that deposit on lung surfaces are cleared over time, the dose metric should be based on retained dose rather than on deposited dose. Unlike the deposited dose, the retained dose of CNT/CNF in the lung depends on the exposure duration taking clearance into account. Thus, an expression similar to Eq. (9) could not be obtained to predict HEC for a lifelong exposure. Instead, an iterative procedure needs to be undertaken in which different human exposure concentrations are selected to calculate the dose (Figure B-3). HEC will correspond to the human exposure concentration for which the calculated retained dose is the same as for the animal. Calculations of HEC based on a dose related to the retained dose have indicated that HEC will always be lower than C_R (Jarabek, Asgharian, and Miller 2005).

GLOSSARY

ACGIH	American Conference of Governmental Industrial Hygienists
APM	aerosol particle mass analyzer
APS	aerodynamic particle sizer
BALF	bronchoalveolar lavage fluid
BAM	beta attenuation mass monitor
BET	Brunauer, Emmet, and Teller
BrDU	bromodeoxyuridine
BW	body weight
CIB	Current Intelligence Bulletin (NIOSH)
CMAD	count median aerodynamic diameter
CMD	count median diameter
CNF	carbon nanofibers
CNT	carbon nanotubes
CNC	condensation nuclei counter
CPC	condensation particle counter
CNS	central nervous system
CRP	C-reactive protein
DF	deposition fraction
DMA	differential mobility analyzer
DMA-APM, DMA	particle mass analyzer
DPBS	Dulbecco's phosphate-buffered saline
DSPC	disaturated phosphatidyl choline
DWCNT	double-walled carbon nanotube
EM	electron microscope
ENM	engineered nanomaterial
EPA	Environmental Protection Agency
FRC	functional residual capacity
GSD	geometric standard deviation
HEC	human equivalent concentration
HPLC	high-performance liquid chromatography
IARC	International Agency for Research on Cancer
ILSI	International Life Sciences Institute
ISO	International Organization for Standardization
LOAEL	lowest-observed-adverse-effect level
LDH	lactate dehydrogenase
LPM	liters per minute
MAC	maximum aerosol concentration
MFTD	maximum functionally tolerated dose
MMAD	mass median aerodynamic diameter
MPPD	multiple path particle dosimetry
mRNA	messenger ribonucleic acid
MOUDI	micro-orifice uniform deposition impactor
MTD	maximum tolerated dose
NM	nanomaterial
NIOSH	National Institute for Occupational Safety and Health
NOAEL	no-observed-adverse-effect level
NIR	near infrared

OECD	Organization for Economic Cooperation and Development
OEL	occupational exposure level
PBS	phosphate-buffered saline
PDGF	platelet-derived growth factor
PMN	polymorphonuclear neutrophils
PPE	personal protective equipment
PSP	poorly soluble particle of low cytotoxicity
PTA	programmed thermal analysis
PUL	region, pulmonary region
SA	surface area
SEM	scanning electron microscope
SMPS	scanning mobility particle sizer
STEM	scanning transmission electron microscope
SWCNT	single-walled carbon nanotube
TB	*tert*-butylalcohol
TEM	transmission electron microscope
TEOM	tapered-element oscillating microbalance
TF	thoracic fraction
TGF	transforming growth factor
TLC	total lung capacity
TV	tidal volume
WHO	World Health Organization